Performance Analysis of Rate Adaptive Wireless Communication System with Regenerative Relaying Using Low Density Parity Check Codes

Von der Fakultät Informatik, Elektrotechnik und Informationstechnik
der Universität Stuttgart zur Erlangung der Würde eines
Doktor-Ingenieurs (Dr.-Ing.) genehmigte Abhandlung

Vorgelegt von

Bushra Bashir Chaoudhry

aus Islamabad, Pakistan

Hauptberichter:	Prof. Dr.-Ing. Joachim Speidel
Mitberichter:	Prof. Dr.-Ing. Ingmar Kallfass
Mitberichter:	Prof. Dr.-Ing. Stephan ten Brink
Tag der mündlichen Prüfung:	19 Dez. 2019

Institut für Nachrichtenübertragung der Universität Stuttgart

2019

Acknowledgements

This thesis is result of my research activities at the Institute of Telecommunication at University of Stuttgart. First of all, I would like to express my deepest gratitude towards Prof. Dr.-Ing. Joachim Speidel, who provided me the opportunity to be part of his team. He was a great mentor and guide. We always had very productive discussions and his insight into the matters helped me both at professional and personal levels. I am really thankful to him for being a constant support while I moved back to Pakistan, during the thesis write-up phase. He always made sure that things work for me.

I am grateful to Prof. Dr.-Ing. Ingmar Kallfass and to Prof. Dr.-Ing. Stephan ten Brink for being the second and the third reviewer and providing me the valuable feedback.

Furthermore, I would like to thank Dr. Syed Ali Hassan at the School of Electrical Engineering and Computer Science at NUST, Pakistan, for one-on-one technical discussions towards the end of the thesis. His ideas, guidance and critical advice helped me through the hard times of my doctorate studies.

A very heartfelt thanks to my former colleagues at the Institute of Telecommunications. They provided me a comfortable working surroundings and let me learn a lot about Germany and Germans. Coffee and ice cream breaks, the legendary lunch at the university cafe, birthday celebrations and the kitchen corner, overall, a very memorable experience. A special thanks for the support staff at the institute. They literally had been there whenever needed. Thankyou Arni, Csaba. Günther, Jessica and Agnes.

I acknowledge and appreciate the work of all the students who carried out their master and bachelor thesis projects with me in this area of research.

A sincere thanks goes to my boss at the Fatima Jinnah Women University, Pakistan,

Prof. Dr. Uzaira Rafique, who had been a great moral support to let me work in a comfortable and flexible environment.

With all my heart I want to thank my mother and my siblings for always believing in me and for always being my moral strength. I want to thank my father, who is no more to see my success but he actually, sowed the seed. I am grateful to my in-laws family too, who encouraged me to pursue my dreams. Furthermore, I am thankful to my family in Stuttgart, who provided me a home away from the home.

A big thanks to some of my special friends also who always listened to me, helped me and kept me motivated to achieve my goal.

A whole-hearted thanks to my wonderful husband, Dawood. He patiently endured my moods and listened to my problems with an open ear. I can not thank God enough for giving me such an amazing companion. A last thanks goes to my little darling, Kashaf, who let me study and prepare for my exam and always provided me energy to work harder. Kashaf, you are the best daughter ever!

December, 2019

Bushra Bashir Chaoudhry

Contents

Abstract

Relay-assisted communication in current wireless systems is used to achieve the higher data rates and better network coverage in a cost-efficient and flexible manner. It is highly likely that relays are going to become an enabling technology for cooperative communications in the era of Internet of things (IoT) in 5G. The regenerative or decode-and-forward (DF) relays are used, decode the data, use forward error correction codes at the relay and then forward it to the subsequent receiver node. The theoretical performance analysis of such wireless systems is much involved. The reason is that there are more degrees of freedom to be taken into account as compared to the point-to-point communication. Moreover, the use of forward error correction codes, e.g. low density parity check (LDPC) codes makes the analytical analysis infeasible.

In this thesis, in the first part we investigate the decode-and-forward relays with LDPC codes and evaluate the bit-error-rate (BER) performance of a couple of decoding algorithms, namely bit-flipping algorithm and sum-product algorithm. The design of the parity check matrix for dual-hop communication system is considered in two ways. Firstly, the dimensions of the parity check matrix are kept the same for encoding at the source and the relay, whereas, in a second way the size of the parity check matrix is different at source and relay. It follows that code rate adaptive relays can be designed, which can adapt to different code rates according to the changing channel conditions. For such systems, we carry out a detailed numerical performance analysis, where we investigate five different code rates for different LDPC codes. Furthermore, the end-to-end BER analysis is carried out with different modulation schemes. The code rate adaptive systems are optimal performance wise but they become more complex, although relays should be low complexity and limited power devices.

In the second part of the thesis, we investigate the optimal placement of the relay. On the basis of the optimal location of the relay, a maximum ratio combining (MRC) system is designed for the cooperative communication, as *cooperative maximum ratio combining*, which achieves the full diversity. A *hybrid* diversity combining model with selection combining and maximum ratio combining has also been explored in the context of DF relays, where at first the relay with signal to noise ratio (SNR) above a threshold SNR is selected and then combined at the destination with a signal directly received from the source using MRC. Towards the end of the thesis, we study a dual-hop but multiple relays system and investigate different transmit power allocation techniques for multiple transmit nodes. Moreover, an optimized power allocation methodology is devised with code rate adaptive relays to obtain an optimized performance under the constraints of energy efficiency and low bit-error-rate.

Kurzfassung

Gegenwärtige drahtlose Kommunikationssysteme verwenden auch relaisgestütze Übertragungstechnik, um höhere Datenraten und bessere Netzwerkabdeckung auf kosteneffiziente und flexible Art und Weise zu erreichen. Mit hoher Wahrscheinlichkeit werden Relais eine wichtige Technologie für das Internet der Dinge (IoT) sein. Regenerierende oder Decode-and-Forward-Relais (DF-Relais) decodieren die Daten mithilfe von Verfahren der Vorwärtsfehlerkorrektur und leiten sie dann an den nachfolgenden Empfänger weiter. Die theoretische Untersuchung solcher drahtloser Kommunikationssysteme ist aufwändig, da dabei mehr Freiheitsgrade berücksichtigt werden müssen als dies bei Punkt-zu-Punkt-Übertragungssystemen der Fall ist. Darüber hinaus macht der Einsatz fehlerkorrigierender Kanalcodes wie z. B. von Low-Density-Parity-Check-Codes (LDPC-Codes) eine theoretische Untersuchung fast gänzlich undurchführbar.

Der erste Teil dieser Arbeit untersucht DF-Relais mit LDPC-Codes und wertet die Bitfehlerhäufigkeit (BER) zweier Decodieralgorithmem, nämlich des Bit-Flipping- und des Summen-Produkt-Algorithmus, aus. Dabei wird der Entwurf einer Codiermatrix für Kommunikationssysteme mit einer Weiterleitung auf zwei Arten betrachtet. Zum einen wird für die Codierung in der Quelle und im Relais eine Codiermatrix von gleicher Dimension verwendet. Zum anderen werden in der Quelle und im Relais unterschiedliche Dimensionen verwendet. Daraus folgt die Möglichkeit des Entwurfs coderatenadaptiver Relais, die sich, abhängig von Kanaleigenschaften, auf verschiedene Coderaten anpassen können. Für solche Systeme wird eine detaillierte numerische Auswertung der Leistungsfähigkeit durchgeführt, wobei fünf verschiedene Coderaten für verschiedene LDPC-Codes untersucht werden. Darüber hinaus wird die BER am Empfänger für verschiedene Modulationsstufen untersucht. Die coderatenadaptiven Systeme sind bezüglich ihrer Leistungsfähigkeit optimal,

werden jedoch durch die aufwändige Verarbeitung komplexer, wenn man bedenkt, dass Relais Geräte mit geringer Komplexität und begrenzter elektrischer Leistung sein sollen.

Der zweite Teil dieser Arbeit untersucht die optimale Position des Relais. Auf Grundlage der optimalen Position des Relais wird ein System mit Maximum-Ratio-Combining (MRC) für die kooperative Kommunikation entworfen (kooperatives Maximum-Ratio-Combining), das volle Diversität erreicht. Im Kontext von DF-Relais wird außerdem ein hybrides Model der Diversitäts-Kombination für Selection-Combining und Maximum-Ratio-Combining untersucht. Dabei werden zunächst Relais mit einem Signal-Rausch-Verhältnis (SNR) oberhalb eines Schwell-SNR ausgewählt und dann an der Senke mit einem Signal, das direkt von der Quelle empfangen wird, unter Verwendung von MRC kombiniert. Am Ende der Arbeit wird ein System mit mehreren Relais untersucht und verschiedene Techniken der Leistungsverteilung für mehrere Sender betrachtet. Darüber hinaus wird ein optimiertes Verfahren der Leistungsverteilung mit coderatenadaptiven Relais vorgestellt, um die bezüglich der Bitfehlerhäufigkeit optimale Leistungsfähigkeit und hohe Energieeffizienz zu erzielen.

List of Acronyms

ACM	Adaptive coding and modulation
AF	Amplify-and-forward
APP	A-posteriori probability
AWGN	Additive white Gaussian noise
BFA	Bit-flipping algorithm
BPSK	Binary phase shift keying
BER	Bit-error-rate
BS	Base station
CC	Cooperative communications
CF	Compress-and-forward
CGSC	Cooperative generalized selection combining
CMRC	Cooperative maximal ratio combining
CR	Code rate
CSC	Cooperative selection combining
CSI	Channel state information
CT	Cooperative transmission
D2D	Device-to-device
DF	Decode-and-forward
EE	Energy efficiency
EF	Estimate-and-forward

EPA	Equal power allocation
EXIT	Extrinsic information transfer
FEC	Forward error correction
GF	Galois Field
GSC	Generalized selection combining
ISI	Inter symbol interference
LDPC	Low density parity check
LLR	Log-likelihood ratio
LOS	Line of sight
LTE	Long term evolution
MIMO	Multiple input multiple output
MRC	Maximal ratio combining
NGMN	Next generation mobile network
NLOS	Non-line of sight
OPA	Optimized power allocation
PDF	Probability density function
PL	Pathloss
QAM	Quadrature amplitude modulation
QoS	Quality of service
rref	Reduced row-echelon form
SC	Selection combining
SIMO	Single input multiple output
SNR	Signal to noise ratio
TS	Time slot
WLAN	Wireless local area network
3GPP	3rd generation partnership project
4G	4th generation
5G	5th generation

List of Symbols

x	Scalar in $\mathbb{R}$ or $\mathbb{C}$
$\mathbf{x}$	Column vector
$\mathbf{X}$	Matrix X
$(.)^T$	Transpose
$(.)^*$	Complex conjugate
$(.)^H$	Complex conjugate transpose
E[.]	Expected value
$\|x\|$	Absolute value of scalar x
$\|\|\mathbf{x}\|\|$	Euclidean norm of the vector $\mathbf{x}$
$\mathbf{I}_N$	Identity matrix of size N
$\mathbf{0}$	Null vector with all zero entries
σ^2	Variance of the Gaussian random variable
γ	SNR
$\overline{\gamma}$	Average SNR
$f(.)$	Probability density function
$p(.)$	Probability density function
$P(.)$	Probability operator
$P(x\|y)$	Conditional probability of x, given y
$L(x)$	Log-likelihood ratio of x
$\log_e$	Natural logarithm
ν	Pathloss exponent

$\Gamma(.)$	Gamma function
$\arg min$	Minimum among arguments
$\mathbf{X}_{(MXN)}$	Matrix $\mathbf{X}$ with dimensions M $\times$ N
η	Energy efficiency

1

Introduction

In the last decade, the ubiquitous computing has become one of the most essential parts of the human life. This everywhere and anywhere presence of the technology has become possible only because of wireless communications. Almost everyone wants Internet for education, research, business and entertainment. Because of the higher demand, the system capacity is reaching its saturation level. To meet this ever rising need of the connectivity, system designers are trying all the means to increase the system capacity. According to [1], [2] *the wireless capacity has doubled every 30 months over the last 100 years*. This increase in capacity was approximately a million folds since 1960s, which has been broken down to yield a 25-times increase from wider spectrum, a 5-fold improvement dividing the spectrum into smaller slices, a 5-fold improvement by designing better modulation schemes and a high 1600-fold gain through decreased cell sizes and transmit distances.

When the radio signal travels a distance, it attenuates or in other words the signal power is reduced at the receiver, this introduces quite a few problems which we will discuss in certain detail later in the 2nd Chapter.

In wireless communication when a signal is sent from the source, it usually takes more than one propagation paths to reach its destination. At the receiver multiple copies of the signal arrive but attenuated and delayed, known as *multipath fading*. Multipath fading is one of the worst effects that a wireless signal experiences, but if the system is designed properly then these multiple copies of the signal can be a *'a bliss in disguise'*, and their time or space separated copies can be used to improve the overall performance of the system. Multi-hop communication involves the relaying

of information comparatively over shorter distances, thus the total distance is being divided into more than one shorter length (hops) between sender and receiver nodes. If a signal regeneration is performed in each node the overall power dissipation of all the hops is less than that hop of the whole distance. The performance gain can be achieved by providing the cooperation via relays which are installed between sender and receiver. This performance gain requires the architectural changes in the wireless communications system. Consequently, this improvement comes with a price of increased complexity of the typical wireless communication system. So a traditional simple point-to-point communication link is broken down into a complex multi-node (multi-hop) link.

A relay is a support node that enhances the data transmission capability of the wireless system. This node lies somewhere between the source and destination. The relay receives the information from the source or preceding relay and processes it in a prescribed way before passing it on to the next node, i.e., next relay or the destination. Cooperation between source and destination can also be achieved by using the existing users in the system for relaying the information. The main idea is that each user is capable of acting as a relay for other users in the network[1]. By relaying, the destination node usually receives different signals and combines them together as if they are coming from a multi-antenna system, so that the spatial diversity can be achieved without mounting more than one antenna elements on the devices. This is known as 'cooperative communication (CC)'. This cooperative communication gave birth to the whole new era of research in wireless communications and recently lots of work has been done in this area [1, 42, 44, 46, 50–55, 58–60, 64, 70–72, 74–82, 84].

Today, very effectual coding schemes like Turbo codes or low density parity check (LDPC) codes on multi antenna, multiple-input multiple-output (MIMO) systems have already made the point-to-point communications to achieve a performance very close to the theoretical limits of the system capacity, the *Shannon capacity*. These coding schemes can be used to encode the data at source, receive it on the relay, decode it, and then re-encode it before sending over to the destination node. We will use the sender-receiver and source-destination pairs interchangeably throughout this thesis.

[1]Though when existing users are employed for relaying the information for other users in the network, their own battery power usage and complexity of the working algorithm increases, which are main tasks of the system designers, because for a wireless user, power is one of the main concerns as it keeps dissipating on the go.

1.1 Motivation

Relay assisted communications have paved their way in almost all major applications of the wireless communication. Relays are used in cellular networks (3GPP Long term evolution has a permanent feature of relaying) and in **4G** wireless local area networks (WLAN, IEEE 802.11s standard). As well, without relaying connection between different nodes of vehicle-to-vehicle (V2V) communications, ad-hoc networks and sensor networks is not possible since they have no pre-established infrastructure to support them [3, 5]. Beyond that 5G will have a device-to-device (D2D) communication [4,75,76] and will resort to relays for non-line of sight (NLOS) communications between them. However, in this thesis we will discuss the regenerative relaying technology in general, without focusing on any particular application area. We consider a relay assisted wireless communication system with LDPC codes and thoroughly analyze the system for different aspects.

Here we will consider a cellular network to develop the understanding for the need of relaying technology. A cellular network is composed of many adjacent cells and each cell is controlled at least by one centralized base station (BS). The basic idea behind cellular system is the 'frequency reuse' using the fact that the signal power falls off with distance to reuse the same frequency spectrum at spatially separated locations [6]. The cell sizes and cell shapes are chosen very carefully as they are the key to the design of a cellular network. A cellular network basically suffers from 3 problems [1]:

1. Capacity: Each cell has a pre-assigned amount of resources like bandwidth (a set of frequencies) and transmit power. As the number of users in a single cell increases the cell becomes unable to serve all the users, so a cell becomes *capacity limited*.

2. Coverage: The received power reduces with the distance and the users at the cell edge experience the diminutive power from their associated BS. As a result a cell becomes *coverage limited*.

3. Interference: As a user terminal approaches the cell edge, it becomes more prone to the interference posed by the adjacent cells. On one hand, it has insufficient received power from its own BS and on the other hand it gets signals from the adjacent cells which are strong enough to make the system *interference limited*.

These three limitations can be mitigated, nonetheless, by making changes in the network architecture to support the efficient communication between source and

destination. These architectural changes can be introduced in the form of relays, which help the cellular networks to increase their capacity and coverage and reduce the interference.

There are different types of relaying that has been discussed in the literature, but the most common are amplify-and-forward (AF) relays, where the relay receives the signal from the preceding node, amplifies it and forwards it to the next node. As a result, signals are received with enhanced signal strength, but at the cost of enhanced noise as each amplifier adds additional noise. On the other hand, decode-and-forward (DF) relay receives information from the previous node, decodes it, re-encodes it and transmits it further to the next node. This is a more complex scenario as compared to AF relaying but of course provides more robust performance with a lower symbol-error-rate (SER) or bit-error-rate (BER). Our considered system in this thesis will use DF type of relays, also known as *'regenerative relays'*.

1.2 Thesis Outline

The remainder of the thesis has been organized as follows: In Chapter 2 we first of all review the fundamental properties of wireless communication and relaying strategies. We will discuss the relay-assisted communications and make general assumptions of the system being analyzed in this work. In Chapter 3 we will discuss LDPC codes to approach capacity along with some basic ideas on encoding and decoding using LDPC codes. Later in Chapter 4 we talk about the multi-hop wireless system focusing on a dual-hop set-up as pilot example. Performance results of dual-hop system with decode-and-forward relays shall be discussed there. Chapter 5 focuses on the cooperative combining of the signals, where we also discuss about the energy-efficiency and power allocation strategies for DF relays. In Chapter 6 eventually, we conclude the main part of the thesis with a short summary of the most important results obtained. We also mention some open areas in the conclusion, which may represent interesting and fruitful research topics for the future.

2

Fundamentals

This chapter provides the overview of the wireless systems, particularly focusing on the relay communications. We will use all the foundations made in this chapter as a prerequisite for the further discussions throughout this thesis. Basic assumptions of the considered system will also be presented here, so that the reader gets a good insight into the system to be further analyzed in the Chapters 3, 4, and 5. We will briefly discuss the wireless channel in Section 2.1, in Section 2.2 we will see the factors that affect the wireless communications majorly. In Section 2.3 we present relays and their operating types with certain details. Under the Section 2.4 the reader gets an overview of the LDPC codes and topic 2.5 finally, concludes the chapter with basic system assumptions.

The next generation mobile networks (NGMN) alliance defines the following requirements for 5G networks in their famous white paper [30]:

- Data rates of tens of megabits per second should be supported for tens of thousands of users
- 1 Giga-bits per second to be offered simultaneously to many terminals on the same office floor
- Several hundreds of thousands of simultaneous connections to be supported for massive sensor deployments
- Spectral efficiency should be significantly enhanced compared to 4G
- Coverage should be improved

- Signaling efficiency should be enhanced
- Latency should be reduced significantly compared to LTE

This increasing demand for data rates needs a thorough analysis of the system. For that, first we will consider what are the wireless channels and what are the challenges to model such channels with an optimized and acceptable performance under the given conditions.

2.1 The Wireless Channel

Like all other channels, a wireless channel is associated with a sender and a receiver with transmit (tx) and receive (rx) antennas mounted on them, respectively. The transmitter sends a message through the 'air' to the receiver, the communication channel is '*wire-less*', since there is no other physical medium involved but air. The wireless environment as an information transmission medium is not only difficult to model but also very unpredictable [6] and unguided, because it keeps changing constantly. Modeling the time-varying nature of the wireless channel is a challenging problem and in last couple of decades lots of research had been carried out to model the wireless channel with different facades, e.g. in references [31–41]. One more thing that we need to emphasize here is that *not only the communication channel is changing constantly* but also the sender and receiver can *change their location/position while communicating wirelessly*, thus an additional factor for modeling the channel.

2.2 Effects on a wireless Channel

Actually, wireless channel is never stable, the time-varying nature of the channel stems to three factors, namely pathloss, shadowing[1] and multipath fading (Figure 2.1). These three factors can be put under the umbrella of two types of variations that occur to a signal traveling in a wireless vicinity: 1) *Large-Scale Fading* and 2) *Small-Scale Fading*. Pathloss and shadowing are called large-scale variations because they usually occur over a large distance[2], whereas multipath fading are small scale variations as they may occur for very small changes (as small as half a wavelength) in spatial positions of transmitter and receiver [8].

[1] also called *shadow fading*
[2] Pathloss: 10-1000m, Shadowing: 10-100m

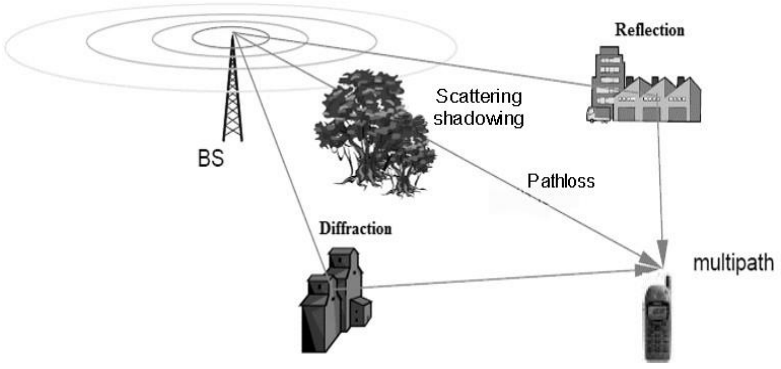

Figure 2.1: Wireless transmission environment

When an electromagnetic wave propagates, it strikes by walls, buildings, terrain, vehicles and other moving or still objects. As a result the wave bears different types of experiences. These varied experiences of reflection, diffraction, scattering [8], and absorption ensue due to the size of the obstruction with which a wave strikes. A classification of the experiences on the basis of obstruction size is

Reflection: This phenomenon occurs when a radio wave hits a wall or any other object of dimensions much larger than its wavelength (λ).

Diffraction: When the radio wave is obstructed by a dense body considerably larger compared to λ and secondary waves are made from behind the obstructing object. This is known to be the main cause of *shadowing*.

Scattering: This occurs when a radio wave hits a body of order of λ or smaller, or when the body is large but has a rough surface. This causes the signal energy to spread in all dimensions.

Absorption: This occurs when a radio signal strikes a surface that absorbs its energy, consequently the signal power attenuates.

After knowing the effects that can occur to a radio wave, let us see the factors that cause these effects in the following subsections.

2.2.1 Pathloss

Pathloss (PL) is the reduction in average received power P_{rx} level as a radio wave propagates through a space where there are no obstructions between tx and rx. It is actually the ratio between transmit power P_{tx} and received power P_{rx}. When a

signal travels a distance d it loses its strength. This power loss is caused by the motion over a large distance and is measured as log-normally distributed variation about the mean [8]. When a transmitter transmits a signal in free-space towards a receiver at a distance d, the pathloss can be defined as

$$P_L = \frac{P_{tx}}{P_{rx}} = \left(\frac{4\pi d}{\lambda}\right)^2 \frac{1}{G_{tx}G_{rx}} \tag{2.1}$$

If we reverse equation$\big(2.1\big)$, it becomes the famous equation of Frii's transmission law, i.e.,

$$\frac{P_{rx}}{P_{tx}} = \left(\frac{\lambda}{4\pi d}\right)^2 G_{tx}G_{rx} \tag{2.2}$$

where G_{tx} and G_{rx} are gains of transmit and receive antenna, respectively and λ is the wavelength of the radio wave. In free-space the received power falls off in inverse proportion to the square of the distance d between transmitter and receiver [6].

There are different pathloss models that capture the received power well. Simple models like free-space or ray-tracing models or empirical models can be used during network planning, e.g. Okumura/Hata or COST 231 (for details please see [6] and the references therein). These models consider transmit and receive antenna heights, and carrier frequency also, along with free-space pathloss specifications. However, they are complex and costly. These models are valuable when tight system specifications are to be met in some given environment. In this thesis we consider the simplified pathloss model[1] that provides the essence of signal propagation without resorting to the complex PL models. The simplified model is a trade-off between complexity and accuracy but provides a basic idea about propagation environment nonetheless,

$$\frac{P_{rx}}{P_{tx}} = K\left(\frac{d_0}{d}\right)^{\nu} \tag{2.3}$$

where K is a constant and depends on antenna heights and average channel attenuation, it implicitly takes care of the free-space pathloss. d_0 is the reference distance in antenna far field and ν is the pathloss exponent, which defines how quickly the received power weakens as compared to the transmit power in a given environment.

The pathloss exponent is different for different environments, for instance outdoor environments like urban, rural, dense or indoor environments like home, office

[1] also known as exponential pathloss model

or factory. Please see Table 2.2 in [6] for pathloss exponents for different environments. For urban macro-cells its range is 3.7 to 6.5 and for a home (indoor) it is typically, 3. So, the value of ν depends upon the propagation environment [6]. We will further talk about the simplified pathloss model in context of regenerative relay assisted communications, once we discuss the suitable relay placement in Chapter 4, Section 4.1.1.

2.2.2 Shadow Fading

Shadow fading is another type of large scale fading and is caused by the objects like a building, a mountain, a tree, a car, or a person etc. The signal traveling through a wireless channel will undergo some random changes due to the blocking objects in the path of signal, the signals are being diffracted from these objects and power decays as the signal travels a given distance. These variations are also caused by the changing reflecting surfaces and scattering bodies. The location, size and other characteristics of these obstructing objects keep changing, so the change they cause is also unpredictable. A special model is needed to take care of these random changes by introducing an additional attenuation factor ψ, i.e., log-normal shadow fading. This model has been proven by extensive measurements and accurately models these random variations in outdoor and indoor environments [6].

$$p(\psi) = (\frac{\xi}{\sqrt{2\pi}\sigma_{\psi_{dB}}\psi})exp\left(- \frac{(\psi_{dB} - \mu_{\psi_{dB}})^2}{2\sigma^2_{\psi_{dB}}} \right), \psi > 0 \tag{2.4}$$

The ratio of transmit to receive power is $\psi = P_{tx}/P_{rx}$, it is random and follows a log-normal distribution. Here in equation (2.4), the probability density function (pdf) of the ψ has been defined where $\xi = 10/ln10$, and $\mu_{\psi_{dB}}$ is the mean of $\psi_{dB} = 10log_{10}\psi$, and standard deviation is $\sigma_{\psi_{dB}}$, both in decibel (dB). The mean and standard deviation can be determined using analytical or empirical methods.

The received power fall-off at a certain distance can be measured by combining the pathloss and shadow fading together, where the additional random attenuation from shadow fading with *zero* mean creates variations about the pathloss, this can be observed in Figure 2.2.

2.2.3 Multipath Fading

When a signal travels in a wireless vicinity, it takes multiple paths to reach the destination. The destination receives a constructive or destructive combination of randomly delayed, reflected, diffracted or scattered signal components [9]. Multipath

fading introduces different variations in the signal amplitude and phase. These variations can be caused by small movements resulting in spatial changes, as small as half a wavelength. There are two direct effects of the multipath fading [8],

1. Time-variation of the channel: Sometimes due to the motion of the tx or rx antenna.

2. Delay-spread of the signal: *Delay-spread* is the difference between the arrival time of first significant multipath component and the last significant multipath component. So this delay spreads the signal and if this spread approaches the symbol interval, there is inter-symbol-interference (ISI) and as a consequence, the signal is distorted. The ISI can be rectified using multi carrier transmission techniques like orthogonal frequency division multiplex (OFDM) or by using equalizers.

Herein, we assume narrow band channels, so that we do not have any delay spread as such since the symbol interval is long enough to ensure that there is no inter-symbol interference. Moreover, we consider a slow fading channel, which remains constant during a symbol interval. If a transmitter transmits $s \in \mathbb{C}$ and the receiver receives $y \in \mathbb{C}$, then the input-output relationship of the equivalent baseband system can be defined as,

$$y = hs + n, \tag{2.5}$$

where $n \in \mathbb{C}$ is the additive white Gaussian noise (AWGN) with *zero* mean and the variance σ^2. $h \in \mathbb{C}$ is the complex channel coefficient. Depending upon the different environments, different models can be used to describe the statistical behavior of such channels. For example, the Rayleigh fading model is frequently applied, which is used to model the behavior of a multipath channel when there is no direct line-of-sight (NLOS) between the tx and rx. The probability density function (pdf) of the magnitude of h follows a Rayleigh distribution [9].

$$p_{|h|}(|h|) = \frac{2|h|}{\Omega} exp\left(- \frac{|h|^2}{\Omega} \right) \tag{2.6}$$

The phase is uniformly distributed between 0 and 2π and h is Gaussian distributed with *zero* mean and variance $\Omega = \mathbb{E}\{|h|^2\}$. Actually, $\mathbb{E}\{|h|^2\}$ is nothing else but average power gain. Another classical model of $|h|$ is the Ricean distribution when there is also dominant line-of-sight (LOS), coming directly from the sender to receiver. Another type of channel model is Nakagami-m distribution. The PDF of

$|h|$ for the Nakagami-m model is defined as [9]

$$p_{|h|}(|h|) = \frac{2m^m|h|^{2m-1}}{\Omega^m\Gamma(m)} exp\left(-\frac{m|h|^2}{\Omega}\right), \tag{2.7}$$

In equation (2.7) along with h a new parameter m has also been introduced, known as 'fading parameter' and its value varies between 1/2 to ∞. This fading parameter helps to model the severity of multipath fading in different propagation environments. The higher the m, the lower the fading is. $\Omega = \mathbb{E}|h|^2$ defines the mean power gain and $\Gamma(m)$ is the well-known Gamma function. When $m = 1$, Nakagami-m fading reduces to the Rayleigh fading that can be easily seen from equation (2.7). Performance analysis of Nakagami-m fading is often much easier as compared to even Ricean fading and it covers a variety of different environments. For the same reasons, in this thesis we will use this more generalized distribution. There are some more distributions for channel coefficient modeling in the literature, for example Weibull distribution, Hoyt distribution and log-normal shadowing to name the few here, but as these are out of scope in this thesis. So, we request the interested reader to please refer to [9] and the references there in. Figure 2.2 shows the ratio of the received power to the transmitted power in decibels (dB) for various factors, which adversely affect the wireless channel.[3]

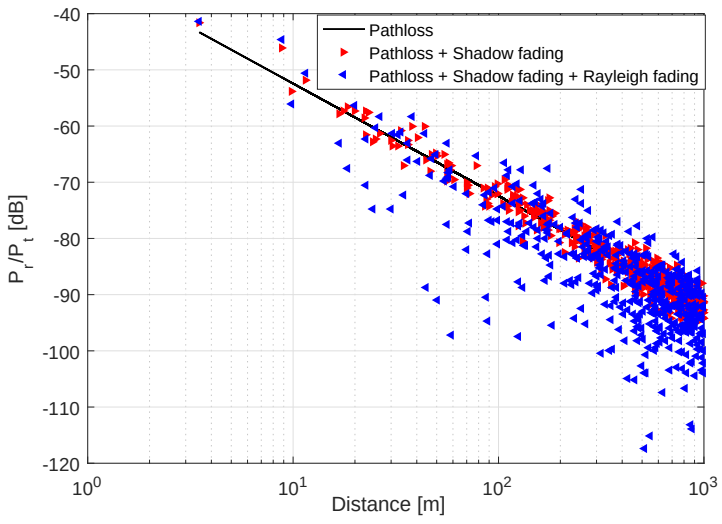

Figure 2.2: Ratio of receive to transmit power as a function of distance for various fading effects [7]

[3]The decibel value of x is $10log_{10}\ x$

2.3 Relayed Communication

In Chapter 1 we have briefly discussed what are relays, why they seem to be a promising area of research, and how they can help to resolve some of the problems posed by the wireless, time-varying channel. In relay-assisted communication relays are used between source and destination to deliver the data and the relay works as a support node. The sender sends the information to the relay that relay processes according to a prescribed set of instructions and forwards the information further to the next node or destination. In this section we will discuss different types of relays, such as the decode-and-forward relays with certain depth, since they are one of the focal points of this thesis.

2.3.1 Types of Relaying Protocols

Broadly speaking, relays can be divided into two types, i.e., transparent and regenerative relaying protocols [1].

Transparent Relaying

With this type of relaying, signal waveform is not being modified, rather very simple operations like amplification or phase rotation of the waveform are done at the relay to reduce the detrimental effects of the wireless channel and then the signal is sent to the next node. This family includes protocols like

Amplify-and-Forward (AF): Simplest form of transparent relaying where a signal is received on a relay from a predecessor, amplified, and sent further on to the next node. But the problem is that noise is also amplified along with the useful signal, hence, the BER performance gets worse.

Linear Process and Forward: Some simple linear operations are performed on the signal, like phase shifting. Such operations are performed in analog domain and after the amplification of the signal. Phase shifting property facilitates the implementation of distributed beam-forming. At the receiver phase information will be needed for phase rotation compensation.

Regenerative Relaying

With this type of relaying, as the name suggests the signal is being modified or regenerated at the relay. The operations are performed in digital baseband and require powerful hardware [1]. Some of the important types of this protocol are the following:

Estimate-and-Forward (EF): The analog signal is amplified and then down converted to the baseband, followed by detection and estimation algorithms. The signal is forwarded to the successor node. The processing done at the relay increases the complexity of the system.

Decode-and-Forward (DF): DF protocols receives the signal, decodes it and re-encodes it before retransmitting to the next node. This encoding and decoding is done by a prescribed protocol, making the system more complex.

The above mentioned types of the relaying protocols are the most common ones in the family of relaying protocols. There are lot more relaying protocols but they are not an area of interest for this thesis, so for details please see [1] and the references therein.

2.3.2 Advantages of Relay-assisted Communication

Relay-assisted communications started with an idea to increase the coverage of wireless communications systems. However, later several new ideas have been introduced to take the full advantage of the relay technology. For example, new cooperation algorithms have been designed to achieve a better BER performance. Moreover, relays help to reduce the effect of pathloss, as we know that the receive power reduces when the signal travels over the distance d. By dividing the whole distance d into shorter lengths, a better individual SNR can be achieved on each hop. Similarly, relay technology also helps to fight against the shadow fading by having stronger signals over shorter distances. If we consider a certain static vicinity where a new BS can not be mounted, placing a relay station somewhere higher than the obstructing buildings, trees or other obstacles can help to reduce the effect of shadow fading, as illustrated in Figure 2.3.

Furthermore, in cooperative relay communication, the diversity combining became possible without mounting multiple antennas at the sources and destination. Signals coming from the multiple and independent paths from the source and the relays can be combined at the destination to achieve diversity. This helps to address the problem of multipath fading, i.e., there is a high probability that not all the independent paths will be in fade and at least one of them will have a strong enough signal to reach the destination.

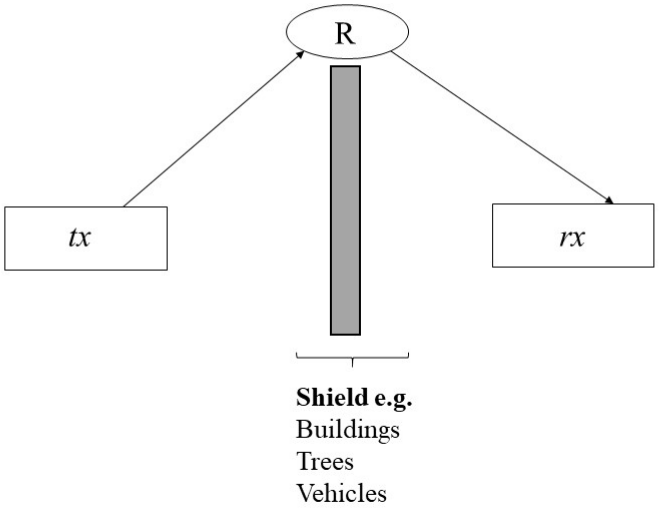

Figure 2.3: Shielding effect of shadow fading

In the following of this thesis we will restrict our discussion to the DF relays. In the next section we will present a brief introduction to LDPC codes and motivate why we choose this type of the block codes.

2.4 Low Density Parity Check Codes

Coding makes it possible for the decoder at the receiver to detect or correct quite some errors that are introduced by the wireless channel [6]. For a coded system the bit-error probability P_b defines the probability that a bit has been received in error. Error correction coding is used to reduce the P_b. The error correcting capability of codes comes with a price, usually the increased complexity and decreased data rates because of additional redundant bits. Examples of such codes are block codes, e.g. Turbo codes or LDPC codes [1] and convolution codes.

Low density parity check codes are forward error correcting (FEC) codes and are a class of linear block codes. They were invented by Gallager in 1960 in his doctoral dissertation [10], but they had been ignored till 1993, when they were reinvented by Mackay and Neal [47]. Since then lots of work has been done on LDPC codes in regard of finding capacity limits, encoder/decoder designs, and their implementation for different channels. LDPC codes can be constructed in a way to achieve the near-capacity performance that means the SNR threshold can be set very near to the theoretical limit, the *Shanon limit*. Actually, the LDPC codes can even beat the

[1] sometimes also known as *'compound codes.'*

best known Turbo codes, when their code length is very large. They can work in close proximity of 0.04dB of the Shanon limit at a BER of 10^{-6} for a code length of 10^7 [48].

LDPC codes are considered as the true competitors of best known Turbo codes. Other than having the BER performance edge over Turbo codes, usually the error floors with LDPC codes are far less evident as compared to Turbo codes. LDPC codes give good performance even when there are data erasures, e.g. in the Internet when the whole packets are lost, LDPC codes often can reconstruct the entire data stream without requiring a repeat request, saving time and bandwidth. Last but not the least, they have low complexity iterative decoders compared to their Turbo counterparts. A major drawback of LDPC codes is that their encoding becomes prohibitively complex when the codeword length is large.

LDPC codes have a special structure of parity check matrix $\mathbf{H}$, a sparse binary check matrix [1]. When every row and column has a fixed number of 0's and 1's, they are called as 'regular LDPC codes'. Luby et al. [14] introduced the 'irregular LDPC codes', which show a better performance as compared to regular codes. Tanner graphs are the graphical representation of parity check matrix $\mathbf{H}$, named after Michael Tanner [15]. The graphical representation is very important for designing the decoding algorithms. Based on the iterative probabilistic decoding, different variations of decoding algorithms for LDPC codes are available, e.g. message passing algorithm (MPA), bit-flipping (BF) or sum product algorithm (SPA).

There are various other types of LDPC codes with different methods to encode them. A detailed discussion on the encoding and decoding process is given in Chapter 3. We will use irregular LDPC codes and see how the Tanner graphs help to design the iterative decoding algorithms. Moreover, we will introduce some basic simulation results on the performance of different decoding algorithms.

2.5 Relay-assisted Communication: Fundamental Assumptions and Targets

In this section we will introduce the reader to some general wireless system assumptions for regenerative relaying. These assumptions are applicable to rather generic scenarios but whenever needed, we will add system specific assumptions.
First of all we consider that relays operate in half-duplex mode, i.e., they can not send or receive at the same time. This assumption is frequently made in relay-

[1] with more 0's and fewer 1's

assisted communications, because relays are supposed to be power limited devices. With half-duplex relaying the transmitted and received signals are kept well separated in time. If relays send and receive at the same time, then self-interference of transmitted and received signals will be very strong that will need accurate cancellation and shielding against this interference. Hence, the full-duplex relays are an impractical solution for the relay-assisted communications [43]. Please be reminded here that we will investigate the half duplex relays, but not one-way relays, which can send information only in one direction. Hence, the half-duplex relays we consider here are capable of sending information in both directions but separated by time or frequency slots.

Further, we assume that all the hops undergo a multipath slow fading, moreover, all the links are corrupted by AWGN with *zero* mean (μ) and variance σ^2. We consider a Nakagami-m distribution for the characterization of the channel fading between different nodes. The Nakagmi-m distribution represents the time-varying nature of the channel in a flexible way, because the fading parameter m specifies the depth of the fading, i.e., for $m = 1$ we have Rayleigh fading and for $m \to \infty$ we have additive white Gaussian noise only. Please see equations (2.6) and (2.7). We assume, that the transmission between different hops takes place on orthogonal channels, which are completely independent of each other but not necessarily identically distributed (n.i.i.d).

Moreover, we assume that all the receiving nodes have perfect channel state information (CSI) of their respective hops, this is necessary for perfect coherent detection of the signals at receiver.

Lastly, we assume that relays are placed right between the source and the destination. For specific cases in upcoming chapters we will investigate the performance of the whole system in detail when relay is put closer to the source or the destination. We will find out the optimal position of the relay to obtain the best BER performance. Positioning the relay at a different point changes the average SNR of the hops but please keep in mind that changing the position of the relay does not affect the fading parameter m and pathloss component ν, they are two independent parameters of the fading environment.

In [49], the DF relays have been throughly investigated under the condition that the system ideally meets the Shannon's channel capacity. However, this dissertation investigates and analyzes the performance of relay-assisted communication under more realistic assumptions with the help of LDPC error correction coding to approach the capacity.

3

Low Density Parity Check Codes

In this chapter low density parity check (LDPC) codes are going to be our focal point. We already motivated in Section 2.4 why we chose these codes. In Section 3.1 we will introduce the reader to some fundamental notions of block codes as well as encoding and decoding methods. In Section 3.2 we introduce the LDPC codes and explain different representations for such codes. The Section 3.3 outlines the decoding algorithms for LDPC codes with an example. In Section 3.4 we conclude the chapter with an explanation of LDPC codes for relay-assisted communications.

The name *low density parity check* codes comes from the fact that they have a low density of 1's in their parity check matrix. There are many approaches to design LDPC codes. For example, Gallager codes have a regular structure and they can be constructed using random column permutations [10]. In [11] Mackay designed LDPC codes having no two columns with more than one overlap of 1's. Richardson et al. [12] and Luby et al. [13], [14] designed the irregular codes which have a parity check matrix that has a non-uniform distribution of 1's in each column and row, respectively. Then there are regular accumulate (RA) codes [16], irregular repeat accumulate (IRA) codes [17], extend irregular repeat accumulate codes (eIRA) [18]. Kou et al. [19] introduced the construction of LDPC codes based on finite geometries.

3.1 Basics of LDPC Codes

3.1.1 Linear Block Codes

A *linear block code* is an error correcting code for which a linear combination of

different codewords results in another codeword.
In a typical digital communication system, the source provides a stream of 1's and 0's as its output. Block coding divides such a stream of bits into chunks/blocks, called a *message block*. This message block can be represented by *a row vector* $\mathbf{u}$ of length k bits,

$$\mathbf{u} = (u_1 \; u_2 \; ... \; u_k) \tag{3.1}$$

where $u_i \in \{0, 1\}$ are the information bits and $i = 1, 2, ..., k$. There can be 2^k distinct message blocks.

3.1.2 Encoding with Block Codes

The encoder at the transmitter (source) performs the encoding of the binary data and allocates redundant bits to the message bits. According to Figure 3.1 the encoder output is a row vector $\mathbf{c}$ of length n, which contains k information bits and $(n - k)$ parity bits.

$$\mathbf{c} = (c_1 \; c_2 \; ... \; c_k \; ... \; c_n) \tag{3.2}$$

where $c_i \in \{0, 1\}$ are the codeword bits and $i = 1, 2, ..., n$. The *code rate* can be defined as

$$CR = \frac{k}{n} \tag{3.3}$$

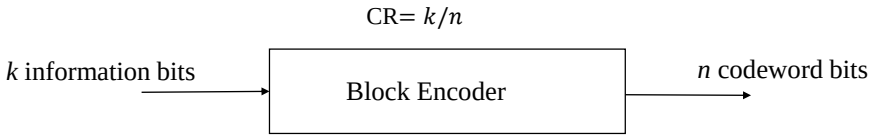

Figure 3.1: Encoder for block codes

As we have k message bits, we will have 2^k distinct codewords as result. The set of 2^k codewords is called a *block code*. A block code of length n and 2^k codewords is called a *linear* (n, k) *code* if and only if its 2^k codewords form a k-dimensional subspace of the vector space of all the n-tuples over the binary field GF(2) [20]. In

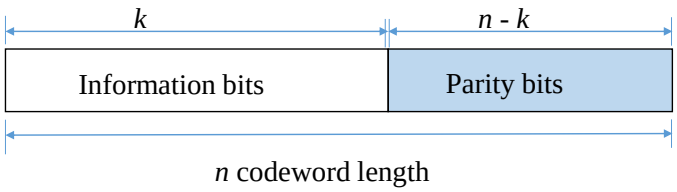

Figure 3.2: Systematic codeword

fact, a binary block code is linear if and only if the modulo-2 sum of two codewords is also a codeword [21].

Given a set of k linearly independent row vectors, i.e., $(\mathbf{g}_1\ \mathbf{g}_2\ ...\ \mathbf{g}_k)$, then the codeword $\mathbf{c}$ can be defined as a linear combination of these k vectors, i.e.,

$$\mathbf{c} = u_1 \bullet \mathbf{g}_1 \oplus u_2 \bullet \mathbf{g}_2 \oplus ... \oplus u_k \bullet \mathbf{g}_k \tag{3.4}$$

$$\mathbf{G} = \begin{bmatrix} \mathbf{g}_1 \\ \mathbf{g}_2 \\ \vdots \\ \mathbf{g}_k \end{bmatrix} = \begin{bmatrix} g_{1,1} & g_{1,2} & \cdots & g_{1,n} \\ g_{2,1} & g_{2,2} & \cdots & g_{2,n} \\ \vdots & \vdots & \ddots & \vdots \\ g_{k,1} & g_{k,2} & \cdots & g_{k,n} \end{bmatrix} \tag{3.5}$$

where $\mathbf{g_i} = \{g_{i,1}\ g_{i,2}\ ...\ g_{i,n}\}$, and $i = 1, 2, ..., k$. The linearly independent vectors form a matrix. The rows of this matrix are used to generate the linear block code. That is why the matrix is known as *generator matrix*. By multiplying the message vector $\mathbf{u}$ with matrix $\mathbf{G}$, the codeword $\mathbf{c}$ is obtained

$$\mathbf{c} = \mathbf{u} \circ \mathbf{G} = (u_1\ u_2\ ...\ u_k) \circ \begin{bmatrix} \mathbf{g}_1 \\ \mathbf{g}_2 \\ \vdots \\ \mathbf{g}_k \end{bmatrix} = u_1 \bullet \mathbf{g}_1 \oplus u_2 \bullet \mathbf{g}_2 \oplus ... \oplus u_k \bullet \mathbf{g}_k \tag{3.6}$$

From equation (3.6) we can conclude that the linear block code can be completely constructed from the k rows of the generator matrix $\mathbf{G}$. The encoder has to store only these rows to perform the encoding process on the input message $\mathbf{u}$.
Please note that the symbol '$\circ$' represents the inner product between *vectors or matrices*, whereas the symbol '$\bullet$' represents the multiplication by a scalar in the field

GF(2) of a vector of the vector space [21]. The generator matrix of a systematic code has the form

$$\mathbf{G} = [\mathbf{I}_1 \mid \mathbf{P}] \tag{3.7}$$

where $\mathbf{I_1}$ is the identity matrix with dimension $k \times k$, that represents the message part of $\mathbf{G}$ and $\mathbf{P}$ is a $k \times (n-k)$ matrix, which generates $(n-k)$ *parity or check* bits of $\mathbf{c}$, composed of linear combinations of information bits. Then the *systematic generator matrix* for a systematic codeword illustrated in Figure 3.2 is

$$\mathbf{G} = \begin{bmatrix} 1 & 0 & \dots & 0 & p_{1,k+1} & p_{1,k+2} & \dots & p_{1,n} \\ 0 & 1 & \dots & 0 & p_{2,k+1} & p_{2,k+2} & \dots & p_{2,n} \\ \vdots & \vdots & \vdots & \vdots & \vdots & \vdots & \vdots & \vdots \\ 0 & 0 & \dots & 1 & p_{k,k+1} & p_{k,k+2} & \dots & p_{k,n} \end{bmatrix} \tag{3.8}$$

From the generator matrix $\mathbf{G}$ the parity check matrix $\mathbf{H}$ can be derived as illustrated in [21]. The parity check matrix is formed by $(n-k)$ independent row vectors $\mathbf{h}_j$, $j = 1, 2, ...n-k$ and can be written as

$$\mathbf{H} = [\mathbf{P}^T \mid \mathbf{I}_2\ ] = \begin{bmatrix} \mathbf{h}_1 \\ \mathbf{h}_2 \\ \vdots \\ \mathbf{h}_{n-k} \end{bmatrix} = \begin{bmatrix} h_{1,1} & h_{1,2} & \dots & h_{1,n} \\ h_{2,1} & h_{2,2} & \dots & h_{2,n} \\ \vdots & \vdots & \ddots & \vdots \\ h_{n-k,1} & h_{n-k,2} & \dots & h_{n-k,n} \end{bmatrix} \tag{3.9}$$

where $\mathbf{P}^T$ is the transpose of the $\mathbf{P}$, and $\mathbf{I}_2$ is the identity matrix with the dimensions $n-k$. The parity check matrix is formed by $(n-k)$ linearly independent rows. The matrix $\mathbf{H}$ is generated in a way that inner product of any row vector $\mathbf{g}_i$ of $\mathbf{G}$ and any row vector $\mathbf{h}_j$ of $\mathbf{H}$ is zero, i.e., $\mathbf{g}_i \circ \mathbf{h}_j^T = 0$ [20]. In the matrix form this can be written as

$$\mathbf{G} \circ \mathbf{H}^T = \mathbf{0} \tag{3.10}$$

From above equation it follows that the parity check equations and any decoded codeword is valid only if

$$\mathbf{c} \circ \mathbf{H}^T = \mathbf{0} \tag{3.11}$$

holds.

3.1.3 Decoding of Linear Block Codes

When a codeword is sent over a noisy channel, errors are added to the encoded data and as a result the received bits are different from the sent bits. Consider that the

sent vector is $\mathbf{c} = (c_1\ c_2\ ...\ c_n)$ and the received vector is $\mathbf{y} = (y_1\ y_2\ ...\ y_n)$, where it is also true that $y_i \in \{0, 1\}$. Then in the received vector $\mathbf{y} = \mathbf{c} + \mathbf{e}$, $\mathbf{e}$ is the vector of erroneous bits added to the codeword. The parity check matrix $\mathbf{H}$ can be used to detect these errors based on the condition given in equation (3.11). This fact can be used to calculate the syndrome vector $\mathbf{s}$ to specify the position of the error in the received codeword as follows

$$\begin{aligned} \mathbf{s} &= \mathbf{y} \circ \mathbf{H}^T = (\mathbf{c} + \mathbf{e}) \circ \mathbf{H}^T \\ &= \mathbf{c} \circ \mathbf{H}^T + \mathbf{e} \circ \mathbf{H}^T \\ &= \mathbf{0} + \mathbf{e} \circ \mathbf{H}^T \end{aligned} \tag{3.12}$$

where $\mathbf{s} = (s_1\ s_2\ ...\ s_n)$. With the syndrome vector the position of the error e_i, for $i = 1, 2, ..., n$, can be detected [21].

3.2 Representation of LDPC codes

LDPC codes can be represented in two ways:

1. *Matrix Representation*

2. *Graphical Representation (Tanner Graphs)*

3.2.1 Matrix Representation

LDPC codes are linear block codes and like all other block codes they can also be represented in the matrix form. The matrix $\mathbf{H}$ represents the parity check matrix of these codes that satisfies $\mathbf{c} \circ \mathbf{H^T} = 0$. LDPC codes are characterized by (n, k), where n is the length of the codeword and k is the length of the message bits *or* (n, w_c, w_r), where w_c denotes the number of 1's per column[1] and w_r is the number of 1's per row. LDPC codes have the property that their *column weight* is much smaller than the codeword length n, i.e., $w_c << n$ and their *row weight* is much smaller than $m = n - k$, i.e., $w_r << m$, for a parity check matrix of dimensions $m \times n$. The parity check matrices of this type are very sparse, that is, the density of 1's in the check matrix is much lower than the density of 0's. This property makes sure that the computational complexity of such codes remains low [13]. An example of a parity check matrix with $m = 4$ and $n = 6$ is as follows,

[1] also known as column weight

$$\mathbf{H} = \begin{bmatrix} 1 & 1 & 0 & 1 & 0 & 0 \\ 0 & 1 & 1 & 0 & 1 & 0 \\ 1 & 0 & 0 & 0 & 1 & 1 \\ 0 & 0 & 1 & 1 & 0 & 1 \end{bmatrix} \tag{3.13}$$

3.2.2 Graphical Representation

LDPC codes can be represented in graphical form as Tanner graphs. Tanner was the first one to introduce such graphical representation and he represented the LDPC codes as *bipartite graphs*. A *bipartite graph* is defined by nodes and connected edges, see the example in Figure 3.3. There are two types of nodes in the graph,

- *Variable nodes or V-nodes:* There are n V-nodes given by the length n of the codeword.
- *Check nodes or C-nodes:* Each C-node represents a parity check equation. The number of check nodes is given by the number of rows $(n - k)$ in the parity check matrix.

The variable and check nodes can be connected to each other with edges. There is a connecting edge between a V-node i and C-node j if the entry h_{ji} in the parity check matrix is equal to '1'.

The graphical representation or Tanner graphs are very important for

- Understanding the iterative decoding algorithms.
- Tracing the message passing between V-nodes and C-nodes during iterations of the decoding algorithm.

After this basic introduction, next we will present an example of the graphical representation of the parity check matrix $\mathbf{H}$. This example shall help the understanding of the decoding algorithm we are going to describe in the next section. However, for more details please see [10, 22, 47].

Example: Graphical Representation of LDPC Parity Check Matrix

A simple graphical representation of a Tanner graph for a linear block code (n, w_c, w_r) with $n = 6$, $w_c = 2$, and $w_r = 3$ and the parity check matrix $\mathbf{H}$ in (3.13) is depicted in Figure 3.3.

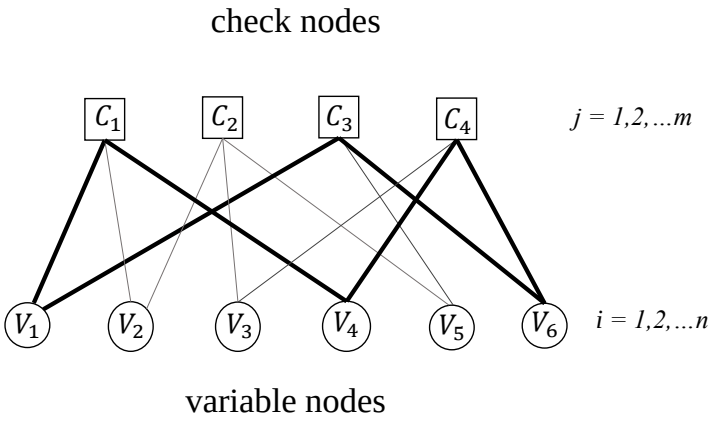

Figure 3.3: Tanner graph with 6 variable and 4 check nodes

In the Figure 3.3 we see that the check node C_1 is connected with variable nodes V_1,V_2, and V_4, since in parity check matrix $\mathbf{H}$ in (3.13), $h_{11} = h_{12} = h_{14} = 1$. From the parity check equation (3.11), it follows by the transposition.

$$\mathbf{H} \circ \mathbf{c}^T = \mathbf{0} \tag{3.14}$$

The parity check equation obtained after replacing $\mathbf{c}$ by $\mathbf{V} = (V_1\ V_2\ ...\ V_6)$

$$\underbrace{\begin{bmatrix} 1 & 1 & 0 & 1 & 0 & 0 \\ 0 & 1 & 1 & 0 & 1 & 0 \\ 1 & 0 & 0 & 0 & 1 & 1 \\ 0 & 0 & 1 & 1 & 0 & 1 \end{bmatrix}}_{\mathbf{H}} \circ \begin{bmatrix} V_1 \\ V_2 \\ \vdots \\ V_6 \end{bmatrix} = \begin{bmatrix} 0 \\ 0 \\ 0 \\ 0 \end{bmatrix} \tag{3.15}$$

The *modulo-2 sum* of the variable nodes connected to the check nodes can be calculated. The sum is 0 when there is an even number of 1's to be added, and it is 1 when odd number of 1's are added to fulfill the parity check equations. Hence, in our example the modulo-2 sum of the V-nodes connected to the check nodes is

calculated as follows

$$\begin{aligned} V_1 \oplus V_2 \oplus V_4 &= 1 \\ V_2 \oplus V_3 \oplus V_5 &= 1 \\ V_1 \oplus V_5 \oplus V_6 &= 1 \\ V_3 \oplus V_4 \oplus V_6 &= 1 \end{aligned} \tag{3.16}$$

The received vector $\mathbf{y} = (y_1\ y_2\ ...\ y_n)$ is a valid codeword only, if it satisfies the condition $\mathbf{H} \circ \mathbf{y}^T = 0$.

Another very important aspect that should be considered while designing the LDPC codes is the avoidance of cycles. A *cycle* in a Tanner graph is known to happen when a sequence of edges starts and ends at the same node. Total number of edges in a cycle is known as the *length of the cycle*. There can be more than one cycles in one graph and the shortest cycle is known as the *girth* of a graph. The existence of cycles reduces the effectiveness of iterative decoding algorithms, because they start and end at the same node. Figure 3.3 shows a cycle of length 6 in bold.

3.2.3 LDPC Codes Construction

As we stated earlier, there is a variety of LDPC codes, which can be constructed in different ways, e.g. [10], [11], [12], [14], [13], [16], [17], [18], [19]. However, on a broader level the LDPC codes can be categorized in two ways.

Regular LDPC Codes

If in a parity check matrix $\mathbf{H}$ the column weight w_c and row weight w_r are constant, i.e., the number of 1's in each row and column is constant, then such a matrix is known as *regular* and the resulting codes are called *regular codes*. The first LDPC codes introduced by Gallager [10] and later by Mackay and Neal [11] are regular. An example of a regular code is shown in (3.13) by $\mathbf{H}$ with $w_c = 2$, $w_r = 3$, and the code rate can be determined as $CR = 1 - (w_c/w_r)$.

Irregular LDPC Codes

If the number of ones are not uniform for each row and column as in case of regular codes, the resultant codes are known as *irregular codes*. The degree distribution of edges connecting from V-nodes to C-nodes is not uniform as well, i.e., in the Tanner graph, the number of edges emerging from one V-node will be different from that in another V-node, unlike regular ones. Irregular codes have been designed by

Richardson [12] and Luby et al. [14] which showed a capacity approaching performance, when the codeword length is considerably long [13]. The irregular LDPC codes can also be described by a degree distribution pair (λ, ρ), that tells us how the edges are distributed between nodes. The polynomial function of V-node degree distribution is

$$\lambda(x) = \sum_{d=1}^{d_v} \lambda_d x^{d-1} \tag{3.17}$$

In equation (3.17), λ_d is the fraction of number of edges connected to V-node of degree d, d_v here represents the maximum number of edges emerging from a V-node. Similarly, the polynomial function for the C-node degree distribution can be written as

$$\rho(x) = \sum_{d=1}^{d_c} \rho_d x^{d-1} \tag{3.18}$$

where ρ_d is the fraction of number of edges connected to the C-node of degree d and d_c here represents the maximum number of edges emerging from a C-node. The code rate $CR(\lambda, \rho)$ for irregular LDPC codes can be defined as

$$CR(\lambda, \rho) = \frac{\int_0^1 \rho(x)dx}{\int_0^1 \lambda(x)dx} \tag{3.19}$$

Different variants for encoding LDPC codes are available in literature and they give very good performance statistics also, specially the randomly generated irregular codes but the problem is that they have a rather high encoding complexity. Anyhow, throughout this thesis we will use the irregular LDPC codes because of their better performance as compared to their competitors like Turbo codes. We will investigate the BER performance of such codes in Chapter 4 and Chapter 5 in certain contexts.

3.3 Decoding of LDPC Codes

There are many decoding algorithms available to decode the LDPC codes: bit-flipping algorithm (BFA), sum-product algorithm (SPA) and message-passing algorithm (MPA) are the few to name, for instance.

Actually, the message-passing is done in all such algorithms and their approximations [13]. The main difference is given by the type of information that is dissemi-

nated between the nodes. Such algorithms perform *local calculations* and pass the results along the edges of the Tanner graph between variable and check nodes. The calculation results are known as *messages*, giving the name *message-passing algorithms* to this genre of algorithms. Several such messages are passed *back and forth* between the nodes before getting the final message, hence, such algorithms are also called "iterative algorithms" because of this property.

Please note that an increase in the codeword length n results in a very large LDPC parity check matrix $\mathbf{H}$. Consequently, the encoder complexity also increases and with very long codeword lengths the encoding process becomes prohibitively complex. Because when we have a very large parity check matrix $\mathbf{H}$, even with a very low density of 1's, after the Gauss-Jordan elimination of $\mathbf{H}$ to get the generator matrix as $\mathbf{G} = [\mathbf{I} \mid \mathbf{P}]$, the submatrix $\mathbf{P}$ will not be very sparse. *A reduced sparsity increases the complexity.* Moreover, with larger matrices more decoding iterations will be needed and consequently, longer delays are involved.

In this thesis, we actually tried to overcome the issue of increased lengths and complexity for encoding and decoding by breaking down such messages into shorter ones using the 'divide and conquer' strategy. The advantage is manyfolds. *Firstly*, it reduces the complexity of the encoding and decoding process and *secondly*, the delays are shorter. *Lastly but largly*, as discussed earlier, relays are resource limited devices. Hence, keeping the block lengths short is beneficial because of quicker processing at the relays with reduced power consumption. Futhermore, in this thesis we will consider two decoding algorithms for LDPC codes, the bit-flipping algorithm and the sum-product algorithm. The former one is a hard-decision decoding algorithm, the latter is a soft-decision decoding algorithm. In the next Subsection 3.3.1, the bit-flipping hard decision decoding algorithm for LDPC codes is discussed in detail. In Subsection 3.3.2 we will describe the details for the sum-product algorithm. Later in the section, we will compare the performance of two algorithms.

3.3.1 Bit-Flipping Algorithm

The bit-flipping algorithm is iterative and keeps passing binary messages (0's and 1's) between the variable and check nodes, until all the parity check equations are satisfied. This is the simplest of all message-passing iterative algorithms, because it works on hard-decision detection of bits. Here is the BF algorithm step-by-step.

Let the sent codeword $\mathbf{c} = (c_1\ c_2\ ...c_n)$ be modulated using binary phase shift keying (BPSK) so that $0 \rightarrow -1$ and $1 \rightarrow 1$, and white Gaussian noise $\mathbf{n}$ is added at

the receiver.

$$\widetilde{\mathbf{y}} = \mathbf{c} + \mathbf{n} \tag{3.20}$$

where $\mathbf{n}$ is the Gaussian distributed random variable with *zero* mean and variance σ^2. After hard decision decoding the corresponding received codeword will be $\mathbf{y} = (y_1\ y_2\ ...\ y_n)$, where $y_i \in \{0, 1\}$.

1- Initialization: (For first iteration only). The contents of the variable nodes V_i are denoted as M_i in each iteration. The initial message bit, M_i, is

$$M_i = y_i$$

The bit M_i $(i = 1, 2, ..., n)$ is assigned to every V-node i and sent to every connected C-node j, believing it to be correct.

2- Check-to-Bit: In the 2nd step every C-node j calculates a response for every bit (variable) node i connected to it to see, if the parity checks are satisfied. This is done on the basis of messages received from other V nodes connected to it, i.e., i' V-nodes, believing the messages to be correct ones, as:

$$E_{j,i} = \sum_{i' \in A_j, i' \neq i} (M_i \mod 2) \tag{3.21}$$

where A_j contains all V-nodes connected to node j. Hence, the resultant message to V-node i is a bit that a check node j considers to be correct, believing that all the other connected V-nodes have sent the correct information. Please note the sent message is labeled as $E_{j,i}$ in the equation (3.21).

3- Codeword Test: If $\mathbf{y} = (y_1\ y_2\ ...\ y_n)$ is a valid codeword ($\mathbf{H} \circ \mathbf{y}^T = \mathbf{0}$) or if the maximum number of *allowed iterations* have been completed, the algorithm terminates.

4- Bit-to-Check: (in all iterations after the first) In this step V-node i decides if its original received bit was correct on the basis of the additional information received from the check nodes j. This decision is made using the majority logic rule. Now check nodes can send another received codeword based on hard decision towards the variable nodes and the process from step 2 keeps repeating.

For a detailed understanding, next, we will apply these steps to an example matrix.

Example 3.2: We will do the example of bit-flipping algorithm using the parity check matrix $\mathbf{H}$ in (3.22).

$$\mathbf{H} = \begin{bmatrix} 0 & 1 & 0 & 1 & 1 & 0 & 0 & 1 \\ 1 & 1 & 1 & 0 & 0 & 1 & 0 & 0 \\ 0 & 0 & 1 & 0 & 0 & 1 & 1 & 1 \\ 1 & 0 & 0 & 1 & 1 & 0 & 1 & 0 \end{bmatrix} \tag{3.22}$$

Graphically **H** can be represented as a graph depicted in Figure 3.4

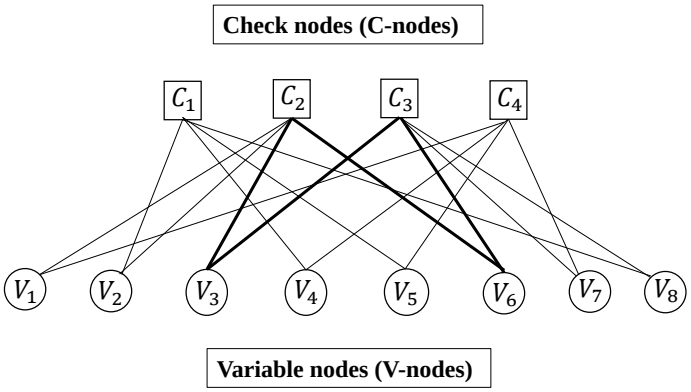

Figure 3.4: Graphical representation of matrix **H** in (3.22)

From the parity check matrix above we can have one of the valid codewords $\mathbf{c} = [1 \quad 0 \quad 0 \quad 1 \quad 0 \quad 1 \quad 0 \quad 1]$. When the bit-flipping algorithm starts, the V-nodes i already have received the codeword $\mathbf{y}$, with one bit in error in the 2nd bit position, i.e., $\mathbf{y} = [1 \quad 1 \quad 0 \quad 1 \quad 0 \quad 1 \quad 0 \quad 1]$ is the received codeword. All the V-nodes send *messages* towards the C-nodes j, correct messages according to their belief. (In our example each V-node is connected to two C-nodes.)

In 2nd step every C-node calculates the response of all the connected V-nodes. From **H**, it is evident that each C-node receives information from the 4 connected V-nodes. When a C-node has received a response from 3 V-nodes, it calculates the response of the 4th V-node on the basis of the information received from three V-nodes, considering them to be correct. For example the first C-node, i.e., C_1 is connected to V-nodes V_2, V_4, V_5, and V_8. The C_1 calculates the response from all 4 variable nodes as under

$$\begin{aligned} E_{1,2} &= M_4 \oplus M_5 \oplus M_8 \\ &= 1 \oplus 0 \oplus 1 \\ &= 0 \end{aligned} \tag{3.23}$$

Similarly,

$$\begin{aligned} E_{1,4} &= M_2 \oplus M_5 \oplus M_8 \\ &= 1 \oplus 0 \oplus 1 \\ &= 0 \end{aligned} \tag{3.24}$$

and

$$\begin{aligned} E_{1,5} &= M_2 \oplus M_4 \oplus M_8 \\ &= 1 \oplus 1 \oplus 1 \\ &= 1 \end{aligned} \tag{3.25}$$

and

$$\begin{aligned} E_{1,8} &= M_2 \oplus M_4 \oplus M_5 \\ &= 1 \oplus 1 \oplus 0 \\ &= 0 \end{aligned} \tag{3.26}$$

The algorithms halts here if all the parity check equations are satisfied. In the Tables 3.1 to 3.4, we will show the received messages of V-nodes. The reader can easily understand how the value of $E_{j,i}$ for all the respective C-nodes is calculated in these tables.

Table 3.1: Calculation of message $E_{1,i}$ at check node C_1

	V_2	V_4	V_5	V_8
rx bits at V-node	1	1	0	1
message $E_{1,i}$	0	0	1	0

Table 3.2: Calculation of message $E_{2,i}$ at check node C_2

	V_1	V_2	V_3	V_6
rx bits at V-node	1	1	0	1
message $E_{2,i}$	0	0	1	0

In the last step, every V-node has two kinds of data, one received from the two C-nodes and one from original received bit y_i it already has. On the basis of majority voting it decides for the bit. If after majority voting the result matches with the

Table 3.3: Calculation of message $E_{3,i}$ at check node C_3

	V_3	V_6	V_7	V_8
rx bits at V-node	0	1	0	1
message $E_{3,i}$	0	1	0	1

Table 3.4: Calculation of message $E_{4,i}$ at check node C_4

	V_1	V_4	V_5	V_7
rx bits at V-node	1	1	0	0
message $E_{4,i}$	1	1	0	0

originally received bit, nothing happens, otherwise the *bit-flip* takes place, Table 3.5.

Table 3.5: Message calculation at V-nodes, based on received messages from C-nodes and prior information

V-node	from C-node1	from C-node2	y_i received	majority voting
V_1	$C_2 \to 0$	$C_4 \to 1$	1	1
V_2	$C_1 \to 0$	$C_2 \to 0$	1	0
V_3	$C_2 \to 1$	$C_3 \to 0$	0	0
V_4	$C_1 \to 0$	$C_4 \to 1$	1	1
V_5	$C_1 \to 1$	$C_4 \to 0$	0	0
V_6	$C_2 \to 0$	$C_3 \to 1$	1	1
V_7	$C_3 \to 0$	$C_4 \to 0$	0	0
V_8	$C_1 \to 0$	$C_3 \to 1$	1	1

The new bit messages from V-node to C-node are $\mathbf{M} = [1 \quad 0 \quad 0 \quad 1 \quad 0 \quad 1 \quad 0 \quad 1]$. The parity checks can be calculated for the test. For the first C-node in our example,

$$\begin{aligned} L_1 &= M_2 \oplus M_4 \oplus M_5 \oplus M_8 \\ &= 0 \oplus 1 \oplus 0 \oplus 1 \\ &= 0 \end{aligned} \tag{3.27}$$

For 2nd C-node

$$\begin{aligned} L_2 &= M_1 \oplus M_2 \oplus M_3 \oplus M_6 \\ &= 1 \oplus 0 \oplus 0 \oplus 1 \\ &= 0 \end{aligned} \tag{3.28}$$

For remaining two C-nodes, parity checks are
$L_3 = 0$
$L_4 = 0$
Hence, there are no unsatisfied parity checks, so the algorithm stops and returns the vector $\mathbf{M} = [1 \quad 0 \quad 0 \quad 1 \quad 0 \quad 1 \quad 0 \quad 1]$, as the decoded codeword.
Please see appendix A.1 for the pseudo-code of the algorithm.

3.3.2 Sum-Product Algorithm

The sum-product algorithm is iterative and very efficient for decoding the LDPC codes. It is based on belief propagation algorithm (BPA), means that the beliefs (probabilities) computed at one node are forwarded to the next node and so on. SPA is very similar to the bit-flipping algorithm, except that BFA accepts only an initial hard decision of received samples as input for the decoder, whereas, in SPA the *'probabilities'* are exchanged between variable and check nodes as initial input for the decoder. These probabilities are known as *'apriori'* probabilities, because they are known to the LDPC decoder already. For the PSK symbols we assume $c_i \in \{-1, 1\}, i = 1, 2, ..., n$, and call them still bits in the following. Thus, the modulator makes a mapping between logical bits and PSK symbols as $0 \rightarrow 1$, $1 \rightarrow -1$.

In the Tanner graph of $\mathbf{H}$, each check node and variable node exchange messages with each other iteratively. The content of every node is updated in each iteration and the decoder computes an *aposteriori probability (APP)*[2] of each codeword bit c_i. The aposteriori probability is given as

$$P_i = P(c_i = 1|y_i) \tag{3.29}$$

where the aposteriori probability is the conditional probability that c_i will be 1, given that sample y_i has been received. APP ratio is known as *likelihood ratio (LR)*, given as under,

$$L(c_i) \triangleq \frac{P(c_i = 1|\mathbf{y})}{P(c_i = -1|\mathbf{y})} \tag{3.30}$$

or *log-likelihood ratios(LLR)*[3]

[2]Iterative decoders require aposteriori probability (APP) as metrics rather than direct observations of the channels [57]
[3]We assume natural log here

$$L(c_i) \triangleq \log_e \left(\frac{P(c_i = 1|\mathbf{y})}{P(c_i = -1|\mathbf{y})} \right) \tag{3.31}$$

i.e., the i^{th} codeword bit is sent to the i^{th} variable node to be 1. All the codeword bits are decoded at *once* in SPA.

Let us assume once again that the sent signal is $\mathbf{c} = (c_1\ c_2\ ...\ c_n)$, the corresponding received vector will be $\mathbf{y} = (y_1\ y_2\ ...\ y_n)$, i.e.,

$$\mathbf{y} = \mathbf{c} + \mathbf{n} \tag{3.32}$$

where $\mathbf{n}$ is AWGN with *zero* mean and variance σ^2. Thus, all $y_i \in \mathbb{R}$. The aposteriori probability for each bit c_i can be computed. For example we will derive the aposteriori LLR in the following by applying the Bayes' rule on equation (3.31)

$$\begin{aligned} L(c_i) &\triangleq \log_e \left(\frac{P(\mathbf{y}|c_i = 1)P(c_i = 1)P(\mathbf{y})}{P(\mathbf{y}|c_i = -1)P(c_i = -1)P(\mathbf{y})} \right) \\ &\triangleq \log_e \left(\frac{P\left(\mathbf{y}|c_i = 1\right)}{P(\mathbf{y}|c_i = -1)} \right) + \log_e \left(\frac{P(c_i = 1)}{P(c_i = -1)} \right) \end{aligned} \tag{3.33}$$

For continuous values of $\mathbf{y}$ the probabilities $P(\mathbf{y}|c_i)$ have to be replaced by probability density functions $p(\mathbf{y}|c_i)$. Making use of conditional Gaussian distribution for received samples y_i

$$p(y_i|c_i) = \frac{1}{\sqrt{2\pi\sigma^2}} \exp^{\frac{-(y_i - c_i)^2}{2\sigma^2}} \tag{3.34}$$

putting (3.34) in equation (3.33), we get for y_i

$$L(c_i) = \underbrace{\frac{2}{\sigma^2} y_i}_{intrinsic} + \underbrace{\log_e \left(\frac{P(c_i = 1)}{P(c_i = -1)} \right)}_{extrinsic} \tag{3.35}$$

In equation (3.35) first part on the right hand side conveys the *intrinsic* or *apriori probability*, P_i^{int}, that is the original probability of the bits independent of the code constraints and it is available right at the start of the algorithm iterations. Whereas, the second part is representing the *extrinsic information* or *likelihood*, P_i^{ext}, is the observation of all the parity checks. In SPA decoding the extrinsic message from C-node j to V-node i, $E_{j,i}$, is the LLR of the probability that bit i causes parity check j to be satisfied. The extrinsic probability P_i^{ext}, obtained in subsequent iterations remains independent of the original apriori probability unless the information is not

returned via *cycle*.

As mentioned earlier, a *cycle* is a path in a Tanner graph that starts and ends at the same V-node. In a bipartite graph, *cycle* length must be even and at least 4, so no cycle is possible if there are less than 4 edges involved. If the Tanner graph is free of cycles, the probabilities remain independent of each other and the *exact* value for APP can be calculated [22].

If we see equation (3.35) it is evident that when bit i is decided as 1, based on the message from a j^{th} C-node, then extrinsic probability, P_i^{ext} is the probability that an odd number of codeword bits in check j are 1 (an odd-parity), i.e.,

$$P_i^{ext} = \frac{1}{2}\left(1 + \Pi_{i' \in B_j, i' \neq i}(1 - 2P_{i'}^{int})\right) \tag{3.36}$$

where B_j represents the set of column locations of the bits in the j^{th} parity check equation of the code. For a binary random variable if P is the probability of -1 and $(1-P)$ is the probability of 1 then L_{c_i} is the likelihood ratio and can also be written as $\log_e\left(\frac{1-P}{P}\right)$, or $(1-P-P) = \frac{e^{L_{c_i}}-1}{e^{L_{c_i}}+1} = tanh\left(\frac{L_{c_i}}{2}\right)$ i.e.,

$$(1 - 2P) = tanh\left(\frac{L_{c_i}}{2}\right) \tag{3.37}$$

Now equation (3.36) can be written into LLR notation as [10]

$$L(P_{i,j}^{ext}) = log_e\left(\frac{1 + \Pi_{i' \in B_j, i' \neq i} \quad tanh(LLR(P_{i'}^{int})/2)}{1 - \Pi_{i' \in B_j, i' \neq i} \quad tanh(LLR(P_{i'}^{int})/2)}\right) \tag{3.38}$$

Next, we describe the formal steps of the sum-product algorithm [22].

1-Initialization (For first iteration only) The initial message, $L_{i,j}$ sent from V-node i to the C-node j is M_i, that is basically the LLR of the received sample y_i given the knowledge of the channel properties. For instance, for an AWGN channel with signal to noise ratio $\frac{E_b}{N_0}$, this will be

$$L_{i,j} = M_i = 4\frac{E_b}{N_0}y_i \tag{3.39}$$

2-Check-to-Bit The extrinsic message from check node j to bit node i is the LLR of the probability that parity-check j is satisfied if bit i is assumed to be a 1:

$$E_{j,i} = log_e\left(\frac{1 + \Pi_{i' \in B_j, i' \neq i} \quad tanh(L_{i',j}/2)}{1 - \Pi_{i' \in B_j, i' \neq i} \quad tanh(L_{i',j}/2)}\right) \tag{3.40}$$

3-Codeword Test The estimated APP of each bit is the sum of the intrinsic and

extrinsic LLRs:

$$L_i = \sum_{j \in A_i} E_{j,i} + M_i \tag{3.41}$$

For each bit hard decision is made

$$y_i = \begin{cases} 1, & L_i \leq 0 \\ 0, & L_i > 0 \end{cases} \tag{3.42}$$

where the reverse mapping $-1 \rightarrow$ "1" and $1 \rightarrow$ "0" is used. Then, if $\mathbf{y} = (y_1\ y_2\ ...\ y_n)$ is a valid codeword ($\mathbf{H} \circ \mathbf{y}^T = \mathbf{0}$), or if the maximum number of allowed iterations have been completed, the algorithm terminates.

4- Bit-to-Check: (in all iterations after the first) For every iteration after the first, the message $L_{i,j}$ sent by each V-node to the C-nodes to which it is connected is similar to (3.41), except that to preserve the independence each V-node i sends a LLR to check node j, which is calculated without using the information from check node j:

$$L_{i,j} = \sum_{j' \in A_i, j' \neq j} E_{i,j'} + M_i \tag{3.43}$$

The above given steps of SPA can be readily applied to an example codeword exactly like the way we did it for the BFA, but the main difference will be that now the messages exchanged between the nodes will be probabilities and not the binary 0's and 1's.

Please see appendix A.2 for the pseudo-code of the algorithm.

3.3.3 Performance Comparison of Bit-Flipping and Sum-Product Algorithms

In this section we will present some results of the decoding algorithms discussed so far. We consider a single hop conventional wireless network with a Nakagami-m fading. Moreover, LDPC code (312,156) and 4-QAM is considered for these results. In Figure 3.5 simulated results for BFA and SPA algorithms clearly demonstrate the well known supremacy of soft decision decoding. *Decoding gain* is defined as the difference between the energy per information bit (E_b/N_0) required by one decoding algorithm as compared to the other. From Figure 3.5 we can see that as compared to SPA, bit-flipping algorithm needs 4dB more power to achieve the BER of 10^{-4} .

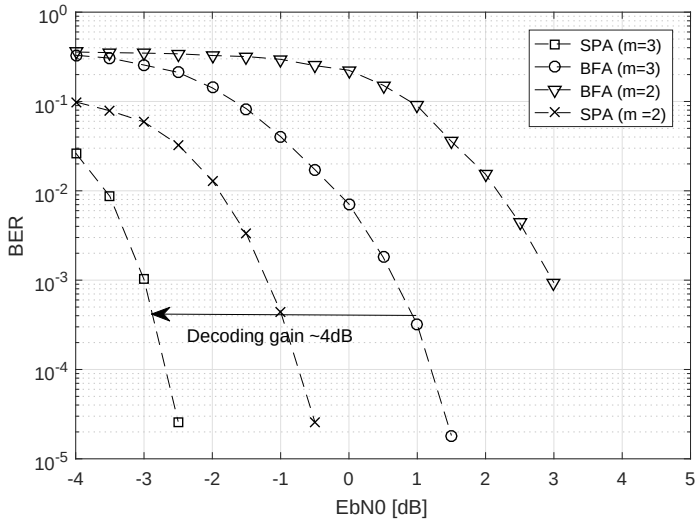

Figure 3.5: Bit-flip and sum-product algorithms performance over Nakagami$-m$ fading channel with 4-QAM, code rate $= 1/2$, $n = 312$

Nonetheless, the good performance gain of SPA has a cost of intricate mathematical operations at the receiver nodes. Hence, for SPA more power and more memory are required. On the other hand, BFA performs binary operations only, which are computationally quite simple. Another detrimental effect of SPA is the additional latency to the overall output as compared to the output of BFA. To our surprise this was not significant because the total run time taken by the two programs[4] was not very different. For our reader we have included some of the run time statistics in Table 3.6, which are quite interesting. When we closely analyze we observe that as expected SPA requires about 3 times more duration for decoding the LDPC codes. The bold entries in Table 3.6 show two aspects. First, albeit the time BFA takes for decoding is almost 2.5 times lesser but overall time taken by the program for both encoding and decoding is not much different. Second, the longest time chunk in encoding and decoding process is taken by the construction of parity check matrix, conforming to the well known fact that it is actually LDPC encoding that takes longer and not the decoding. Consequently, in this thesis we have mostly used SPA for our experimental work because of the following two reasons. Foremost, it gives substantial performance gain against BFA. Further, because if we see total time taken by the whole process of encoding and decoding, the difference is trivial whereas, the results of the SPA decoder are far more accurate.

[4]in MATLAB

Table 3.6: Comparison of time taken by bit-flipping and sum-product algorithm, $n = 312$, 4-QAM, fading parameter=3

	Bit-Flip Algorithm (BFA)	**Sum-Product Algorithm** (SPA)
Total time taken by prog	783.017s	916.533s
time taken by decoding	**94.802**s	**215.175**s
time taken by encoding	646.123s	690.524s
time taken by check matrix	**438.181**s	**469.747**s

3.4 LDPC Codes for Relay-Assisted Communications

The idea of cooperation via relays was first introduced by van der Meulen [59] in 1971, where he discovered the upper and lower bounds on the capacity of the relay channel. Cover and El Gamal [60, 61] improved these bounds significantly in their very inspirational paper later in 1979.

Since the last decade quite some research was done on the design of LDPC codes for relay channels [43, 62–65]. However, main focus of thesis is not the design of new LDPC codes but to take the existing codes and investigate whether they are candidate for half duplex relays. We use LDPC codes for relay-assisted transmission in two ways, which are presented in the next two subsections with brief details.

3.4.1 Non-Rate Adaptive Relays

We consider that S transmits a systematic codeword $\mathbf{u}_1$. The codeword $\mathbf{u}_1$ can be described by a parity check matrix $\mathbf{H}_1$ of dimension $m \times n$. Assuming a perfect decoding at relay R, a new systematic codeword $\mathbf{u}_2$ is generated using a new parity check matrix $\mathbf{H}_2$ with the same dimension. From relay the codeword $\mathbf{u}_2$ is transmitted towards the destination D. The code rate remains the same on both hops and it can be determined as $CR = k/n$. Hence, always the same code rate is used on both hops and there is no code rate adaptation.

3.4.2 Rate Adaptive Relays

In this case, source S transmits a codeword of length n towards a relay station. We call this codeword $\mathbf{u}_1$, which can be described by a parity check matrix $\mathbf{H}_1$ of dimension $m_1 \times n$. The code rate at the source S will be calculated as $CR = k_1/n$, with $k_1 = n - m_1$. Assuming a perfect decoding at the relay R, a new codeword $\mathbf{u}_2$

is generated using a new parity check matrix $\mathbf{H}_2$. $\mathbf{H}_2$ will have different number of check bits m_2. The number of check bits is decided on the basis of the channel state information received from the destination. With better channel conditions higher code rate can be chosen, i.e., a lesser number of check bits. Consequently, the new parity check matrix will be devised with new dimension, which will have same length n but different number of parity check bits m_2. Now at relay, the code rate can be determined as $CR = k_2/n$. Hence, in this case the decoupled code rates are used at source and relay.

3.4.3 Maintaining the Sparsity of the Parity Check Matrices

The key characteristic of LDPC codes is their sparse parity check matrix. While implementing the details of parity check matrix $\mathbf{H}$, system designers need to maintain its sparsity. In this work, we have also tried to keep $\mathbf{H}$ sparse. We consider the irregular parity check matrix $\mathbf{H}$, which generates systematic codewords. A *systematic parity check matrix* generates a codeword in systematic form, i.e., the parity/check bits are attached at the front or end of the source message. The systematic codeword also brings some advantages, e.g. the original message symbols do not get scrambled and only the check bits need to be computed. Moreover, with systematic codewords the encoder and decoder implementations remain simple and easy.

The parity check matrix $\mathbf{H}$ can be decomposed into two parts as under

$$\mathbf{H} = [\mathbf{P}^T \mid \mathbf{I}_2] \tag{3.44}$$

where, as mentioned earlier, $\mathbf{I}_2$ is the identity matrix with dimensions $(n-k)\times(n-k)$ and $\mathbf{P}^T$ has dimension of $(n-k)\times k$. The Gauss-Jordan elimination is applied to reduce the parity check matrix into *reduced-row echelon form (rref)* and subsequently, $\mathbf{H}$ becomes systematic. The *rref* can be achieved by performing elementary operations on the rows or columns. Moreover, for having a systematic codeword the second part of the $\mathbf{H}$, has not only to be the identity matrix but also a non-singular matrix. To ensure the non-singularity of the matrix $\mathbf{I}$ after attaining the systematic parity check matrix, we perform *columns permutations* to rearrange the columns of irregular rref matrix $\mathbf{H}$. The row operations are avoided for a certain reason that by performing row operations again may change the sparsity of the matrix, i.e., may result in dense matrices. If decoding is done with such a parity check matrix $\mathbf{H}$, it will take longer and eventually result in slow decoding. Hence, the parity check matrices we are using in this work are always irregular, row-reduced echelon form

and systematic parity check matrices.

4

Link Adaptation in Decode-and-Forward Relaying Systems

Decode-and-forward (DF) relays have drawn a great deal of research interest, e.g. [44], [51], [70], [71], [72], [73], [74] because of being a practical and effective relaying strategy. It has been shown that the relay transmissions equipped with error control codes can improve the system performance considerably [28, 70, 71].

This chapter outlines the main results of LDPC coded relay assisted communications. In Section 4.1 we will describe the model of general multi-hop system, whereas in Section 4.2, the performance of a dual-hop systems in terms of error probability is discussed in detail by considering the different parameters of the system. In Section 4.3 we describe the link adaptive relaying in dual-hop systems and present the results for the same in Section 4.4.

4.1 General Multi-hop System Fundamentals

We consider in Figure 4.1, a general multi-hop or N-hop wireless system, which includes more than two nodes: a source node S, $N-1$ relay nodes, and a destination D node. Here the relays are assumed to operate in a regenerative decode-and-forward mode, i.e., the relay first performs the decoding and re-encoding of the data and then sends it to the next node. We assume half-duplex relays with time-division based half-duplex[1] scheme. We suppose that a predecessor node only sends data to its successor node, so every node actually sends data to its immediate next

[1]Information can only be sent or received, in one time interval

node and ignores any other signals coming from any other node. Additionally, for the time being we presume that all the nodes between source and destination use the same modulation scheme. Consequently, none of the nodes need any buffers to store the additional bits, since the bits received from the predecessor node are forwarded immediately to the next node. The transmission time between source and destination has been divided into N equal length time slots. This N is always equal to the number of hops of the system under discussion. The destination receives the signal at the N^{th} time slot. Moreover, during a time slot i only the i^{th} hop will be active, where $i = 1, ..., N$.

Figure 4.1: General multi-hop set-up

Mathematically, the channel model can be written as

$$y_i = x_i h_i + n_i, \qquad i = 1, ..., N \tag{4.1}$$

where x_i is the transmitted signal from the i^{th} hop in the time slot i. During time slot i, only the i^{th} hop will be active. The received signal is y_i on $(i+1)^{th}$ node, furthermore h_i are the channel coefficients on different hops. We assume that channel coefficients on different hops are independent of each other and the channel shall be frequency flat. Nakagami-m fading is considered on these links and all the links are subject to independent but not necessarily identical fading. Additive white Gaussian noise is added at the respective receiving nodes, where

$$n_i \sim CN(0, {\sigma_i}^2), \qquad i = 1, ..., N \tag{4.2}$$

hence, the noise is complex Gaussian distributed with *zero* mean and variance ${\sigma_i}^2$. The instantaneous signal to noise ratio (SNR) γ_i on the i^{th} hop can be calculated by considering the transmit power P_i as,

$$\gamma_i = \frac{P_i}{{\sigma_i}^2} |h_i|^2, \qquad i = 1, ..., N \tag{4.3}$$

Moreover, we suppose that all the nodes have perfect channel state information (CSI) of the links on which they receive data, thus facilitating perfect coherent detection. Generally, in this thesis, we will consider only the path with multiple hops (dual hops) for data transmission, i.e., the path via relays. Although there can be exceptions where we will have to consider the direct path between the source and the destination also but that we will always mention explicitly. Whenever used, the direct channel between a source and destination will be characterized by a channel coefficient h_{sd}, where subscript sd denotes the direct path from source to destination.

4.1.1 Average SNR for a Two-hops system

If we consider a two-hops system with only one relay between S and D as depicted in Figure 4.2, then the average SNR on both hops can be calculated by assuming a simple pathloss model. Any position of the relay station can be translated directly into the corresponding average SNR $\bar{\gamma}$ on all the involved links.

Assuming that the average SNR between source and destination is given by $\bar{\gamma}$ and all nodes have same noise figure as well as the same transmit power P. The average SNR $\bar{\gamma}_1$ at relay and average SNR $\bar{\gamma}_2$ at destination can be computed as

$$\begin{aligned} \bar{\gamma}_1 &= \frac{\bar{\gamma}}{(d_1)^{\nu}} \\ \bar{\gamma}_2 &= \frac{\bar{\gamma}}{(d_2)^{\nu}} \end{aligned} \tag{4.4}$$

where d_1 and d_2 denote the distances, source to relay and relay to destination, respectively. Furthermore, ν is the corresponding pathloss exponent[2].
Please see Appendix B.1 for details.

4.2 Performance Analysis of LDPC Coded Systems

Generally, it is very difficult if not completely infeasible to calculate the bit-error-rate analytically for LDPC coded systems. Due to the iterative evolution of the probability density functions of LDPC decoders, the performance analysis is mostly restricted to the extensive simulations or density evolution. We mentioned in Chapter 3 that for sum-product algorithm the messages passed from V-nodes to C-nodes are the summation of LLR's, actually. The incoming LLR's from the C-nodes to the V-nodes are equivalent to the convolution of their pdf's except the V-node that gets the message. Because of iterative message passing it becomes very difficult to

[2] ν varies for outdoor and indoor environments and its typical value is between 2 and 6

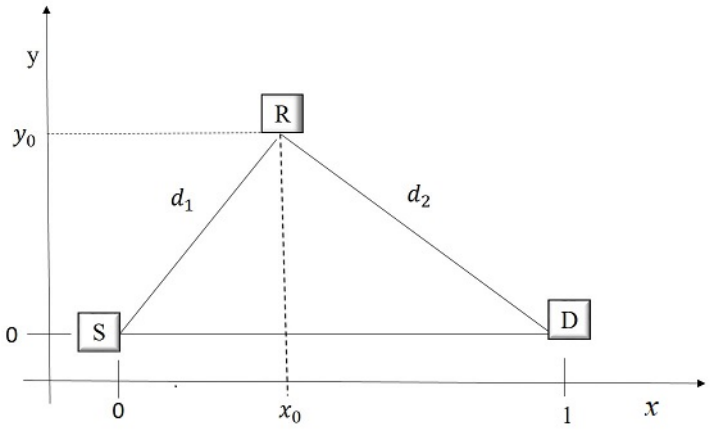

Figure 4.2: Relay location in a 2-D Cartesian coordinate system

update the pdf's for every node in each iteration. Subsequently, the calculation of analytical BER of LDPC codes becomes prohibitively difficult. For the same reason different approximations can be used to analyze the LDPC coded systems, namely Gaussian approximation (GA) [68], density evolution (DE) [69], and EXIT charts [66, 67].

A wireless channel endures many impairments, for example the thermal noise modeled as AWGN, pathloss and reduction in signal power because of distance traveled by the signal, shadowing and multipath fading caused by the propagation environment. When a signal is transmitted from its source, different copies of the signal take independent paths, which undergo attenuation, distortion, delays and phase shifts. All this results in degraded system performance [26]. It can be seen in Figure 4.3 that fading affects a binary phase shift keying modulated wireless system adversely and we need about $\sim$ 20dB additional SNR to get the same BER of 10^{-3} with the same modulation scheme and transmit power P.

Relays can be of great help for mitigating the effects of fading. In this section we will present a thorough numerical analysis of different parameters of the system and show how a change of these parameters effects the system error rate performance. We will perform a numerical analysis, supported by rigorous Monte Carlo simulations. The decode-and-forward relays have better performance than their serious contenders, like AF relays because in those systems the amplified noise travels to the destination along with the actual signal and increases the bit-error at D. For DF relays with successful decoding and re-encoding, noise amplification at relays can be avoided. Nonetheless, if the channel quality of $S - R$ link in a two-hops system is bad so that decoding errors may occur, which propagate to the destination then

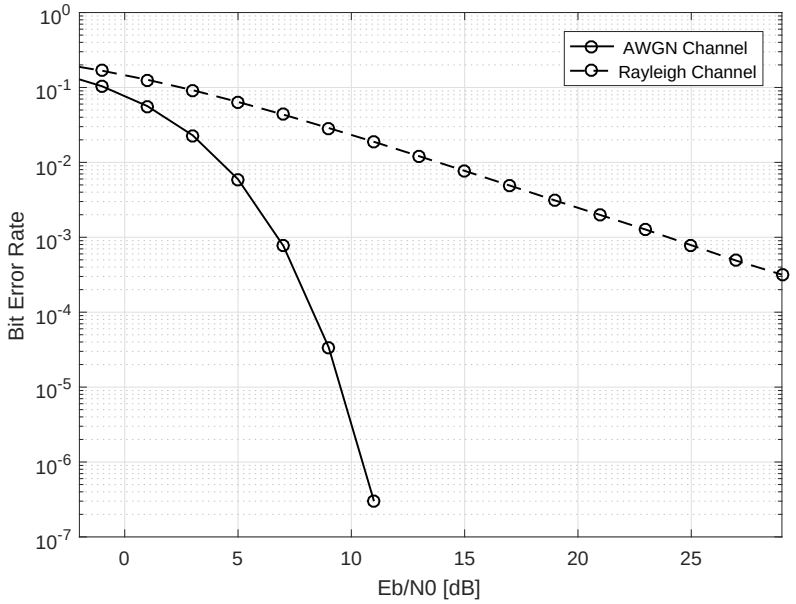

Figure 4.3: Comparison of uncoded system for AWGN and Rayleigh fading channels, modulation = BPSK, Bits = 10^7

there will be a serious performance degradation even worse than for AF relays. In the upcoming paragraphs, we will outline our analysis of the system with good and poor $S - R$ links.

4.2.1 General Considerations for a Dual-hop System

We consider a two-hops wireless communication system, where the sourse S communicates to the destination D via a relay R. We assume that the channels $S - R$ and $R - D$ are independent and not necessarily identically distributed. Nakagmi-m fading is assumed on both hops. For numerical analysis we have considered 4-QAM, LDPC code with length $n = 312$ and a code rate $CR = 1/2$.

In a dual-hop system, an end-to-end transmission is considered error-free, if transmission on both $S - R$ and $R - D$ links is error-free. However, there are chances that the errors introduced by the $S - R$ link might reverse on $R - D$ link and eventually an error-free end-to-end transmission be still possible. So actually, the end-to-end performance is always not the average sum of errors on both (all the involved) hops which initially seems a feasible idea, but an erroneous decision at the destination can correct the false decision made at relay. Of course this is not always true and an erroneous decision at the relay might not be compensated at the destination, i.e., we will still have an erroneous transmissions.

In Figure 4.4, we see that if the direct link $S - D$ and the $S - R$ link have an

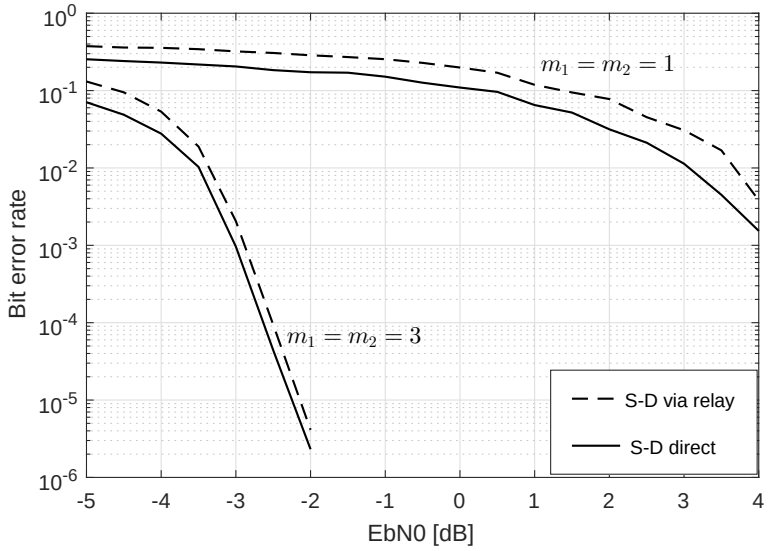

Figure 4.4: End-to-end BER performance of LDPC coded dual-hop link with same average SNR on both hops, relay position: $x_0 = 0.5$, $y_0 = 0$, CR 1/2, LDPC codeword length $n = 312$, Nakagami-m fading

equal SNR then a slightly better BER performance can be observed at D from the direct link as compared to the link via relay. The reason is that if not carefully placed there must be some un-corrected errors at the relay which propagate to the destination. Consequently, the performance of the cooperative link will be worse than the direct link. Moreover, this is evident here that after some performance gain on the direct link, with increasing average SNR at relay, the performance of both the systems become almost the same. This is due to the fact that if the channel conditions on $S - R$ link are becoming better then a very few or zero errors propagate to the destination and practically both the systems become alike. However, this thesis focuses on methods, how a cooperative link can give an improved error-rate performance. We will demonstrate how the optimal position of the relay in 2-D Cartesian coordinate system affects the BER performance of the system. In the upcoming discussion, we will also explore that the performance gain of the cooperative link can be maximized as compared to a direct link.

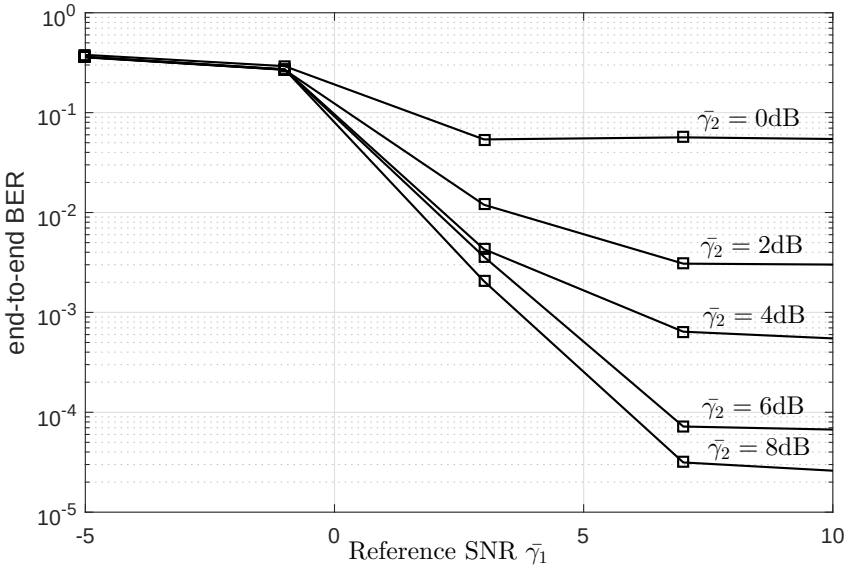

Figure 4.5: BER performance of LDPC (312,156) encoded dual-hop link, Nakagami-m fading, $CR = 1/2$, $x_0 = 0.5$, $y_0 = 0$, $m_1 = m_2 = 3$ with variable SNR $\bar{\gamma}_1$ on first hop and fixed SNR $\bar{\gamma}_2$ on second hop

In Figure 4.5, we change the average SNR $\bar{\gamma}_1$ on 1st hop, i.e., from $S - R$ link and keep the average SNR $\bar{\gamma}_2$ on 2nd hop fixed. As we can see, for an increasing $\bar{\gamma}_1$ the error-rate drops quickly till a certain point. This certain point is known as *transition point*. After this point although the average SNR on first hop is still increasing the end-to-end BER performance does not improve anymore. We can observe two types of regions here in Figure 4.5. The first region is known as the *waterfall region*, whereas the second region is the *errors floor region*. In the start of the transmission as the channel quality on first hop is poor and as it improves with increasing SNR, the system performance also improves. But as the $\bar{\gamma}_2$ is fixed so the number of errors that are going to appear at the destination are completely determined by $\bar{\gamma}_2$. Furthermore, $\bar{\gamma}_2$ also determines the transition point after which errors floor occur. Actually, as the SNR gets better and better on the first hop there will be a negligible number of un-corrected errors at the relay, but at the same time after this point the performance becomes $R - D$ link dependent. There are two reasons for the compromised performance after the transition point, foremost, that after quick decrease of error rate in water fall region the performance becomes dependent on $\bar{\gamma}_2$. Secondly, as LDPC codes use iterative decoders, these decoders are optimal for longer length codes but for shorter length codes they become sub-optimal because of the cycles in the Tanner graphs of LDPC codes. These cycles hold the LDPC codes from behaving optimally and as a result the errors floor occur.

Next, we study the effect of fading severity on dual-hop wireless communication system by keeping the fading parameter of one hop constant and varying it on other. In Figure 4.6(a), we keep $m_1 = 3$ and change the m_2 between 1 and 6. We see in Figure 4.6(a) that when we have less severe fading on first hop, i.e., $m_1 = 3$, the performance of the system gets better and better with increasing m_2. However, we can observe poor BER for first two curves in Figure 4.6(a), i.e., for $m_2 = 1, 2$. Reason being that the link from $R-D$ has sever fading and good channel conditions on 1st hop do not help in achieving good BER performance results. The results of Figure 4.6(a) completely comply to the results we achieved in Figure 4.5. In Figure 4.6(b), we set $m_2 = 3$ and vary m_1 between 1 and 6. As we know, when $m_1 = 1$, we have Rayleigh fading on the first hop, hence, there must be uncorrected errors at the relay which propagate to the destination. Consequently, the BER is very high. As the fading gets less severe on the first hop, which can be achieved by increasing the value of fading parameter m_1 on first hop, we see a performance improvement. Furthermore, please note that the performance improvement is maximum when the channels on both hops are in good conditions, this fact can be observed in Figure 4.6(a) and 4.6(b) from 3rd to 5^{th} curves (top to bottom). Additionally, for $m_2 > m_1$ or $m_1 > m_2$, i.e., when the channel conditions on one hop get worse than on the other hop then that hop becomes the bottle-neck of the system. Evidently, this can be said that the channel with sever fading or lower values of m becomes the bottle-neck of the system. Moreover, in dual-hop (multi-hop) system, good channel conditions on one channel does not guarantee the overall good system performance.

Furthermore, if observed carefully, there is a considerable performance difference in the 2nd curve of Figure 4.6(a) and 4.6(b). The reason is that for $m_1 = 2$ and fixed $m_2 = 3$, there will be decoding errors that propagate to the destination and despite having the better channel conditions on 2nd hop, the performance is poor as compared to the case when $m_2 = 2$ and fixed $m_1 = 3$.

Now, we will present the results for effect of using different code rates in dual-hop systems. Nevertheless, we assume same code rates on both hops and there is no code rate adaptation on any of the two hops. It is very much evident from Figure 4.7(a) and Figure 4.7(b) that we will have a better BER performance with decrease in code rate CR. If we compare the two figures, this is also obvious that having equal code rates on dual hops has a substantial performance edge. Likewise, it can also be observed that when the channels on both hops are independent but identically distributed (i.i.d) fading channels, i.e., the value of fading parameters $m_1 = m_2 = 3$ as in Figure 4.7(a), we have better BER performance for the same code rate. In

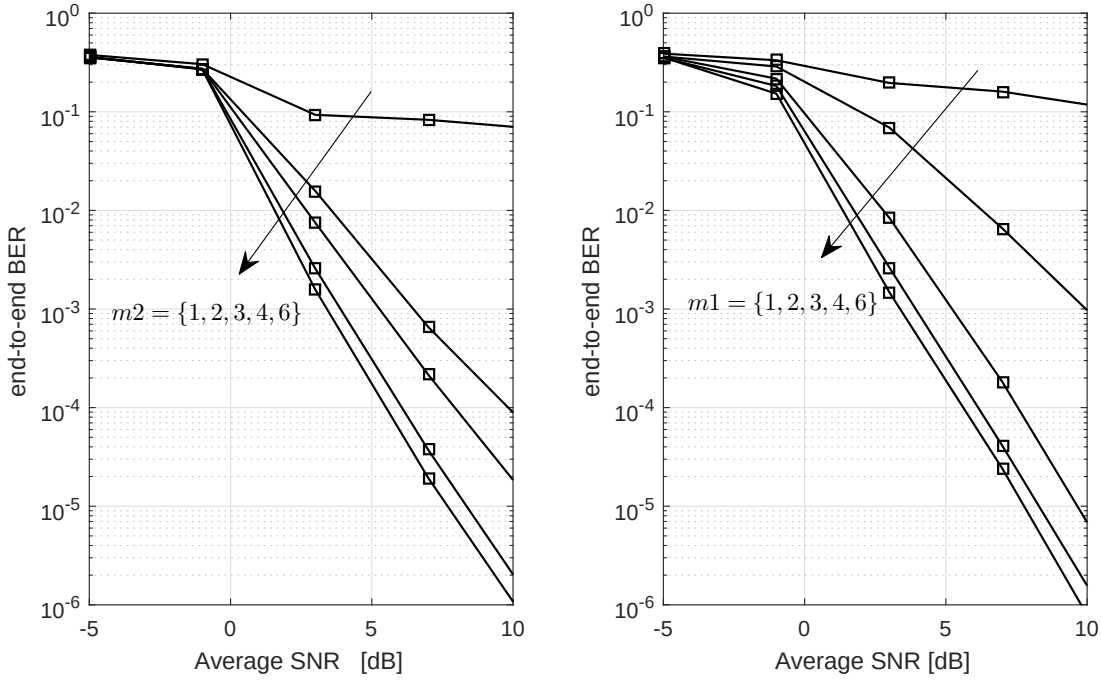

(a) Fading parameter on first hop $m_1 = 3$ **(b)** Fading parameter on second hop $m_2 = 3$

Figure 4.6: BER performance of dual-hop system when fading parameter m on one hop is changed and kept constant on the other hop, 4-QAM, $x_0 = 0.5$, $y_0 = 0$, LDPC (312, 156), $CR = 1/2$

Figure 4.7(b), we have non-identical but independent distribution (n.i.i.d) of fading and it is obvious from the simulation results that when the fading is non-identical on two-hops, BER performances will be worse than the i.i.d fading channels. This happens because the channel with intense fading becomes the holdup of the system. Consequently, the end-to-end error rate becomes higher.

Effect of relay positioning is shown in Figure 4.8. Here we wanted to see under what conditions relays are more advantageous compared to the direct transmission between sender and receiver. We have employed simple model of the Section 4.1.1 to see the impact of relay positioning on an end-to-end BER performance. We consider the simple exponential pathloss model by putting the relay on direct line between source and destination, by keeping the $y_0 = 0$, i.e., there is no change in the position of relay on y-axis. We only change the position of relay on x-axis. From the results we can see that if the relay is placed between $0.3 < x_0 < 0.7$, it gives the best performance for $m_1 = m_2 = 3$. For $m_1 = m_2 = 1$, the best placement of relay is in the range of $0.4 < x_0 < 0.6$. This is clear that best results are obtained when the relay is placed right inbetween the S and D, i.e., at $x_0 = 0.5$. Nevertheless, in

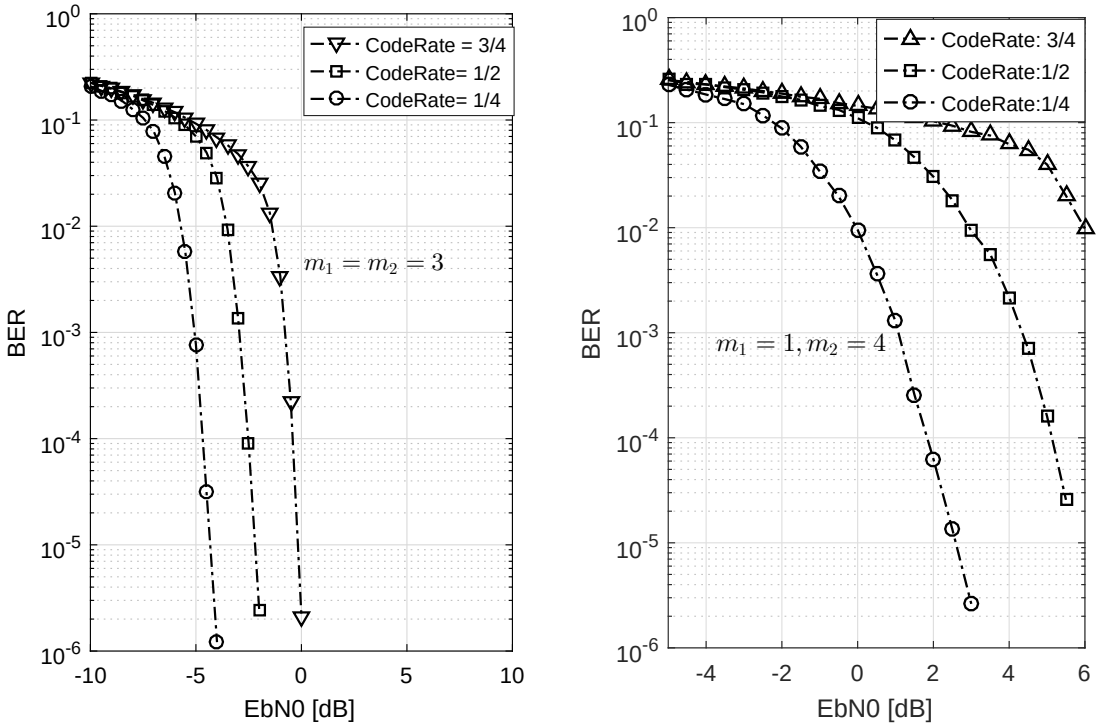

(a) i.i.d channels in dual-hop

(b) n.i.i.d channels in dual-hop

Figure 4.7: End-to-end BER performance comparison of relayed communications with 3 different code rates: identical and non-identical fading channels on two-hops, LDPC (312,156), $x_0 = 0.5$, $y_0 = 0$, 4-QAM

the next chapter we will discuss relay placement from a different perspective and prove that placing a relay closer to S is more beneficial. Figure 4.8 is also a proof that with changing intensity of fading, distance range for right placement of relay also changes. When relay is placed on $x_0 = 1$ or $x_0 = 0$ then the two-hops system practically becomes a single hop system and functions under the performance bounds of single hop systems.

4.3 Link-Adaptation in Relayed Systems

The cooperative transmission (CT), where relay forwards the data of the source, has been proven to bring beneficial impact on the performance of wireless systems [42]. As we mentioned in Chapter 2, multi-hop wireless systems have the ability to combat detrimental effects of wireless channel by dividing the transmission path between the source and the destination into multiple shorter paths that increases the average SNR on each hop and hence, elevates the overall network coverage. Despite all the advantages of multi-hop networks, the end-to-end *success probability* is the product

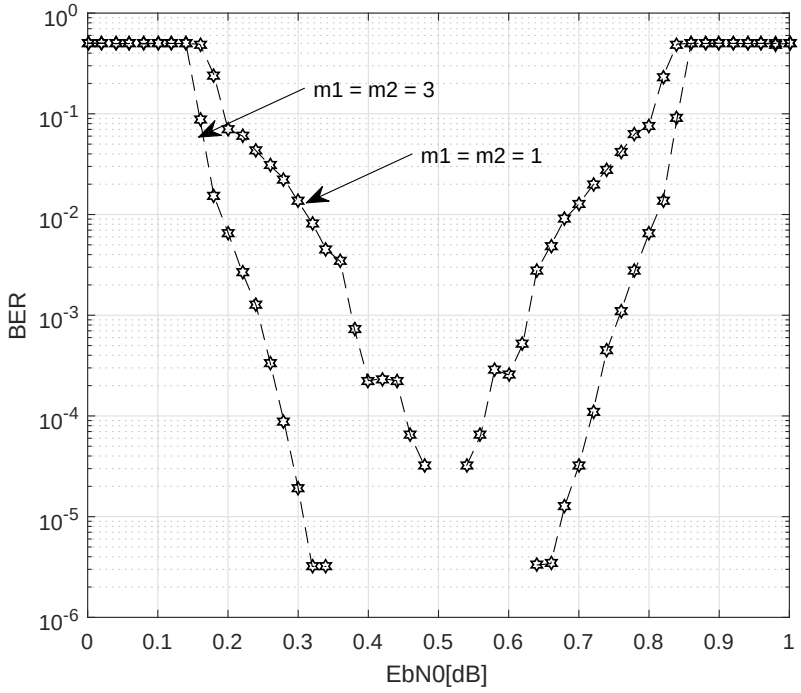

Figure 4.8: Changing relay position x_0 between 0.1 to 0.9 (Figure 4.2) for $y_0 = 0$, codeword length $n = 312$, 4-QAM

of all the success probabilities of the intermediate hops. Therefore, in addition to performance improvement using the SNR advantage of CT, multiple hops that employ forward error correction (FEC) codes help to achieve a BER performance by exploiting the inherent properties of FEC. This can be done, e.g. by changing the code rate on different hops according to the quickly changing conditions of the wireless channel which otherwise would be hard to maintain while having fixed data rates [46].

In many previous works, researchers have been using link adaptation techniques, or more specifically, adaptive coding and modulation (ACM) in cooperative networks. Andreas Müller et. al in [44] and [51], discuss the decode-and-forward (DF) multi-hop systems without considering any particular encoding scheme at source and/or relay. The authors perform the hard decision decoding at both relay and destination nodes and adapt to different modulation schemes according to the changing channel conditions. The authors in [52] have adapted to modulation schemes but without employing the FEC codes. Yet, some people have carried out research on using different types of codes, rather than changing the code rates of the same type of codes, they switch between different types of codes, for instance, in [54], researchers use two different codes, namely, LDPC and Reed Solomon (RS) codes,

with same code rate. In [56], LDPC codes have been proposed with different puncturing and extension techniques, but these codes were used for single hop systems. Moreover, these schemes come with a price for calculation of bits positions for punctured bits and sending this information to the receivers for successful decoding. In this section, we focus on link adaptation strategy of compatible code rates, where a single relay helps the source to deliver its information to the destination. Specifically, if the channel conditions on a link are becoming better, higher code rates can be used, with poor channel conditions lower code rates are employed.

The results are compiled using extensive Monte Carlo simulations and the results verify that an adaptive code rate system is more efficient than a fixed-rate one. Some of the results are the manifestation of the obvious fact that performance of the relaying system gets better with better channel conditions. This can be demonstrated using a higher value of m, where m is the fading parameter in Nakagami-m model of fading. But this effect becomes invisible as m gets higher and higher and after a certain value the performance increase is almost negligible.

We consider a two-hops wireless system which includes three nodes: a source node S, a relay node R and a destination node D. There is no direct link between S and D and the source node communicates with the destination only via a relay, where the relay is assumed to operate in a regenerative DF mode. We suppose that the relay not only decodes the source information but also regenerates the encoded sequence to send it further, hence, the name *"regenerative relaying"*.

We assume, as mentioned before, a time-division based half-duplex relaying over Nakagami-m channels. Each transmission is assigned a time slot (TS). Ideally if S and R transmit with the same code rate, then in the first time slot, TS-1, the source S sends the data to the relay. In second time slot, TS-2, S remains silent and R transmits the decoded and re-encoded sequence to the destination D. We assume that the source and the relay transmit with the same transmit power, P, such that the received signals at the relay and the destination are given as

$$y_r = \sqrt{P} x_s h_{sr} + n_r, \tag{4.5}$$

$$y_d = \sqrt{P} x_r h_{rd} + n_d, \tag{4.6}$$

In the above equations, x_s and x_r are the transmit symbols from source and relay, whereas the channel coefficients between source to relay $(S - R)$ and relay to destination $(R - D)$ links are given as h_{sr} and h_{rd}, respectively. In (4.5) and (4.6), n_r and n_d are the additive white Gaussian noises with *zero* mean and variance σ^2,

added at R and D, respectively.

Further, it has been assumed that all the nodes are equipped with single antenna elements and the wireless channel on both links undergoes a frequency flat fading. The channel coefficients h_{sr} and h_{rd} are independent and identically/non-identically distributed and follow the Nakagami fading, each with a probability density function described as

$$f(x) = \frac{2}{\Gamma(m)}\left(\frac{m}{\Omega}\right)^{m} x^{2m-1} exp\left(-\frac{m}{\Omega}x^{2}\right), m \geq 0.5 \tag{4.7}$$

In (4.7), Ω is the mean power of the random variable, i.e., channel here. All the nodes are supposed to have perfect channel state information of links on which they receive data, thus facilitating the perfect coherent detection. Once again LDPC codes are used at the source to encode the information sequence and the log-domain sum product algorithm is used to decode the LDPC coded sequence at the intermediate relay node and finally at the destination. We used the log domain version of SPA, because log domain calculations change the multiplications into additions, a suitable solution for relays being the power-limited devices.

4.3.1 Rate-Adaptive LDPC Encoding

For encoding with LDPC codes, we generate an (n, k) irregular LDPC code by keeping the code rate (CR) variable, where code rate can be defined as k/n, i.e, for every k bits of useful information, LDPC encoder generates a total of n bits, of which $(n-k)$ are redundant. In the Table 4.1 we have listed example LDPC code with different CR. The redundant bits are used to detect and correct the errors at the receiver node.

At the source, we generate a sparse parity check matrix, $\mathbf{H_1}$ with $(n-k)$ rows and n columns. For $\mathbf{H}_1$, a corresponding generator matrix $\mathbf{G}_1$ is generated to encode the given sequence as $\mathbf{x}_s = \mathbf{u} \circ \mathbf{G}_1$[3], where $\mathbf{u}$ is the input sequence then $\mathbf{x}_s$ is the encoded sequence. After encoding, $\mathbf{x}_s$ is modulated using M-ary quadrature amplitude modulation, i.e., M-QAM with $M = 4, 16$ and is transmitted by the source in TS-1. At the relay station, the received sequence $\mathbf{y}_r$ is decoded using log domain SPA. The decoded sequence $\mathbf{u}'$ at the relay is encoded again as $\mathbf{x}_r = \mathbf{u}' \circ \mathbf{G}_2$. $\mathbf{G}_2$ is the generator matrix at relay, corresponding to $\mathbf{H}_2$. After M-QAM modulation $\mathbf{x}_r$ is transmitted by the relay in TS-2. The destination D decodes the received sequence $\mathbf{y}_d$ using the log-domain SPA again. Both $\mathbf{H}_1$ and $\mathbf{H}_2$ are irregular parity

[3] $\circ$ represents the inner product between vectors or matrices in GF(2).

check matrices. $\mathbf{H}_1$ and $\mathbf{H}_2$ can be different or same. The parity check matrices are reduced-row echelon form (rref) to maintain the sparsity. We are using a soft decision decoder here, because as we know from the Section 3.3.3, although, bit-flipping algorithm (BFA) itself is quite quick but the total time taken by BFA and SPA both for encoding and decoding has only a slight difference. Further, using log-domain SPA results in better BER performance with an acceptable delay as compared to BFA.

As variable rate LDPC codes are considered here, if S sends an information at a certain code rate CR, then R receives the sequence and decodes it using the same parity check matrix, $\mathbf{H_1}$. Before we proceed further, what happens at the relay, we ought to make some assumptions, which are as follows:

1. Our system works under a constraint of target BER δ_0.

2. Ideally, CSI is already known to the receiver nodes, i.e., relay and destination. Based on this CSI, a *code rate index*, r_{index}, is fed back to the transmitting node on a control channel. Only a few bits are required on the feedback channels[4].

3. We divide the transmission of data into three different scenarios on the basis of CSI feedback, as under:

   (a) **Case 1:** When channel conditions are same on both hops, the same code rate CR is used. No temporal data storage will be done at relays.

   (b) **Case 2:** If the channel conditions are becoming worse on $R-D$ link than $S-R$ link, more redundant bits will be needed to maintain the target δ_0, at the destination. Hence, CR will be lowered and $\mathbf{H}_2$ will be updated according to new dimensions. In this case remaining bits will be stored in the relay buffer. The buffered bits will be sent in the next time slots depending on the CSI feedback.

   (c) **Case 3:** If the channel conditions are getting better on $R-D$ link than $S-R$ link, CR can be increased, i.e., more information bits can be sent with lesser redundant bits. In this case, bits from previous transmissions, stored in the buffer can be grouped together with the bits received from the S, in the current TS. They will be encoded with a modified generator matrix, say $\mathbf{G}_2$. The modified generator matrix will calculate the information and check bits according to the new code rate. They are sent to

[4]Relays are two way devices. Forward and feedback channels work in half duplex mode though.

the destination. Destination decodes the longer sequence with modified parity check matrix $\mathbf{H_2}$.

Note: For the Case 3, relay can not only send its current information but also the buffered bits from the previous transmissions, according to the channel conditions. Besides, Case 3 can compensate for the time delay resulted from a situation discussed in Case 2. Because in Case 2, according to our assumption, the information sequence at relay is divided into smaller chunks and sent in multiple time slots. So, on average we need the same amount of time as if the data rate was the same for the source and relay node.

4. The buffer at the relay is of infinite length, therefore, no overflow occurs ever.

5. Our system can support 5 data rates initially and adapts to any code rate (Table 4.1), depending on the channel conditions.

Table 4.1: Different code rates CR for LDPC codes, codeword length n = 312

Code Rate CR	**Information Bits** k	**Check Bits** $(n-k)$	**Code Rate Index** r_{index}
1/4	78	234	0
1/2	156	156	1
3/4	234	78	2
5/6	260	52	3
7/8	273	39	4

The received signals $\mathbf{y}_r$ and $\mathbf{y}_d$ in (4.5) and (4.6) represent the valid codewords after hard decision, only if they satisfy the following parity check equation

$$\mathbf{H} \circ \mathbf{y}_a^T = \mathbf{0}, \quad a \in \{r, d\} \tag{4.8}$$

i.e., $\mathbf{H} \circ \mathbf{y}_a^T$ is a zero vector of dimensions $n \times 1$.

The decoder is provided with the *parity check* matrix, along with the *a priori probabilities* of the transmitted bits, which have to be known before running the LDPC decoder [22]. Here, we will request the reader to please refer to Chapter 3, Section 3.3.2 for details on the decoding process using SPA. In Section 3.3.2 we described in detail how the estimate of each codeword bit c_i is made. Moreover, we know that decoding terminates if $\mathbf{y_a}$ turns into a valid codeword, or if the maximum number of iterations has reached.

4.4 Numerical Analysis of Link-Adaptation in Relay-assisted Communications

When the same code rate is used on both hops, then there are no bits to buffer at the relays. However, the major drawback is that the performance of the system is dominated by the poor quality hop. The overall system performance will be degraded and spectral efficiency will be lowered, no matter how good are the conditions on the other hop. Such a hop becomes the bottle neck of the system and ultimately, both the nodes have to transmit with the most robust code rate [44].

In our proposed scheme, by keeping the modulation order fixed on both hops, we use decoupled code rate adaptation on these hops, which ensures that the system can maintain an end-to-end target BER, δ_0, along with a desired spectral efficiency. On the other hand, the temporal storage of data in a buffer and using more than one time slots for the transmission of data from relay to destination might add further delay in overall time required for the transmission of data from source to the destination [44]. Nonetheless, to the best of our knowledge the CR adaptation has not been done in this manner. It is not a simple task to implement such code rate adaptive system at relays, since relays are smaller devices with limited memory and power. As we described before in Chapter 3, Section 3.3 that we kept lengths of codeword blocks short, so that with smaller parity check matrices a quick encoding is done at relays with least power consumption.

We have provided the *code rate selection* algorithm in appendix A.3. During the very first transmission, source transmits with the most robust code rate. Every CR has a corresponding r_{index}, where $index \in \{0, 1, ..., 4\}$ and r_0 is the lowest (robust) index corresponding to $CR = 1/4$ and r_4 represents the $CR = 7/8$. Relay receives, decodes and forwards the data again with r_0. The advantage of using r_{index} is that on feed back channels just a few bits for the *code rate index* are fed back as CSI to the respective source nodes. This first transmission takes 2 time slots.

In the subsequent transmissions, if the instantaneous BER δ_{inst} is smaller than δ_0, then r_{index} is lowered, only if it is already more than the most robust rate. If it is already the lowest code rate then the data is encoded with the same code rate. After receiving the r_{index} from relay node, source node encodes with the corresponding CR, to maintain the target BER δ_0. Exactly, in the similar manner, when relay receives r_{index}, it looks for the corresponding code rate and encodes the message with the new CR. At the end of the transmission, destination and relay again send the feedbacks to their respective source nodes. This sequence keeps repeating until

source/relay still have no data to transmit. When all the data has been transmitted from source to destination, BER is calculated from end-to-end and checked against overall average BER δ_0.

For Monte Carlo simulations, we have used LDPC codes with different code lengths. For every block length n, 10,000 frames have been delivered to the destination with 20 decoding iteration. Five different code rates have been used with M-QAM, $M \in \{4, 16\}$ and a fading parameter $m \in \{1, 3\}$ has been selected to collect the results. Figure 4.9 shows the results with 4-QAM when there is no buffering of data at the relays and same code rate was used on both links. For two different values of m, the BER curves show that the performance degrades as the code rate increases. On the other hand, it becomes inevitable to have a lower BER performance for $m_1 = m_2 = 1$, i.e., Rayleigh fading, when the code rates are higher. For code rates of 3/4, 5/6 and 7/8, there is negligible difference in the BER performance for $m_1 = m_2 = 1$. Better performance is achieved as the m changes from 1 to 3 for both hops. In Figure 4.10, the same trends can be observed with 16-QAM. However, the BER performance deteriorates as a consequence of using higher order modulation.

Figure 4.11 shows the number of effective bits received via relays in one frame, the *effective bits* can be defined as the *number of information bits*, which actually get transmitted from S to D. We demonstrate the results for one end-to-end transmission when a fixed code rate of 3/4 is maintained on the first hop and variable rate is chosen on the second. For instance, for the lowest rate of 1/4 on second hop, we need 4 time slots and 3 times more redundant bits than effective bits have to be transmitted on second hop. For the transmission from relay, if the code rate is 1/4, then only k bits are transmitted and remaining bits are stored at relay buffer. This effect not only adds to the latency in transmission but also increases the complexity of processing. We can see as the code rate increases less redundant bits are sent, resulting in reduced latency, with no buffering of data at the intermediate node. Therefore, it always will be a trade-off between a highly reliable system with very low BER at a low SNR, where latency is no issue *or* a system with an acceptable BER performance where late response is intolerable.

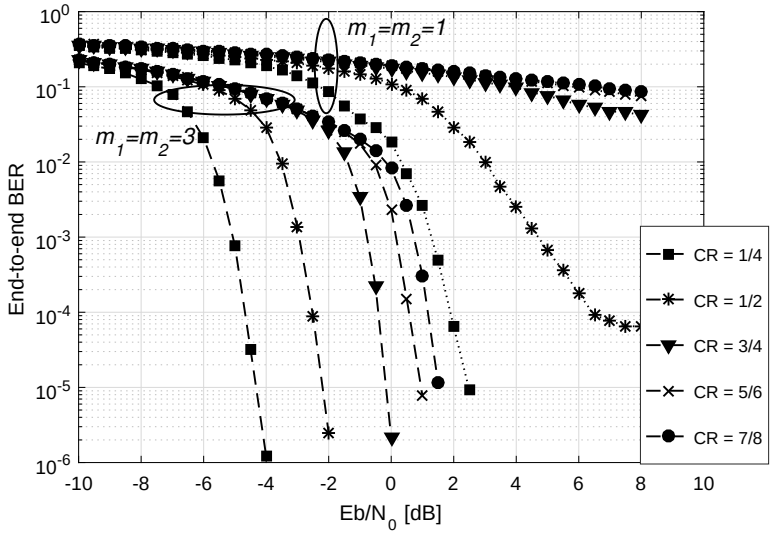

Figure 4.9: BER performance of a dual-hop system at the destination node with different code rates, LDPC codeword length $n = 312$, 4-QAM, $x_0 = 0.5$, $y_0 = 0$

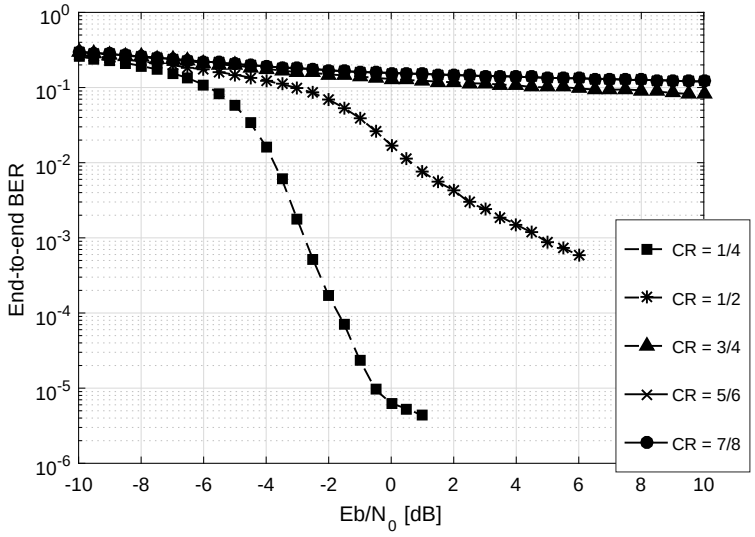

Figure 4.10: BER performance at the destination node for LDPC codeword length $n = 312$, 16-QAM, $m_1 = m_2 = 3$

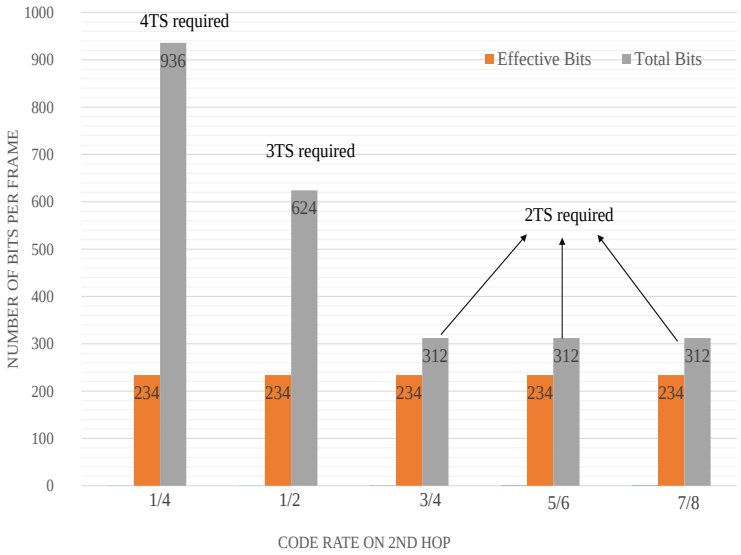

Figure 4.11: A two-hops system with LDPC codeword length $n = 312$, fixed code rate on first hop $= 3/4$ and a variable rate on second hop, 4-QAM, $m_1 = m_2 = 3$

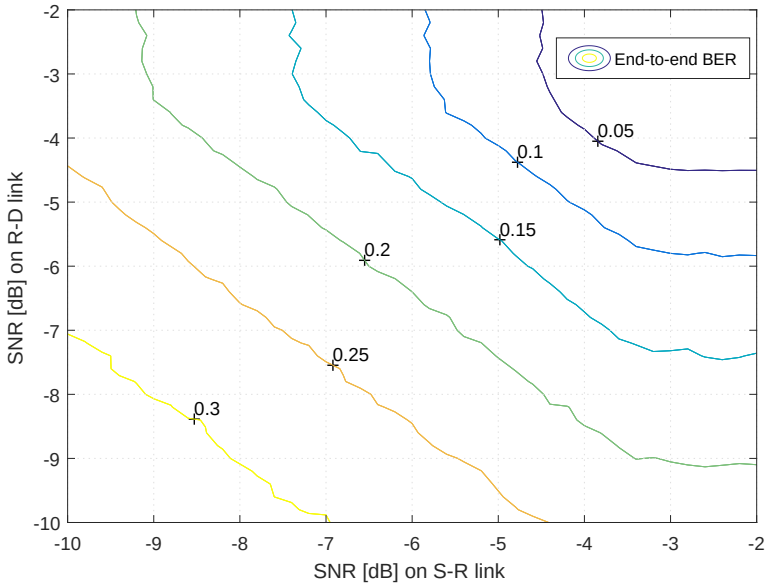

Figure 4.12: A contour of end-to-end BER on two-hops relaying system, code rate=1/2, 4-QAM, $n = 312$, $m_1 = m_2 = 2$

The contour of the destination BER against SNRs on both hops is shown in Figure 4.12. It can be observed that if a higher SNR is available on the first hop, then to maintain a certain target BER of δ_0, a lower average SNR on second hop should still work to maintain a consistent performance. This conforms with the

idea that by breaking down the transmission path into shorter paths, if we have good SNR on one link, we can still maintain a minimum end-to-end BER with worsened conditions on the other hop. However, we are completely aware of the fact that a good BER performance can not be achieved in such a scenario, as the poor link becomes the bottle neck of the system, only a bear minimum performance is achievable.

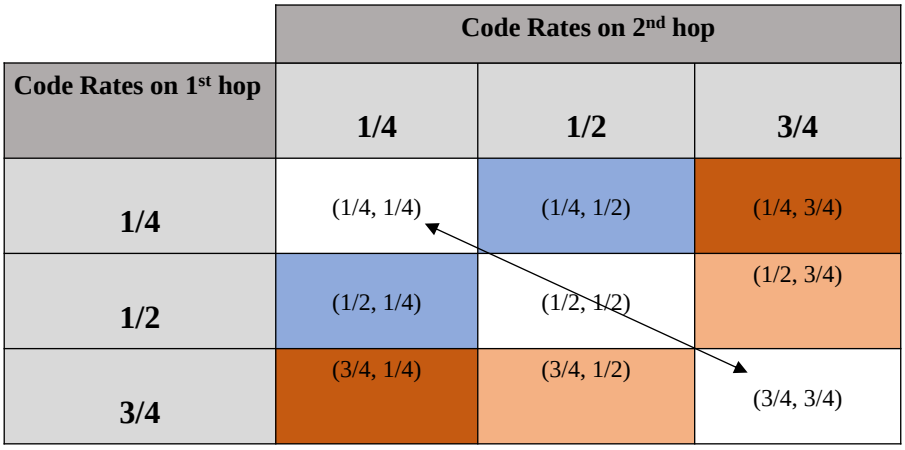

Figure 4.13: An illustrative summary for different code rates, (1st hop CR, 2nd hop CR) for simulations

As mentioned earlier, an algorithm, which changes the code rate on both hops according to changing channel conditions is developed. The designed system supports five different code rates, 4-QAM, and 16-QAM modulations. Figure 4.13 presents a summary of different code rates and compares the performance for different rates on different hops. If we look closely, on the main diagonal, we have the most favorable code rates, which are same for both hops and there is no need of data buffering at the relay. Rest, if noticed carefully, we see boxes of different colors. E.g. for the light blue boxes with $CR = (1/4, 1/2)$ and $CR = (1/2, 1/4)$, we should not expect the same performance despite the symmetry. Actually, there is a difference in performance as shown in Figures 4.14(a), because the first hop with higher CR will experience some decoding errors at relay, which will propagate to the destination, increasing the end-to-end BER. A similar consideration can be done for $CR = (3/4, 1/2)$ and $CR = (1/2, 3/4)$ as illustrated in 4.14(b).

Based on simulated results we can see that the fading effects can be mitigated not only by the use of regenerative relays but also by link adaptive techniques employing variable rates on dual-hop wireless networks. We conclude that link adaptation can attain better performance yet with an increased complexity and transmission delay, especially for lower code rates. For higher rates complexity of processing at relay and overall delay reduces. Hence, each scenario needs a trade-off between complexity and BER performance.

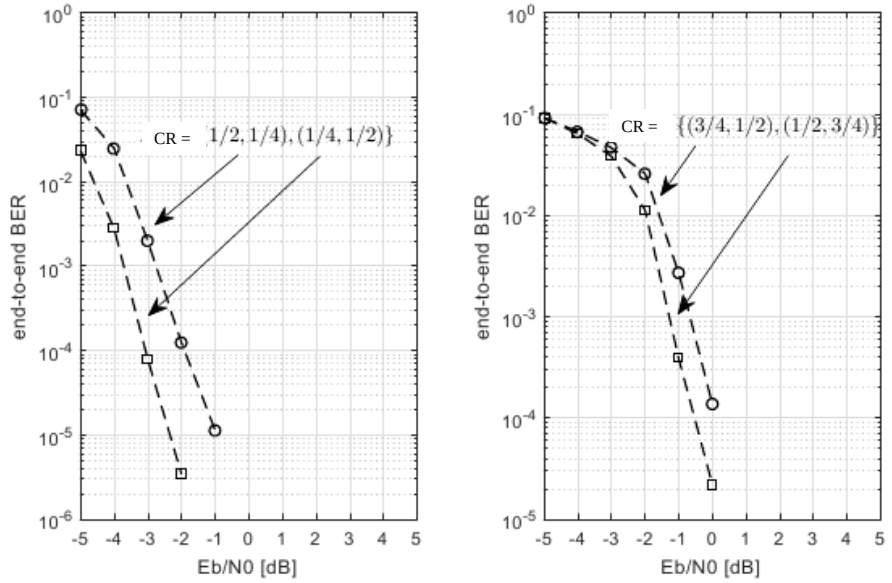

(a) CR pairs comparison: $(1/2, 1/4)$ and $(1/4, 1/2)$

(b) CR pairs comparison: $(3/4, 1/2)$ and $(1/2, 3/4)$

Figure 4.14: BER performance comparison of rate adaptive links for different pairs of code rates on two-hops, $m_1 = m_2 = 3$, $x_0 = 0.5$, $y_0 = 0$, $n = 312$)

5

System Synthesis and Performance Analysis of Cooperative Combining

Diversity combining is considered one of the best techniques to maximize the gain of wireless communications. In this chapter we briefly describe the relay assisted communication in context of diversity combining. We apply different combining techniques like selection combining, maximum ratio combining, and a combination of the two as generalized selection combining. Further, we extend our investigations to a system where power allocation on multiple-relays has been done in an optimized manner. In the last section we discuss the numerical results of the power allocation strategies and demonstrate the effect of optimized power allocation (OPA) against equal power allocation (EPA).

5.1 Introduction

As we discussed in former chapters the reason for a bad performance of a wireless systems can be attributed with deep fades of the channel. Consider a system, where there is only one transmit tx and one receive rx antenna. Then there will be only one propagation link between this pair of tx and rx. If the transmission is in a deep fade, the communication is disrupted, because there is no alternative path between the tx and rx. Hence, the performance of the system will be poor. Naturally, multiple links can be introduced between the tx and rx pair. For example, if we have 4 rx antennas and 1 tx antenna, there will be 4 independent transmission paths between source and destination. The probability that all of them will be in deep fade is

much lower than the probability of single link being in deep fade, since other links are there and the signal can propagate through these alternative links.

Actually, the principle of *diversity* employs that *'there are many'* paths between a pair of transmitter and receiver. The main purpose is to *send the same data/information on independent paths*, these independent paths are combined in such a way that the overall fading effect reduces. Diversity combining exploits the fact that there are lesser chances of independent signal paths to be in deep fades simultaneously. Hence, the diversity helps to improve the deteriorating nature of the channel.

Diversity can be achieved in different ways [26], for example by installing multiple antennas at transmitter or receiver, this is known as *antenna diversity*. In this diversity type antennas are put apart on a sufficient distance[1], so that the signals received look like coming from independent paths. The multiple antenna elements are separated by the distance, such a diversity is also known as *space diversity* in literature. This is important to know that with space diversity independent paths are considered without any increase in the transmit power, rather this type of combining increases the SNR at the receiver as compared to the SNR that would be achieved using only one receive antenna [6]. This is the most common type of diversity.

There are few more methods which can be used for diversity combining, e.g. *frequency diversity*, where a narrowband signal is transmitted over different carrier frequencies and all the carriers are separated by the coherence bandwidth of the channel. Basically, with carriers that are separated by a coherence bandwidth, the idea is to spread the signals over the wide spectrum of carriers so that different copies of the signal undergo independent fading. This type of diversity not only needs spare bandwidth but also additional transmit power to send the same signal over multiple carriers.

Another way to achiever the diversity is by using tx or rx *antennas polarization*. This method also does not come without a price, i.e., only two types of polarization can be achieved at most, vertical and horizontal polarization and there is an extra 3dB power loss when dividing the signals between two differently polarized antennas [6].

To complete the discussion on diversity combining we will mention another important type, where directional antennas restrict the beam-width of the receive antenna to a certain angle, hence, the name directional or angle diversity. This type

[1]for omni directional transmit and receive antennas in a uniform scattering environment this distance is approximately half a wavelength at least [6]

of diversity needs antennas to be smart, otherwise no gain can be obtained. For that reason smart antennas have been introduced, which can be steered to the incoming angle of the strongest multipath component. For further details please see [23].

In the upcoming sections we will observe how diversity combining with LDPC codes further improves the BER performance of the system over fading channels.

5.2 Diversity Combining

In this section we will first introduce the simple maximum ratio combining and then step-by-step map it to the cooperative MRC.

5.2.1 Maximum Ratio Combining (MRC)

Maximum Ratio Combining is one of the classical types of antenna diversity where signals are combined on the receiver side. With MRC, the signal sent from the source is received on different receive antennas. This is called *receiver diversity* (1 tx and multiple rx antennas), i.e., the same source signal is received at two or more received antennas (also called single input multiple output (SIMO)). The same signal reaches the destination traversing through independent fading paths, these signals are combined and then passed through a demodulator. Combining multiple signals at soft-bit level before channel decoding is an important way to achieve the diversity gains. In MRC, the instantaneous SNR is equal to the sum of the SNR's from all the links [6].

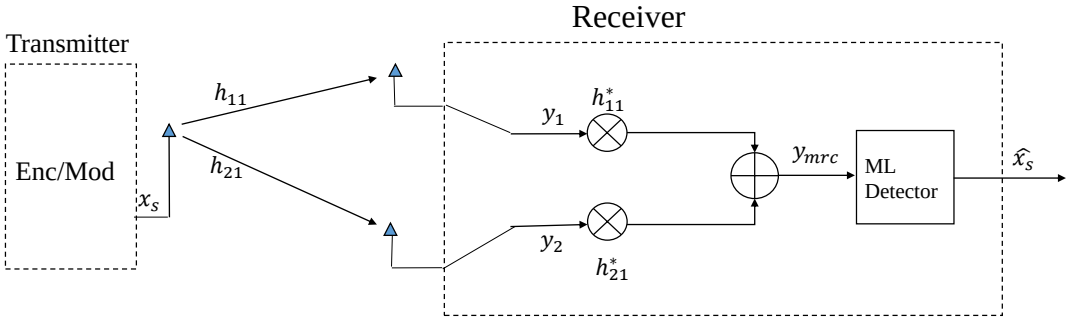

Figure 5.1: Maximum Ratio Combining Setup

Please consider the example of a single input multiple output system, i.e., 1 tx

antenna, 2 rx antennas will be considered. The mathematical model for Figure 5.1 can be described as

$$\begin{aligned} y_1 &= x_s h_{11} + n_1 \\ y_2 &= x_s h_{21} + n_2 \end{aligned} \tag{5.1}$$

where x_s is the signal to be transmitted, y_1 and y_2 are the received signals at antenna 1 and antenna 2, respectively at the receiver. The complex fading channel coefficients h_{11} and h_{21} are independent, identically distributed and *zero* mean random variables with frequency flat spectrum. To have the independent fading at rx 1 and rx 2, these receive antennas are put on a certain distance, at least half a wavelength at the receiver. The white Gaussian noise n_1 and n_2 is added to the signal x_s at antenna 1 and antenna 2. The noise has a *zero* mean and variance σ^2. Moreover, the noise at two different antennas is completely uncorrelated.

The signals y_1 and y_2 are combined together after reception at different antennas. The combined output y_{mrc} will be

$$\begin{aligned} y_{mrc} &= \sum_{\mu=1}^{2} h_{\mu 1}^{*} y_{\mu} \\ y_{mrc} &= \sum_{\mu=1}^{2} h_{\mu 1}^{*} \big[h_{\mu 1} x_s + n_{\mu} \big] \end{aligned} \tag{5.2}$$

The equation (5.2) is the last expression for the maximum ratio combining. This is a very much covered topic in books and literature of digital communications, so we will request the interested reader to see the text books on wireless communication for further details, e.g. [6].

5.2.2 Cooperative Maximum Ratio Combining (CMRC)

Cooperative diversity combining has been proven an efficient strategy to enhance the communication reliability in slow fading wireless environment [42]. In multiple-input multiple-output (MIMO) systems, multiple antenna elements are deployed at transmitter and receiver to provide the spatial diversity. There is another way to achieve the same with the help of relays. If we consider cellular networks, multiple antennas at the receiver are already used in uplink transmissions, e.g. at the base stations. But in downlink transmissions, for example from BS to mobile station (MS), it is difficult to install multiple antennas at the mobile device because of size-limitations and the cost of multiple down-conversions of radio frequency (RF)

paths. Likewise, relay transmissions offer enhanced coverage and resilience against shadowing. In such cooperative links, the message sent by the source arrives at the destination through diverse paths: (i) directly from the source to the destination (ii) and path(s) via relay nodes.

In [27] CMRC has been discussed without using any FEC codes at the source and the relays. Moreover, an equivalent model of $S-R-D$ path has been considered. Rather than combining the SNR from $S-D$ and $R-D$ links, authors compute $SNR = SNR_{SD} + SNR_{eq}$ where SNR_{eq} is the SNR from equivalent path of $S-R-D$. It had been shown that when $S-R$ and $R-D$ have low SNR (for example 0dB), the system performs worse but providing $S-R$ link with an extra 30dB gain gives the good performance. In [29] fixed-gain amplify-and-forward relays had been studied for Nakagami-m fading channels and an exact MRC performance analysis has been done, but without considering any error correcting codes. More in [29] it has been considered that destination is deployed with a multi-antenna system and then the signals coming from the relay and the source branches are combined at multi-antenna destination. It has been argued that in this two-hops system the weaker link becomes the bottle neck of the system.
From [27], we know that providing the $S-R$ link with more power can enhance the performance of CMRC protocol, so, in our set-up we provided the 1st hop with a higher SNR value by placing the relay closer to the source. By keeping the relay closer to S, we ensure that SNR on the $S-R$ link is always higher than on the $R-D$ link. Later, a collective receive SNR is calculated at the destination by applying the MRC method. By applying MRC on $S-D$ and $R-D$ link an equivalent SNR is calculated, which provides a good BER performance even for very low SNR at destination. At relay, the decoding errors are kept low by applying LDPC codes. To best of our knowledge this is a unique scenario, where we investigate the BER performance of cooperative maximum ratio combining (CMRC) system using LDPC codes at source and relay.

We consider the general two-hops, three nodes wireless system as illustrated in Figure 5.2. Mathematically, the receive signals can be written as

$$\begin{aligned} y_{sd} &= x_s h_{sd} + n_{sd} \\ y_{sr} &= x_s h_{sr} + n_{sr} \\ y_{rd} &= x_r h_{rd} + n_{rd} \end{aligned} \tag{5.3}$$

where x_s and x_r are the transmit signals from source and relay, respectively, in

TS-1 and TS-2. y_{sr} is the received signal at the relay in 1st time slot. y_{sd} and y_{rd} are the received signals at the destination in TS-1 and TS-2, respectively. The channel coefficients from source to destination $S-D$, source to relay $S-R$, and relay to destination $R-D$ are h_{sd}, h_{sr}, and h_{rd}. Nakagami-m frequency flat fading is considered on these links. The overall signal to noise ratio is defined by the SNR of the $S-D$ link. Additive white Gaussian noise is added at the receive nodes as n_{sd}, n_{sr}, and n_{rd} with *zero* mean and σ^2 variance.

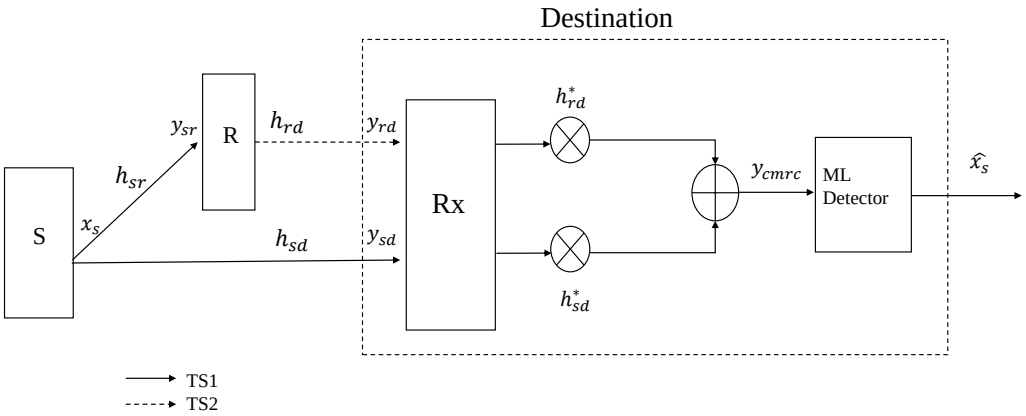

Figure 5.2: Cooperative maximum ratio combining (CMRC)

In [42] and [63] it has been shown by Laneman et al. that full diversity can be achieved with MRC if relay node *only* forwards the error-free data from the relay. The practical implementation of such a system is only possible with some forward error correcting codes. LDPC[2] codes are considered very powerful amongst the forward error correcting codes. With SPA decoding at the relay, a correct decoding sequence can be attained, i.e., 'a replica of the input sequence'. So the information sequence from source and relay are almost the same sequences, as per assumption of traditional MRC model.

The "cooperative" model provides us with an opportunity to combine the signals coming from two different paths, in a dual-hop system, in two different time slots. We will consider a signal coming directly from the source to the destination and another arriving via relay. The combined receive SNR γ_{comb} is the sum of $\bar{\gamma}$ and $\bar{\gamma_2}$ from two independent channels: source to destination and relay to destination

[2]For details on LDPC encoding and decoding, please see Chapter 3

respectively,

$$\gamma_{comb} = \bar{\gamma} + \bar{\gamma_2} \tag{5.4}$$

We are familiar with the fact that when the distance between two nodes is decreased, the SNR value is increased. Consequently, $\bar{\gamma_1} > \bar{\gamma_2}$, if distance between source and relay is less than the distance between the relay and the destination, i.e., $d_1 < d_2$, assuming identical transmit powers (Please see Figure 4.2). Here, $\bar{\gamma_1}$ denotes the average SNR of the first hop. This fact gives rise to the idea that when we put a relay closer to the source or destination, we can attain a better SNR at the respective receiver. Subsequently, in this work we place the relay in a closer vicinity of the source node that helps us to presume the conventional maximum ratio combining model for the regenerative relay-assisted communication system without making any changes to the mathematical model.

In Figure 5.2, the signals y_{sd} and y_{rd} are coming from two independent fading channels, they are multiplied with the conjugate of the channel coefficients h^*_{sd} and h^*_{rd} and are combined at the destination. The sum is fed to the maximum likelihood (ML) detector. Obviously, MRC requires the channel to be known at the receiver [6]. We can mathematically formulate it as follows

$$\begin{aligned} y_{cmrc} &= \sum_{\mu \in \{s,r\}} h^*_{\mu d} y_{\mu d} \\ y_{cmrc} &= \sum_{\mu \in \{s,r\}} h^*_{\mu d} \big[h_{\mu d} x_\mu + n_{\mu d} \big] \end{aligned} \tag{5.5}$$

The estimated symbol $\hat{x_s}$ can be obtained like

$$\hat{x}_s = arg\min_{x_s} |(h^*_{sd} y_{sd} + h^*_{rd} y_{rd}) - (h^*_{sd} h_{sd} + h^*_{rd} h_{rd}) x_s|^2 \tag{5.6}$$

h^*_{sd} and h^*_{rd} are also called the *weights* or *combining coefficients*. These weights are optimal when there are no decoding errors at the relay [24]. Hence, another reason for keeping the relay placed closer to the source. With persistence to our supposition, i.e., a higher SNR at the relay ensures a successful decoding of data, i.e., *no decoding errors at the relay.*
For detailed derivation please see appendices B.2 and B.3.

For having an error-free information sequence at the relay, this is very important to answer, where the relay should be placed. The optimal location of the relay helps to maximize the performance gain of the cooperative maximum ratio combining

technique. For the set-up under consideration, we put the relay always closer to the source, i.e., $10\% - 40\%$ of the total distance d. Successively, a higher SNR at relay can be achieved, which helps to have a zero or negligible BER, and the sequence at the output of the relay is an exact *replica* of the data sent from the source.

This is one of the prerequisites of the maximum ratio combining technique that the data received at two (multiple) rx antennas should come from the same source, i.e., *(the sent information should be same!)*, but on uncorrelated and independent fading channels.

5.2.3 Numerical Results and Discussion for CMRC

In this section, we present the Monte Carlo simulation results of CMRC system. The fading channels we considered here are imposed by Nakagami-m fading and fading parameter m is assumed to be same on all the links. The pathloss exponent is chosen as $\nu = 3$. We apply an LDPC code of length $n = 312$ which is given by IEEE 802.11n WLAN standards [25]. The modulation 4-QAM and an initial code rate $CR = 1/2$ has been chosen. Figure 5.3 shows the results for a direct transmission $S - D$ and a transmission via a relay $S - R - D$ and compares them with proposed diversity technique CMRC. Note, in case of $S - R - D$ transmission without CMRC, the destination just receives the signal from the relay and ignores the signal coming from the direct path between the source and destination. The optimal distances for the placement of relay had been chosen here. As we know, from our numerical analysis in Chapter 4 that relay at $0.5d$ gives best performance for two-hops communications. Although, $0.3d$ is one of the optimal distances to be considered when working with CMRC.

In Figure 5.4 we have considered CMRC for higher order square M-QAM. We compare the results for $M = 4$, 16 and 64, with identical Nakagami-m channels, where fading parameter on all links is kept same, i.e., $m = 3$. As expected, the higher order modulation schemes require higher SNR to achieve the same BER. In Figure 5.5 we compare the cooperative maximum ratio combining and cooperative selection combining (CSC) for 4-QAM with 3 different code rates and nonidentical Nakagami-m channels. In CSC signals coming from the direct path between $S - D$ and path via relay $S - R - D$ are combined at the destination in a way that the path with highest SNR will be selected. From Figures 5.5(a) and 5.5(b), it is evident that CMRC performs better than CSC in terms of BER, reason being that CMRC takes into account the SNR of all the signals coming from all the uncorrelated and independent communication links. Whereas, CSC only considers the link with

highest SNR and ignores the other links.

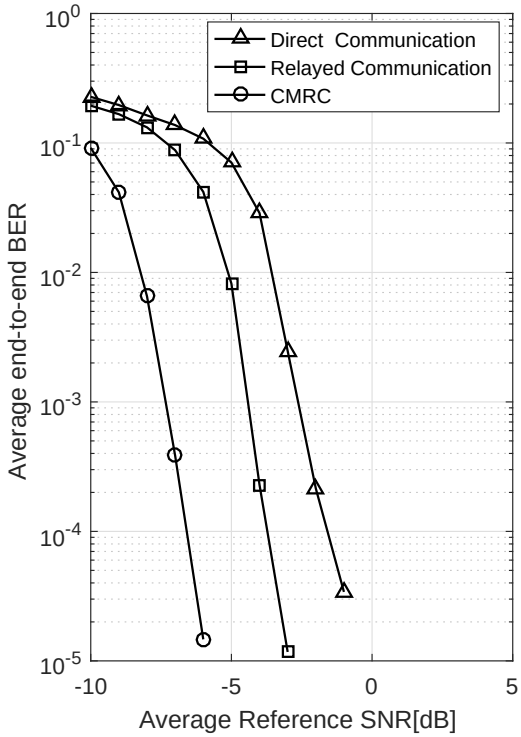

Figure 5.3: A comparison of three types of set-ups, i) direct communication with distance d ii) communication via one relay at 0.5d, iii) cooperative maximum ratio combining, $x_0 = 0.3, y_0 = 0$, $m = 3$ (same for all links), $n = 312$, 4-QAM and $CR = 1/2$, Nakagami-m fading

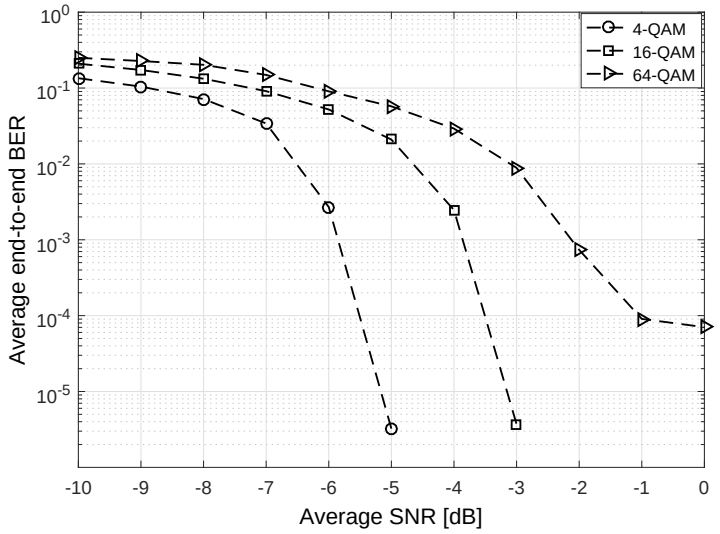

Figure 5.4: BER performance of cooperative diversity system CMRC for M-QAM, where $M = \{4, 16, 64\}$, $CR = 1/2$, LDPC (648, 324), $m = 3$ (same on all links)

In case of CMRC there are two paths, $S-D$ and $R-D$, but CSC chooses one out of these two. The path via relay will have higher SNR in almost all cases as compared to the direct link between S and D, because of shorter distance between relay and destination.

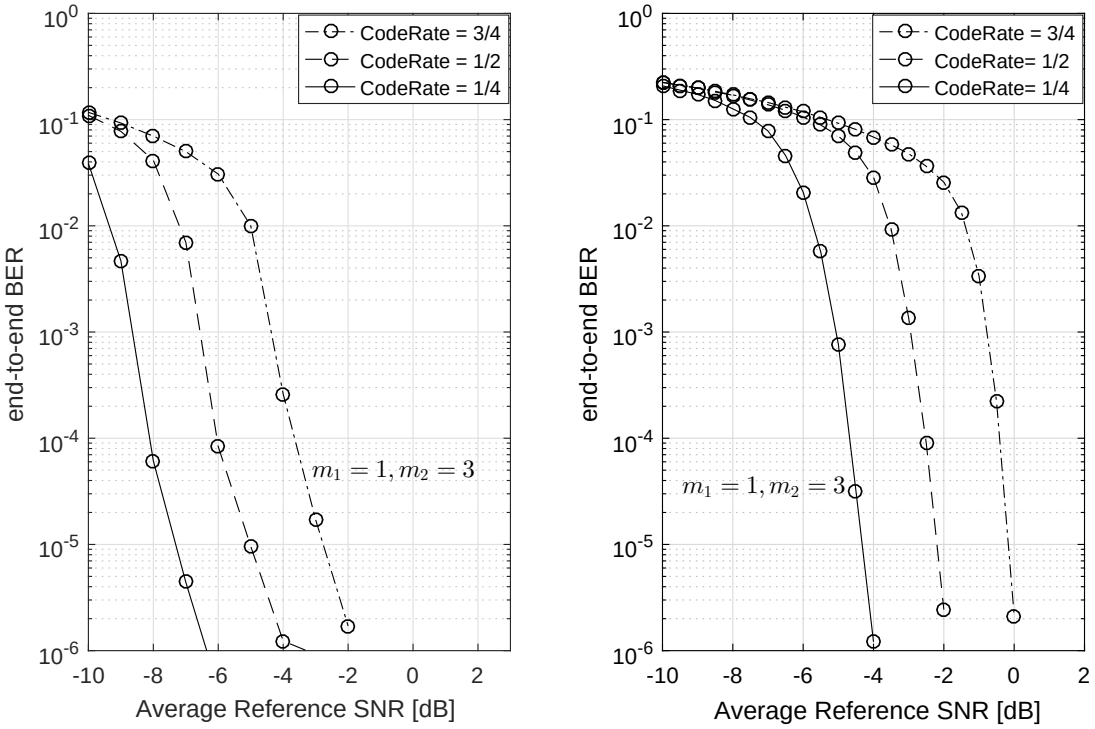

(a) Cooperative maximum ratio combining (CMRC), relay position $x_0 = 0.3d$

(b) Cooperative selection combining (CSC), relay position $x_0 = 0.3d$

Figure 5.5: BER performance comparison of CMRC and SCS with LDPC codes, $n = 312$, 4-QAM and $CR = \{1/4, 1/2, 3/4\}$, nonidentical Nakagami$-m$ channels, $m_1 = 1$ (for S-R and S-D link), $m_2 = 3$ (for R-D link)

In Figure 5.6 we checked our system by holding the relay at different positions from the source. Our assumption that the decoded sequence at the relay output is an exact replica of the sequence sent from the source, when the distance between source and relay is kept between 10 and 40% of the total distance of $S-D$ has been verified numerically. We also increased the distance to more than 40%, that is, the relay moves further away from the source[3], subsequent to this, significant decoding errors occur at the relay and consequently, our prerequisite that the transmit signal of the relay is the replica of the transmitted signal of the source is not fulfilled anymore. An an end-to-end BER at the destination is increased and the same performance margin

[3]not shown here in the Figure 5.6

can not be achieved. We conclude that for good end-to-end BER performance, the relay has to be placed closer to the source at 0.1d-0.4d when the pathloss exponent is between 2 and 3.

Please note, another very important aspect, which is visible from the Figure 5.6 is that the best end-to-end BER performance is achieved when the relay is placed at 0.4d. When the relay is put closer to the source for example at 0.1d or 0.2d, although, we have an exact replica of the information sent from the source but because of pathloss on the 2nd hop the average SNR at the destination will be lower. Consequently, the BER performance is worse than that for 0.4d.

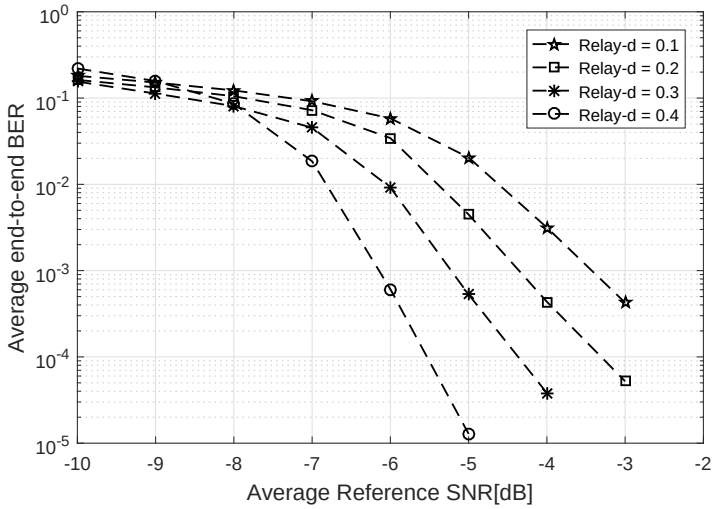

Figure 5.6: BER performance of cooperative diversity system for different relay positions, LDPC (312, 156), 4-QAM modulation, pathloss exponent $\nu = 2$

In our modeled dual-hop system the optimal weights for CMRC had been achieved by obtaining an error-free sequence at the relay. Based on our simulations, we can see that the impact of fading on the BER can be mitigated not only by the use of a decode-and-forward relay but also by applying the cooperative maximum ratio combining technique at the destination on received signals from relay and source. Diversity provides a receiver with replicas of the same signal that are combined at the receiver to attain a gain. In Figure 5.3 a *diversity gain* of about 3dB can be observed in case of CMRC as compared to the cooperative communication via a relay for 4-QAM and $CR = 1/2$.

5.2.4 Cooperative Generalized Selection Combining

As we had been discussing in the last couple of paragraphs, combining the signals

at destination can improve the system performance, significantly. Although, MRC provides an optimum performance gain but it has high complexity implementations involved at the receiver. Because receiver requires to estimate, weigh, and combine all the paths accordingly. On the other hand, selection combining (SC) is not complex to implement because it requires to estimate the channels and selects only one channel with highest instantaneous SNR. However, the lower implementation complexity of SC results in performance loss [86]. A trade-off between complexity and performance had been proposed in [85] in the form of a *hybrid model for selection and maximum-ratio combining*. This model is also called generalized selection combining (GSC). GSC had been studied in literature mostly in context of multi-antenna systems like in [64, 65]. Traditionally, in multi-antenna systems also known as MIMO systems, the generalized selection combining is done at the destination by combining the signals coming from the multiple but independent paths. At the multi-antenna destination as shown in Figure 5.7, K antennas out of L with highest instantaneous SNR, higher than a threshold SNR are considered for the selection combining. After this, on the 2nd level, the signals from K antennas are coherently combined using MRC method by weighing all the paths with the respective gains of the paths. Hence, signals are combined at two levels. By applying such a unification of signals, actually more diversity gain can be achieved as compared to the SC or MRC alone [85]. GSC provides a double layer of diversity that achieves a better error rate performance. Besides, providing the lower BER, GSC also bridges the gap between SC and MRC by maximizing the performance and minimizing the overall complexity [64].

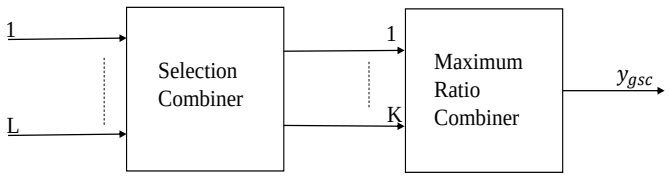

Figure 5.7: Generalized selection combining set-up

GSC technique is equally applicable to the relay-assisted communications. In a two-hops multiple relays system, on first level signals are combined using SC method, i.e., the relays, which will have receive SNR above a threshold SNR will be selected to forward the signals to the output. On the second level, signals coming from the se-

lected relays and source are combined using MRC. For the cooperative transmission, we will call GSC as *cooperative generalized selection combining* (CGSC).

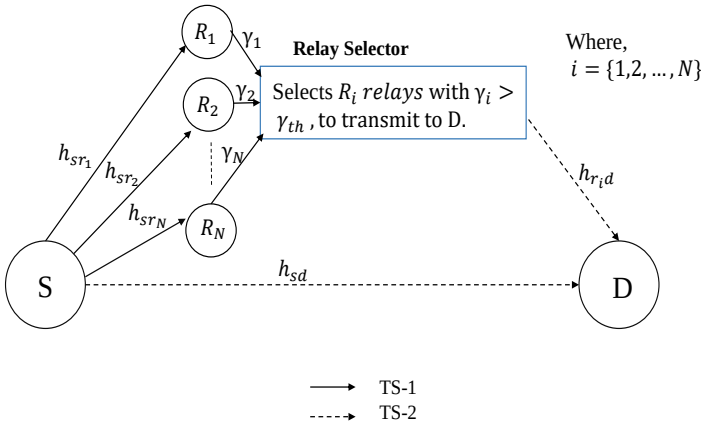

Figure 5.8: Cooperative generalized selection combining for multiple DF relays

In Figure 5.8, we have illustrated the basic system set-up for CGSC technique, where 1st hop has the multiple channels between source and N relays and 2nd hop also has multiple channels between N relays and destination. All the channels, i.e., h_{sr_i}, and $h_{r_i d}$ follow a Nakagami-m fading, where $i = 1, 2, ..., N$, indicates a relay. Relays are put at a certain distance d_i from the source. We integrate the effect of relay positioning by considering a composite model for large-scale and small-scale fading, i.e., pathloss and Nakagami fading. The pathloss effect can be incorporated by considering the distance d_i, where, d_i is the propagation distance between S and R_i. The distance between a relay R_i and destination D can be calculated as $(1-d_i)$. The transmit power P has been normalized to 1. As per GSC technique, the relay R_i is selected only if it has the instantaneous SNR γ_i above a threshold SNR γ_{th}.[4]. where

$$\gamma_i = \frac{P\,|h_{sr_i}|^2}{\sigma^2}; \qquad i = 1, 2, ..., N \tag{5.7}$$

[4]The relay selection is done on the basis of instantaneous SNR, γ_i only, because in [82], this has been argued that while calculating the end-to-end SNR, the relay with maximum SNR contributes most to the output SNR. Furthermore, for general S-R-D configuration, the end-to-end data rate is the minimum of S-R and R-D links, so of course if R-D link is good but S-R link is not good effective data rate will be less. Therefore, we always assume an equal SNR on R-D links, then main contribution comes from the S-R link.

It is assumed that channel state information of h_{sr_i}, h_{r_id} and h_{sd}, is completely available to the respective destination nodes. The instantaneous SNR of channels $S-D$, $S-R_i$, R_i-D can be represented as γ_{sd}, γ_i, and γ_{r_id}, respectively. Therefore, all the relays with instantaneous SNR greater than the threshold SNR γ_{th} should be eligible to take part in data transmission on the 2nd hop, irrespective of the channel conditions on R-D link. Hence, at destination the data from all the relays with $\gamma_i > \gamma_{th}$ can be combined with the data directly coming from the source, using MRC technique. However, when multiple relays are selected on the basis of a certain threshold SNR, the overall complexity of the system does not reduce significantly. Selecting a single relay, is the best relaying option in terms of the resulting complexity and overhead and most of the times the relay with the maximum SNR is the one that contributes most to the output SNR [82, 83]. For these reasons we demonstrate the CGSC technique for a case, where on first level only one relay is selected and on 2nd level only two signals are combined at the destination, i.e., one coming directly from S and the other one coming via relays. It follows that for CGSC, we have $K = 1$, and $L = 2$, i.e., only 1 relay is selected out of N relays and there are always only 2 signals to combine at the destination. This simplifies the scenario with an additional performance gain. Thus, now the selection criteria is defined slightly in a different manner and the relay R_i with *maximum* instantaneous SNR γ_i is selected only.
Mathematically it can be written as,

$$\gamma_{sel} = \max(\gamma_1, \gamma_2, ..., \gamma_N) \tag{5.8}$$

The decoding and encoding of data is done at the selected relay R_i. Moreover, R_i transmits the encoded sequence to the destination, where destination combines it with the signal coming from the direct path between S and D, by applying MRC.

In the second stage, after applying MRC, the total SNR at destination can be, approximately, given as

$$\gamma_{cgsc} = \gamma_{sel} + \gamma_{sd} \tag{5.9}$$

It is evident from the Figure 5.9 that CGSC performs best of all the combining techniques. A very low BER performance can be attained at a low SNR. If we compare the simulation results of Figure 5.9 with Figures 5.5(a) and 5.5(b), we can observe that CGSC provides the BER of 10^{-6} at an SNR of -7.8dB, which was achieved at -6.5dB with CMRC. Moreover, as compared to SC, CGSC provides a gain of $\sim$4dB for the BER of 10^{-6}, which validates that CGSC is the most supe-

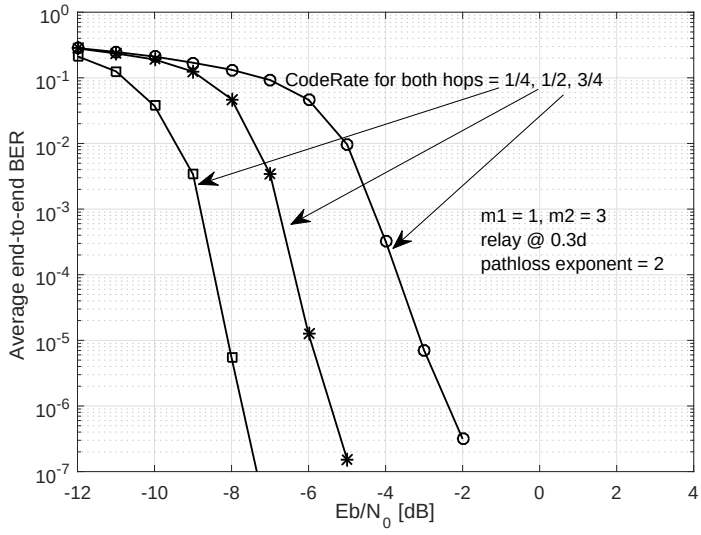

Figure 5.9: CGSC BER performance, Nakagami-m fading with, changing fading parameter and 4-QAM,

rior diversity combining technique, amongst all the combining techniques we have discussed in this chapter.

5.3 Power Allocation Techniques in Decode-and-Forward Multiple Relays Network

5G communications is already underway and promises to provide higher data rates and reduced latency. One of the ways to achieve an accelerated performance is to use the network resources efficiently with the aid of sophisticated techniques which are under rigorous research these days. On another perspective, energy consumption is a major concern in future wireless communication networks which has to be dealt very effectively to ensure the energy-efficient solutions for the end users. Especially in mobile devices energy is a scarce resource and needs to be reserved [62].
A number of conflicting constraints should be considered while designing the wireless communication systems. The bit-error-rate, broadcast transmissions, limited bandwidth, and higher energy consumption are some of the examples of such constraints. At the physical layer, the *higher error rates* are due to the multipath-broadcast nature of the wireless channels especially in downlink scenario. This is in addition to the *interference*, which is present in the network. The available *bandwidth* in wireless networks is much less than the wired networks, so it has to be used efficiently. Similarly, *energy* is a scarce resource, however, the wireless networks require high

energy while transmitting the data from source to the destination.
From equation (5.7), it is obvious that for a given physical environment of a wireless communications system, the only adjustable (tailored according to need) parameter is the transmit power P. In this section we will allocate the power to different transmit nodes under the constraint of energy efficiency, i.e., we will assign the transmit power in a way so that energy efficiency of the system can be maximized. Furthermore, breaking down the total distance into shorter lengths with the help of relays does not only reduce the energy consumption, but also provides better network coverage with a lower BER. The amount of energy required to transmit the data depends on the *distance* between the transmitter and receiver.
As discussed in Chapter 4, in addition to the performance improvements using the SNR advantage of cooperative communications, multiple hops employing the FEC codes can help to achieve a desirable BER performance by exploiting the inherent properties of FEC. This can be done, e.g. by changing the rate of data transmission on different hops according to the quickly changing conditions of the wireless channel, which otherwise would be hard to maintain with fixed code rates [46]. In the past decade, the focus of most of the researchers has been on designing the two-hops or multi-hop systems without any consideration of link adaptation techniques, e.g. in [43, 48, 50]. Nonetheless, some of the researchers have been using rate adaptation techniques or more specifically, adaptive coding and modulation (ACM) in cooperative networks. Andreas Müller et. al in [45] and [51], discuss the decode-and-forward multi-hop systems with ACM, without considering any particular encoding scheme or optimized power allocation at source and/or relay(s). Moreover, authors do not consider optimized power allocation at transmitter. The authors in [52] have adapted to different code rates and different modulations, but they also do not allocate a fair share of transmit power to each transmitting node. In [77], the researchers consider the optimum power allocation technique under the constraint of union bound minimization. Moreover, the authors only consider a two-hops but single relay network, where there are no FEC codes applied at the source or at relay. The authors in [78] study the optimized power allocation in certain situations. They consider the minimization of Chernoff bound on BER performance, but do not consider FEC codes on transmitting nodes. Hence, to best of our knowledge we have considered a unique scenario, which bridges the gap between the two groups of the researches who either consider the code rate adaptation, without taking into account the fair allocation of transmit power *or* consider the optimized power allocation on multiple transmitting hops without code rate adaptation. In this section, we investigate a two-hops

multiple relays system for different power allocation techniques under the constraint of maximization of energy efficiency. The system under consideration provides a comprehensive framework for optimum power allocation in multiple relays network when variable code rates are applied according to CSI. We numerically investigate the allocation of transmit power in such a manners that it guarantees the provision of quality of service (QoS) in terms of lower BER and maximal energy efficiency.

5.3.1 Transmission Model

We consider a two-hops wireless system, with a source node S, a destination node D and multiple intermediate relay nodes R_i. The relay nodes are located at different positions between vicinity of S and D as shown in Figure 5.10. There is no direct link between S and D and the source node communicates with the destination via relays only. The relays are assumed to operate in a regenerative DF mode. A time division based half-duplex relaying has been considered, i.e., there are two phases of the data transmission. In the first phase or time slot (TS-1), S encodes the data with a specific *code rate* using LDPC codes and broadcasts it towards relays. The relays receive the data and decode it. In the second phase or time slot (TS-2), the data is encoded at the relays with same or varying code rates and sent towards the destination D. The destination receives the data from all the relays on orthogonal channels and performs decoding. The AWGN has been assumed on all the receivers with *zero* mean and same variance per real dimension.

The received signal at the i^{th} relay is given as

$$y_{r_i} = \sqrt{P_s} x_s h_{sr_i} + n_{r_i}, \tag{5.10}$$

where x_s is the transmitted symbol from the source with the transmit power P_s. In (5.10) the channel coefficient between the source and i^{th} relay is given as h_{sr_i} and n_{r_i} is the additive white Gaussian noise sample added at the i^{th} relay. It has been assumed that all the nodes are equipped with single antennas and the wireless channel on all links undergoes a frequency flat fading. The channel coefficients are independent and identically distributed and follow a Nakagami-m distribution. Moreover, we assume that all the nodes have perfect channel state information of the links on which they receive data, hence, a perfect coherent detection is possible at the receiver.

Likewise, at the destination D, the received signal from the i^{th} relay can be repre-

sented as

$$y_{d_i} = \sqrt{P_i} x_{r_i} h_{r_i d} + n_d, \tag{5.11}$$

where x_{r_i} is the is the transmitted symbol from the i^{th} relay with transmit power P_i. $h_{r_i d}$ is the channel coefficient between the i^{th} relay and the destination and n_d is the AWGN sample added to the received symbol at the destination. The destination receives signals from the multiple relays on orthogonal channels.

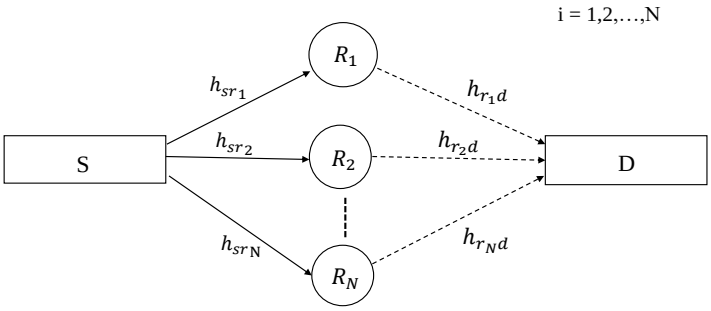

Figure 5.10: Multiple decode-and-forward relays network

We generate an (n, k) irregular LDPC code by keeping the code rate CR *same* in one end-to-end transmission. This is the first considered scenario, which implies that same code rate is applied at the source and at all the relays irrespective of the channel conditions. The code rate is defined as $CR = k/n$, where for every k bits of useful information, LDPC encoder generates a total of n bits and $n > k$, of which $(n - k)$ are the redundant bits. In Chapter 4 in Table 4.1, we have enlisted the five different code rates for an example LDPC code, which are used in our simulation results as well.

At the source, we generate a sparse parity check matrix, $\mathbf{H}$, with $(n - k)$ rows and n columns. A corresponding generator matrix $\mathbf{G}$ is generated to encode the given sequence as $\mathbf{x}_s = \mathbf{u} \circ \mathbf{G}$, where $\mathbf{u}$ and $\mathbf{x}_s$ are the input and output of the encoder, respectively. M-ary quadrature amplitude modulation with $M = \{4, 16\}$ is employed by the source in TS-1. At the relay station i, the received sequence is decoded using log domain SPA. The decoded codeword $\mathbf{u}'_i$ at i^{th} relay is encoded again as $\mathbf{x}_{r_i} = \mathbf{u}'_i \circ \mathbf{G}_i$. Please recall from the Chapter 3, Section 3.4, $\mathbf{G}$ and $\mathbf{G}_i$ can be same or different depending upon, whether the code rate adaptation is done at relays or not. After M-QAM modulation, it is transmitted by the relay in TS-2.

The destination then decodes the received information using the log-domain SPA.

After demodulation, the received vectors $\mathbf{y}_{r_i}$ and $\mathbf{y}_{d_i}$ constructed from (5.10) and (5.11) are valid codewords only if they satisfy the parity check condition, i.e.,

$$\mathbf{H} \circ {\mathbf{y}_{ri}}^T = \mathbf{0}, \tag{5.12}$$

$$\mathbf{H}_i \circ {\mathbf{y}_{di}}^T = \mathbf{0} \tag{5.13}$$

where $\mathbf{H}_i$ is the parity check matrix corresponding to $\mathbf{G}_i$. The above products in equation 5.12 and 5.13 are zero vectors of dimension $(n-k) \times 1$. For each bit, the hard decision is made using sum product algorithm[5].

5.3.2 Post-detection Combining at Destination

To improve the performance of the wireless communication links, several copies of the data coming from different paths, (here from the relays) are combined. As all the copies are combined after detection (decoding) of the signals, therefore, we call it *post-detection combining*.

In this section, we shall discuss the post-detection combining at the destination, of the signals coming from different relays. The signals received from each relay are decoded separately using LDPC decoder and are combined in a single matrix $\mathbf{Y}_{pdc}$ of dimensions $(N \times k)$, where N is the number of relays. Each column of the matrix is decided on the basis of *majority voting rule*, i.e., if a bit (0 or 1) has more than 50% occurrences it will be selected as the detected bit, as shown in Figure 5.11.

5.3.3 Power Allocation (PA)

Power allocation is an important aspect of wireless communications and much research has been done in this regard [77–82, 84]. All the transmitting terminals, be it multiple antennas, two hops/multiple hops relay assisted communications or multiple-sources/multiple-relays, require different types of strategy to distribute the power to all the transmitting terminals. In multi-hop wireless networks, the instantaneous SNR, γ_i, at the i^{th} relay can be calculated by considering the transmit power P_s, i.e.,

$$\gamma_i = \frac{P_s}{\sigma^2} \left| h_{sr_i} \right|^2, \tag{5.14}$$

Energy efficiency (EE), η, is the maximum number of information bits transmitted successfully, per Joule of energy consumed at the transmitter. In other words,

[5]For sum product algorithm details, please see Chapter 3, Section 3.3

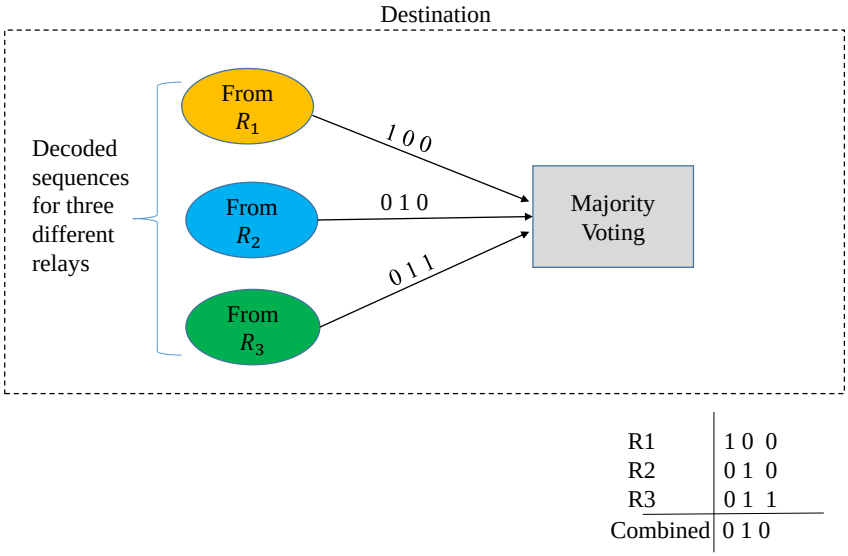

Figure 5.11: Post-detection combining with majority voting rule

EE is the amount of data transmitted per unit power. Mathematically, for a single link between S and relay R_i, it can be defined as,

$$\eta = \frac{log_2(1+\gamma_i)}{P_{tot}} \tag{5.15}$$

Similarly, the instantaneous SNR, γ_{d_i} at D form a relay i can be defined as

$$\gamma_{d_i} = \frac{P_i}{\sigma^2} |h_{r_i d}|^2 , \tag{5.16}$$

where P_i is the transmit power of relay i and energy efficiency at D can be defined as follows

$$\eta = \frac{log_2(1+\gamma_{d_i})}{P_{tot}} \tag{5.17}$$

In (5.15) and (5.17), P_{tot} is the sum of the normalized powers at the source and all relays, i.e.,

$$P_{tot} = P_s + \sum_{i=1}^{N} P_i, \tag{5.18}$$

After defining the certain terms, in the following paragraphs we consider the transmit power allocation under certain conditions to achieve a target BER. For discussion on energy usage and energy efficiency, a couple of different scenarios are considered where transmit power allocation is performed in different manners. The scenarios

are as follows.

5.3.4 Equal Power Allocation (EPA)

Equal power allocation to all transmitting nodes reduces the computational complexity of a wireless network, keeping in view the simplicity of the power allocation algorithm. In this section, we investigate the equal power allocation in two contexts, as follows.

1. Equal power allocation, without code rate adaptation (EPA-I)
   In this case, we assume that the same code rate is applied on both hops. Hence, relays do not perform any temporal buffering because of the same input and output data rates. This assumption makes the implementation of such a network straightforward. For EPA-I there is no power adaptation and no code rate adaptation at relays but equal transmit power is allocated to every transmitter regardless of its needs.

2. Equal Power allocation with code rate adaptation at relays based on feedback from destination (EPA-II)
   EPA-II also uses equal power allocation but code rate adaptation is done here, i.e., a higher code rate can be adapted if channel conditions are becoming better. With bad channel conditions, a lower code rate is chosen to send the data from the relays. However, the transmit power at relays remains the same.

For EPA, in (5.18) P_i denotes the transmit power of the i^{th} relay, under the constraint that

$$P_i = P_i^{max}, \quad \forall i \tag{5.19}$$

where $P_i^{max} = P_s$, yielding $P_i = P_s \ , \quad \forall i$.

5.3.5 Optimized Power Allocation (OPA)

When equal transmit power is provided to all the transmitting nodes in network, a certain performance margin can be obtained but EPA scenarios do not maximize the system efficiency. However, this performance gap can be bridged by providing the relay nodes with an optimized power. Following that idea, we consider to distribute the power in a different manner.

We consider that the source S and all the relays R_i share a certain pool of power, where the source always transmits with half of the total power. Whereas, each relay transmits with a power allocated to it on need basis. Hence, all the relay nodes get

a fair share of transmit power. The optimized power allocation ensures the system efficiency by fair allocation of transmit power at multiple relays.

We treat this type of power allocation as an optimization problem. The transmit power is allocated in a way, such that it maximizes the energy efficiency of the system. We consider that the source always emits with a fixed transmit power P_s. The optimization problem is formulated as

$$\begin{aligned} \max_{P_i} \quad & \eta, \quad i = 1, ..., N \\ \text{s.t} \quad & \sum_{i=1}^{N} P_i \leq P_i^{max} \end{aligned} \tag{5.20}$$

and $P_i^{max} = P_s$.

In above equation η is given by (5.17). An i^{th} relay can transmit with the maximum transmit power $P_i = P_s$ or a power less than P_s. However, the sum of transmit powers at all the relays should not be exceed the P_s. This constraint in (5.20) limits the maximum transmit power to maximize the EE. In case of OPA, supposedly, a relay sends with a higher code rate when the channel conditions are good. Different code rates CR will be selected on the basis of CSI feedback from the receiver node. We presume that a good channel condition means a high channel gain. On the basis of the *waterfilling algorithm* notion, we allocate more power to the channels with higher gain. Consequently, every relay gets a fair share of transmit power according to its needs. We will distribute power among multiple relays in this regard and as we mentioned earlier, S transmits with half of the total transmit power P_{tot}. OPA works under the assumption that high channel gain deserves more transmit power allocation. It is different from EPA-II methodology because there is not only the code rate adaptation on the basis of CSI feedback as in EPA-II but also the power will be allocated on need basis. The numerical analysis of all the PA protocols we have discussed so far, is presented in the next section along with simulation results.

5.4 Numerical Results and Discussion

For Monte Carlo simulations, we have used different code lengths of LDPC codes. Five different code rates have been used with 4-QAM. A Nakagmi-m fading factor, i.e., $m = 3$ and data rate $CR = 1/2$ had been used to collect the results, unless otherwise mentioned.

5.4.1 EPA

In Figure 5.12, the BER performance for various numbers of relays is shown. We see that as the number of relays increases, we get a better BER performance, e.g. for 3 relays we have a BER of 10^{-5} for an SNR of -3.0dB approximately, whereas for 7 relays the required SNR to achieve the same BER of 10^{-5}, reduces to -4.5dB. Figure 5.13 shows that if we decrease the amount of transmit power by a factor of 2 for the same system, the system performance also decreases. This can be observed by comparing Figure 5.12 and Figure 5.13.

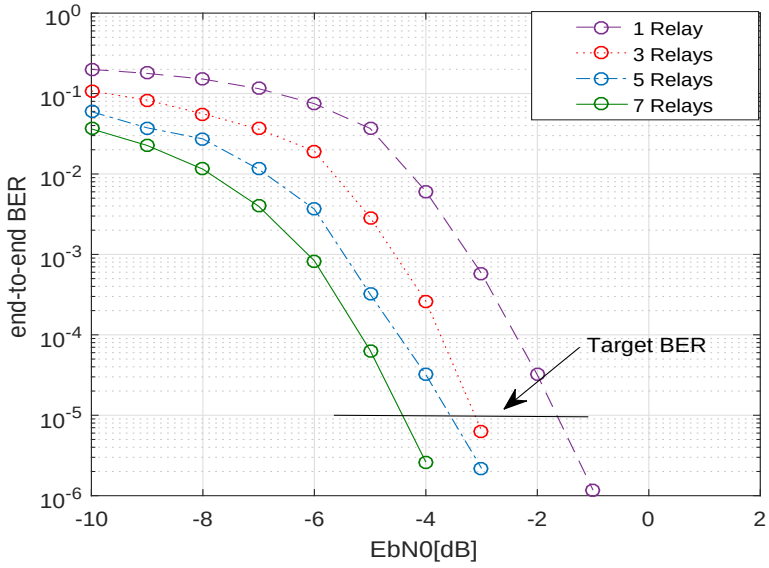

Figure 5.12: EPA-I: BER of system with multiple relays with equal transmit power, code rate 1/2, codeword length $n = 648$, Nakagami-m fading, $m_1 = m_2 = 3$, 4-QAM

It is evident from the two figures that when transmit power is halved, the target BER of 10^{-5} for 7 relays is achieved at an SNR of -1.5dB, approximately. Hence, approximately a 3dB extra SNR will be needed to achieve the target BER when transmit power is decreased by a factor of 2. Figure 5.14 represents the relationship between energy efficiency of the system versus the number of cooperative relays. We can see that as the number of relays increases, the energy efficiency η drops very quickly. This is because the total transmit power is increased with the increasing number of relays, however, the data rate is not increased at the same pace. In other words, the resultant SNR to attain a certain target BER does not increase as quickly, consequently, energy efficiency decreases. Nonetheless, this is also clear that when the transmit power is still allocated equally but decreased by a factor of

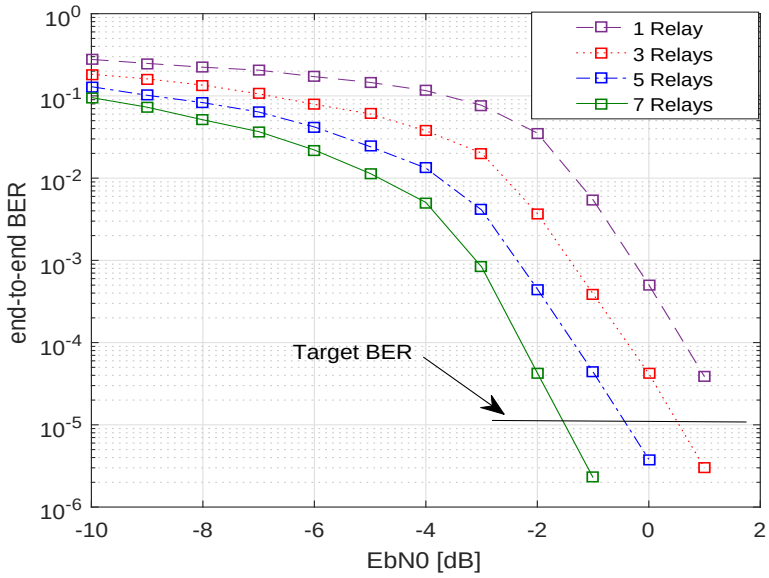

Figure 5.13: EPA-I: BER of system with multiple relays with equal transmit power (decreased by a factor of 2), code rate 1/2, codeword length $n = 648$, Nakagami-m fading $m_1 = m_2 = 3$, 4-QAM

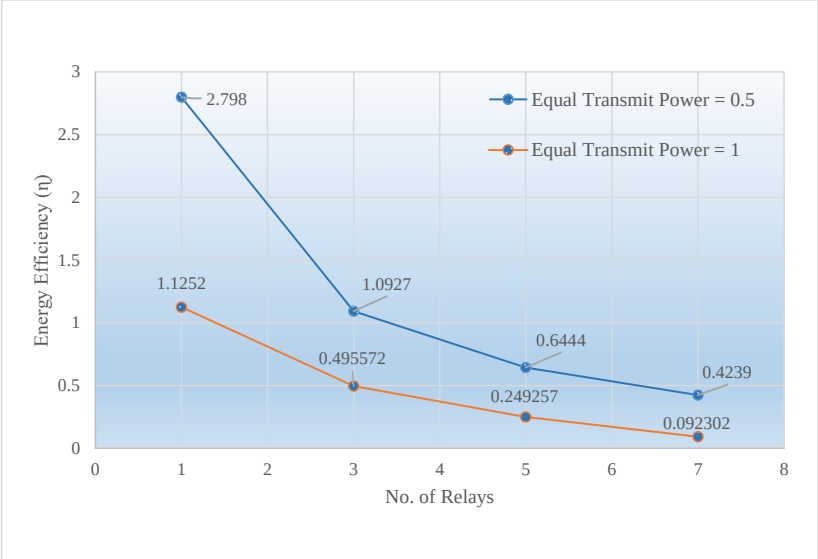

Figure 5.14: Energy efficiency *vs* number of relays for target BER $= 10^{-5}$, code rate 1/2, codeword length $n = 648$, 4-QAM

2, we see an improvement in the energy efficiency of the system.

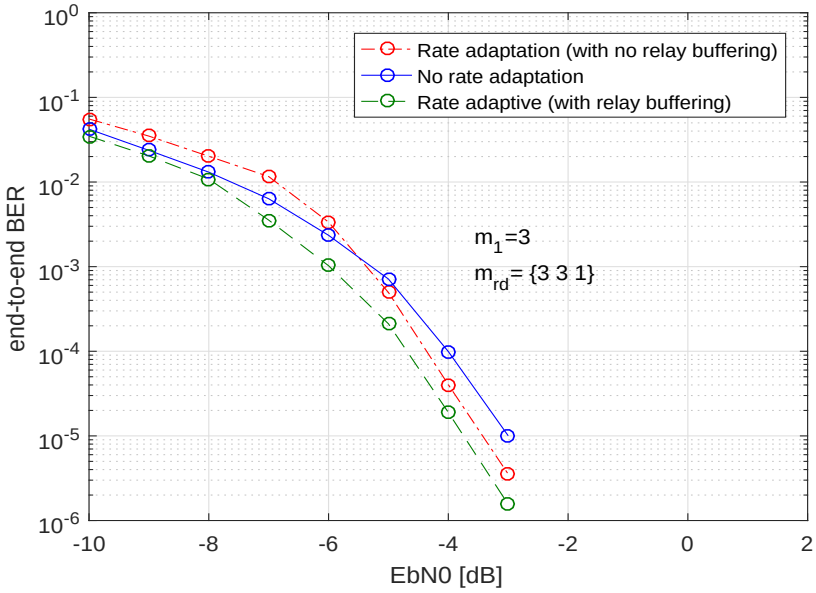

Figure 5.15: BER of multiple relays (3 relays) with equal transmit power (decreased by a factor of 2) , codeword length $n = 648$, CR at source 1/2, 4-QAM

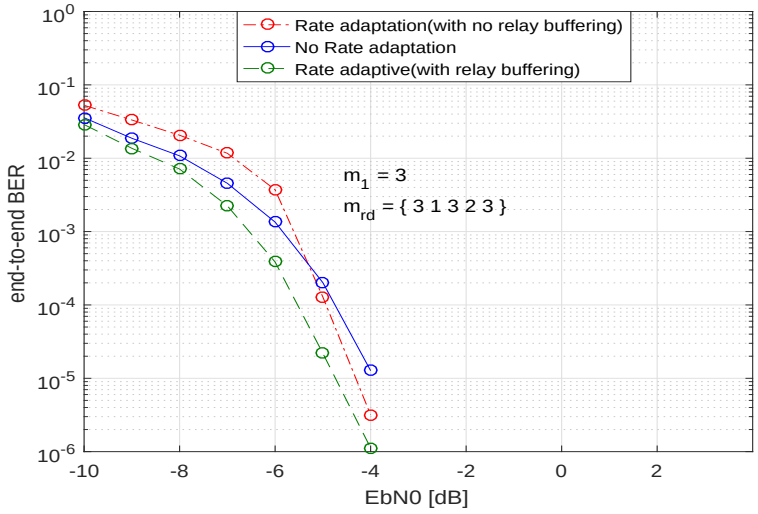

Figure 5.16: BER of system with multiple relays (5 relays) with equal transmit power (decreased by a factor of 2), codeword length $n = 648$, CR at source 1/2, 4-QAM

5.4.2 OPA

In Figures 5.15 and 5.16, we analyze our system for optimized power allocation strategy with different conditions. In Figure 5.15 we can observe the 3 curves, the first (red) curve shows the BER performance of the system when the system adapts

to the different code rates but does not do any temporal storage of the data at the relays. In this case, if a relay has to send the data at a lower code rate than the rate with which it has received the data, no bits are buffered at the relay and after sending the required bits according to the new chosen code rate, the remaining bits are disposed off.

Example: We consider 3 relays with LDPC codeword of length $n = 648$. We observe that if the source S sends data with a code rate of 3/4, then the decoded sequence length, i.e., k will be 486 bits. For the 1st relay when the relay adapts CR according to the channel conditions and if it adapts to a new code rate of 1/2 then it sends 324 bits only and disposes off the remaining 162 information bits. Moreover, a new parity check matrix $\mathbf{H}_1$ with revised parameters, k and $n-k$ is defined at the relay. For the relay 2, if the same output code rate as input code rate, i.e., $CR = 3/4$ is chosen then no bits will be disposed off. If at relay 3, only 162 information bits are transfered because of worst channel conditions on the link between relay and destination, as $m_{rd} = 1$, hence, rest of the bits are disposed off at relay 3. Consequently, destination receives the data from first relay with a code rate of 1/2, i.e., D receives 324 information bits in a frame, from the 2nd relay with a code rate of 1/4, the destination receives 162 bits and from 3rd relay with a code rate of 3/4, D receives a frame of length 486 bits. Consequently, when all the three frames are received from the relays, they are of different lengths. In Figure 5.17 we have outlined the whole scenario. We observe that by disposing off the remaining bits, system can avoid the overhead of buffering the information at relay(s). Besides, there are lower delays in the information transmission. Moreover, destination combines the only bits which are received in the same time-slot on orthogonal channels from all the relays. Please note, we have used Nakagami-m factor as m_1 for the first hop, i.e., for the channels between source and multiple relays and it is denoted as m_{rd} for the links between relays and destination. Moreover, the above example addresses a rather generic scenario, and does not necessarily uses the same parameters as for the simulation results in Figure 5.15.

Furthermore, in Figure 5.15, the second (blue) curve demonstrates the BER performance of the system when there is no code rate adaptation, the input code rate and output code rate at the relay are same. The last (green) curve shows the bit-error-rate performance when the system applies the code rate adaptation based on channel conditions and also buffers the remaining bits at the relay. In this case, not only the bits are temporarily stored at the relay but they are also sent using the extra time-slots. As a result the destination receives the complete sequence from

each relay in multiple time-slots. Then D applies the post-detection combining on all the sequences received from relays. If we compare all three curves, we see that at the start the worst performance is shown by the system which applies the code rate adaptation without buffering any information at relays. Still, at a higher SNR this curve surpasses the performance of the code rate non-adaptive system and shows a very close performance to the system that does a temporal buffering of data at the relays, reason being that because of having multiple relays, the destination receives the multiple copies of the data sequences. If some of the information sequences are of not of same length, system can still achieve a good diversity gain. This fact is more evident when the number of relays increases. The advantages of this approach are manyfold, i.e.,

1. No temporal buffering of the data at the relays
2. Lesser processing at the relays
3. Lesser power consumption, as less information has to be sent
4. Shorter time delays

Hence, the OPA approach where code rate adaptation is done with no intermediate data buffering at relays but post detection combining is done on sequences of unequal lengths, appears to be a promising solution for multiple relays. Moreover, this approach also ensures the maximal energy efficiency by allocating the optimal share of transmit power to the transmitting nodes.

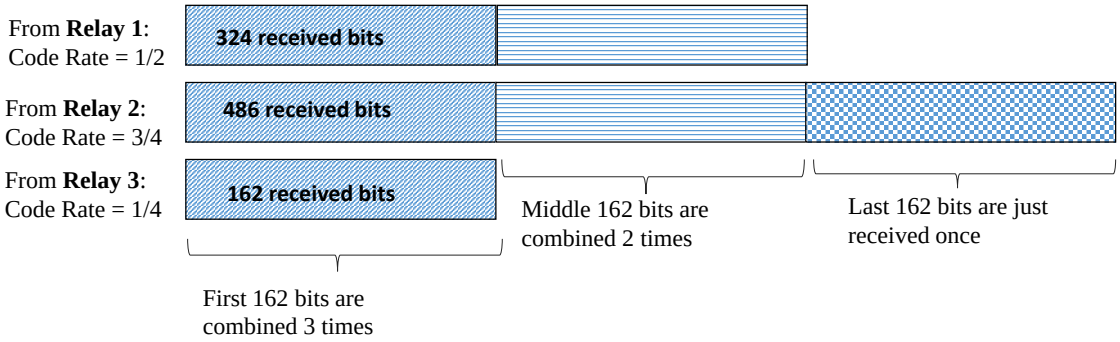

Figure 5.17: OPA Example: Number of effective information bits, received and combined (from 3 relays), codeword length = 648, $m_1 = 3$, $m_{rd} = \{3, 3, 1\}$, source code rate 3/4, 4-QAM

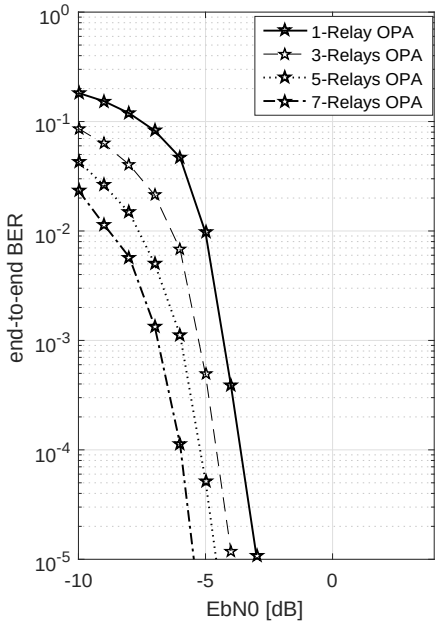

Figure 5.18: OPA: BER of system with multiple relays, codeword length = 312, $m_1 = m_2 = 3$, 4-QAM, varying code rates CR

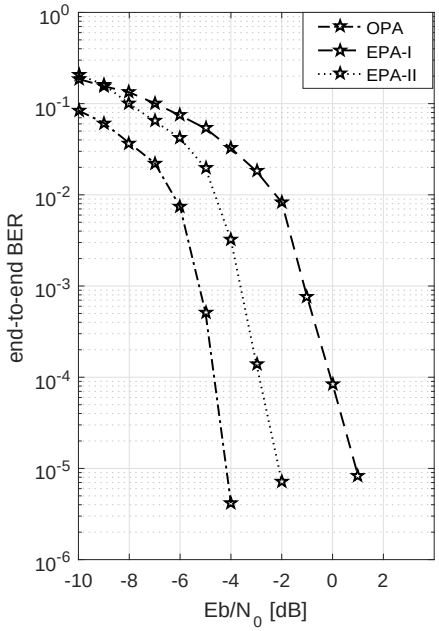

Figure 5.19: BER of multiple relays (5 Relays) with 3 PA schemes, (independent but not identically distributed (n.i.i.d) Channels), 4-QAM

Figure 5.18 shows the results of optimized power allocation and adaptive code rates. An identical Nakagami-m factor is considered on both hops, on all channels between source and multiple relays and relays and destination, i.e., $m_1 = m_2 = 3$. This is clear from Figure 5.18 that when transmit power is allocated optimally, with

increasing number of relays the BER performance becomes better and better. Figure 5.19 shows the performance of three different PA schemes, which we have studied in this work. As shown in Figure 5.19, results are collected for n.i.i.d Nakagami fading, i.e., value of fading factor m between two hops is different. OPA provides a performance gain of ∼5dB and ∼2dB as compared to EPA-I and EPA-II, respectively. From our discussion we know that EPA-I and EPA-II are simpler strategies of power allocation, as compared to the OPA. Because like in EPA-I, there is no transmit power adaptation in EPA-II but only the code rates adaptation is done under the CSI feedback. Table 5.1 presents an overview of the PA strategies. Positively, OPA not only improves the BER performance of the system but it also maximizes the energy efficiency of the system. As we can see, OPA is the superior power allocation technique because it takes into account the real time channel conditions and calculates the instantaneous SNR, and maximizes the energy efficiency of the system.

Table 5.1: Overview of three power allocation strategies

	EPA-I	**EPA-II**	**OPA**
Code rate adaptation	×	✓	✓
Power adaptation	×	×	✓

Furthermore, when there is code rate adaptation for the relay to destination link, a considerable gain can be attained with post-detection combining even without buffering the information at the intermediate relays. This method not only has many advantages over the technique with information buffering at the relays, but it also reduces the complexity of the over all system and helps the relays to consume less power and reduces the overall system delay.

6

Conclusion

Wireless communication between sender and receiver nodes via relays has been our focus in this thesis. Decode-and-forward relays are employed and investigated for this purpose. We have carried out the numerical analysis of the relay-assisted communications in terms of bit-error-rate performance, when relays are capable of encoding and decoding the information using the inherent properties of the LDPC codes. In this work, we have examined the several scenarios for time-division based half-duplex decode-and-forward relays, where different system parameters are optimized to enhance the system performance.

The main research results are presented in Chapters 4 and 5. In Chapter 4, an error rate analysis for dual-hop system has been carried out in detail. From the simulation and numerical results, we conclude that decode-and-forward relays can outperform their counterparts, such as, amplify-and-forward (AF) relays. For the dual-hop system we determined the optimum relay position and we conclude that with changing intensity of the fading, the optimum relay position range also changes. Besides, we determined from the comparison of two types of LDPC decoding algorithms that although bit-flipping algorithm (BFA) itself is a faster algorithm as compared to sum-product algorithm (SPA) but the overall time taken by the two algorithms for whole process of encoding and decoding is only slightly different. However, SPA gives almost a 4dB *decoding gain* at a BER of 10^{-4}. Additionally, in Chapter 4, we analyze the performance of rate adaptive relays, where relays are able to adapt to the changing conditions of the channel. The relays can adapt to the 5 different code rates (CR), on the basis of channel state information (CSI). An algorithm has been

designed for the task of rate adaptation. The rate/link adaptive coding was one of the main methodologies, which was explored in this thesis.

In Chapter 5, on the basis of the scenarios presented in the Chapter 4, some more results are demonstrated. One major part of the Chapter 5 is dedicated to the *diversity combining* techniques for relay-assisted communications. It has been seen that classical methods of diversity combining are equally applicable to the cooperative communications and they can also provide full diversity. For the cooperative maximum ratio combining communication (CMRC) our results show that a relay provides a substantial performance gain, if it is put closer to the source node between 10% to 40% of the total distance between source and destination when Nakagami fading parameter m on the 1st hop is set to at least 2, i.e., comparatively a less sever fading than Rayleigh fading. A method of generalized selection combining as cooperative generalized selection combining (CGSC) is presented, where the signal from selected relay/relays are combined at the destination with the signal from the direct path. We found, CGSC outperforms all the other diversity combining techniques used in this work. A numerical analysis of energy efficient DF relaying strategy is presented in Chapter 5, which concludes that the energy efficiency can be maximized for independent and identically distributed (i.i.d) channels if optimized power is allocated to the channels on both hops of the dual-hop multiple relay systems. The Chapter 5 also provides an overview of power allocation techniques for some scenarios. The simulations results show that relays, if used in combination with FEC codes, can provide a better network coverage, help to fight the fading better, and provide very low error-rates. We emphasize, as relays are power limited devices they should not carry out long mathematical and logical operations. Such operations not only increase the complexity of the relay processing but also result in additional delays. However, if relays are rate adaptive with buffers and use power allocation on the basis of instantaneous CSI, they must have to use the complex algorithms, which increases the complexity of these devices. So, DF relays are useful devices but in many applications they require a trade-off between complexity and performance.

A

Various Algorithms

In this appendix we present some of the algorithms, which we have either explored or developed in this thesis. The three algorithms are as under:

A.1 Bit-Flipping Algorithm

Algorithm 1 Bit-Flipping Algorithm

function DECODER(R)
  $I = 0$ ▷ Step1: Initialization
  for $i = 1 : n$ **do**
    $M_i = y_i$
  end for

  repeat
  for $j = 1 : m$ **do** ▷ Step2: Check node to variable node
    for $i = 1 : n$ **do**
      $E_{j,i} = \sum_{i' \in B_j, i' \neq i} (M'_i \mod 2)$
    end for
  end for

  for i = 1:n **do** ▷ Step3: Codeword test
    if the message $E_{j,i}$ disagree with y_i **then**
      $M_i = (y_i + 1 \mod 2)$
    end if
  end for

  for j=1:m **do** ▷ Step4: Variable node to check node
    $L_j = \sum_{i' \in B_j} (M'_i \mod 2)$
  end for

  if all $L_j = 0$ or $I = I_{max}$ **then**
    Finished
  else$I = I + 1$
  end if
  until Finished
end function

A.2 Sum-Product Algorithm

Algorithm 2 Sum-Product Algorithm

function DECODER(r)
$I = 0$ ▷ Step1: Initialization

  for i = 1:n **do**
    for i = 1:m **do**
      $L_{j,i} = R_i$
    end for
  end for
  repeat
  for j = 1:m **do** ▷ Step2: Check node to variable node

    for $i \in B_j$ **do**
      $E_{i,j} = log_e\left(\frac{1+\Pi_{i\prime\in B_j, i\prime\neq i} \quad tanh(L_{i\prime,j}/2)}{1-\Pi_{i\prime\in B_j, i\prime\neq i} \quad tanh(L_{i\prime,j}/2)}\right)$
    end for
  end for
  for i = 1:n **do** ▷ Step3: Codeword test
    $L_i = \sum_{j\in A_i} E_{i,j} + R_i$
    $z_i = \begin{cases} 1, & L_i \leq 0 \\ 0, & L_i > 0 \end{cases}$
  end for
  if $I = I_{max}$ **then** or $Hz^T = 0$
    Finished
  else
    for i=1:n **do** ▷ Step4: Variable node to check node

      for $j \in A_i$ **do**
      $L_{i,j} = \sum_{j'\in A_i, j'\neq j} E_{i,j'} + R_i$
      end for
    end for$I = I + 1$
  end if
  until Finished
end function

A.3 Code Rate Selection Algorithm

Algorithm 3 Code Rate Selection

buf = [ ] ▷ Initialization
$\delta_0 = 10^{-x}$ ▷ Target BER
if $t = 1$ **then** ▷ First transmission
    $r_{index} = r_0$
else ▷ 2nd/further transmissions
    if $\delta_{inst} > \delta_0$ **then**
        if $r_{index} = r_0$ **then**
        $r_{index} = r_{index}$
        else
        $r_{index} = r_{index-1}$
        end if
        $u'' = [\ ]$
        buff= y_i ▷ y_i is received data, stored in buffer
        Split the data into n shorter data streams
        for i = 1:n **do**
            function CodeGenerator(M, N, y_i) ▷ Generates a new parity check matrix
                return (u, H)
            end function
            function Decoder(L_i, H) ▷ L_i are log likelihood ratios
                return u'
            end function
        $u'' = [u'', u']$ ▷ Appending the data
        end for
    else
        $r_{index} = r_{index+1}$
        $buff = buff - bi$ ▷ bi, stored bits in buffer
        function CodeGenerator(M, N, y_i)
            return (u, H)
        end function
        $u' = [u, b_i]$ ▷ Appending the data
        function Decoder(L_i, H)
            return u''
        end function
    end if
end if

B

Various Derivations

B.1 Average SNR Calculation at Relay and Destination

Signal-to-noise ration (SNR) is the ratio of signal power to noise power at the receiver. To calculate the signal power at the receiver, the distance of the receiver from the source and the fading model must be taken into account. For a dual-hop wireless communications system if the distance between source and destination is d, any position of the relay can be translated into average SNR of both the links. If the distance d is normalized to one, the source node is considered to be located at the origin $(x, y) = (0, 0)$ while the destination is placed at $(x, y) = (1, 0)$ of the 2-D Cartesian coordinates system. For any arbitrary position (x_0, y_0) of the relay, by Pythagorean theorem, the distance d_1, between the source and the relay can be calculated as

$$d_1 = \sqrt{(x_0^2 + y_0^2)} \tag{B.1}$$

Similarly, the distance between relay and the destination can be calculated as

$$d_2 = \sqrt{((1 - {x_0}^2) + {y_0}^2)} \tag{B.2}$$

If the average SNR between S and D is represented as $\bar{\gamma}$

$$\bar{\gamma} = \frac{P|h|^2}{N_0} \tag{B.3}$$

Considering the same noise figures and transmit power P, for all nodes, the average SNR between source and the relay, $\bar{\gamma}_1$, can be written as

$$\bar{\gamma}_1 = \frac{\bar{\gamma}}{(d_1)^\nu} \tag{B.4}$$

where, ν, is the corresponding *pathloss* exponent, used to incorporate the effect of power loss with distance. Likewise, the average SNR between relay and the destination can be calculated as follows

$$\bar{\gamma}_2 = \frac{\bar{\gamma}}{(d_2)^\nu} \tag{B.5}$$

B.2 Calculation of SNR in CMRC

Let us consider the equation (5.3) once again,

$$\begin{aligned} y_{sd} &= x_s h_{sd} + n_{sd} \\ y_{sr} &= x_s h_{sr} + n_{sr} \\ y_{rd} &= x_r h_{rd} + n_{rd} \end{aligned} \tag{B.6}$$

we can see from (B.6) that y_{sd} and y_{rd} are the signals to be combined at the destination. Here, $|h_{sd}|$ and $|h_{rd}|$ are Nakagami distributed channel coefficients and n_{sd} and n_{rd} are random and Gaussian distributed noises with *zero* mean and variance σ^2. Here, all signals and channel coefficients are assumed real. The expected value of the two noises can be written as

$$\mathrm{E}\{|\mathrm{n_{sd}}|^2\} = \mathrm{E}\{|\mathrm{n_{rd}}|^2\} = \sigma^2 \tag{B.7}$$

Hence, each noise component has a noise power σ^2. Further, because two noises are added to the signal components on orthogonal channels, separated by time slots, they are uncorrelated. i.e.,

$$\mathrm{E}\{\mathrm{n_{sd}n_{rd}}\} = 0 \tag{B.8}$$

(B.8) implies that n_{sd} and n_{rd} are uncorrelated and as they are Gaussian so they are independent also. Further, to simplify the derivation let us assume, h_{sd} and h_{rd} are real coefficients and write the received symbols in vector form as follows:

$$\begin{bmatrix} y_{sd} \\ y_{rd} \end{bmatrix} = \begin{bmatrix} h_{sd} \\ h_{rd} \end{bmatrix} x_\mu + \begin{bmatrix} n_{sd} \\ n_{rd} \end{bmatrix}, \quad \mu \in \{s, r\} \tag{B.9}$$

Moreover, equation (B.9) can be written as in vectors form

$$\mathbf{y}_{\mu d} = \mathbf{h}_{\mu d} x_{\mu} + \mathbf{n}_{\mu d} \tag{B.10}$$

There are two received symbols at the destination to be combined, y_{sd} and y_{rd}. A new symbol y_{cmrc} is introduced here, which actually represents the *weighted combination* of y_{sd} and y_{rd} as follows,

$$y_{cmrc} = w_{sd} y_{sd} + w_{rd} y_{rd} \tag{B.11}$$

where, w_{sd} and w_{rd} are the *combining weights*. In the vector from these weighted combinations can be represented as

$$= \begin{bmatrix} w_{sd} & w_{rd} \end{bmatrix} \begin{bmatrix} y_{sd} \\ y_{rd} \end{bmatrix} \tag{B.12}$$

$$= \mathbf{w}_{\mu d}^{T} \mathbf{y}_{ud} \tag{B.13}$$

where we already know that $\mathbf{y}_{\mu d}$ is a vector,

$$\mathbf{y}_{\mu d} = \begin{bmatrix} y_{sd} \\ y_{rd} \end{bmatrix} \tag{B.14}$$

and

$$\mathbf{w}_{\mu d} = \begin{bmatrix} w_{sd} \\ w_{rd} \end{bmatrix} \tag{B.15}$$

In this system model (B.13), the equation (B.10) can be incorporated as under,

$$= \mathbf{w}_{\mu d}^{T}(\mathbf{h}_{\mu d} x_{\mu} + \mathbf{n}_{\mu d}) = \underbrace{\mathbf{w}_{\mu d}^{T} \mathbf{h}_{\mu d} x_{\mu}}_{\text{Signal Component}} + \underbrace{\mathbf{w}_{\mu d}^{T} \mathbf{n}_{\mu d}}_{\text{Noise Component}} \tag{B.16}$$

Therefore, the signal to noise ratio for (B.16) can be written as,

$$\gamma = \frac{|\mathbf{w}_{\mu d}^{T} \mathbf{h}_{\mu d}|^2 P}{\mathrm{E}\{|\mathbf{w}_{\mu \mathrm{d}}^{\mathrm{T}} \mathbf{n}_{\mu \mathrm{d}}|^2\}} \tag{B.17}$$

where, P is the transmit power of the signal x_{μ}. Let us now calculate the noise and signal power.

Noise Power

As,

$$\mathbf{w}_{\mu d}^{T}\mathbf{n}_{\mu d} = \begin{bmatrix} w_{sd} & w_{rd} \end{bmatrix} \begin{bmatrix} n_{sd} \\ n_{rd} \end{bmatrix} = w_{sd}n_{sd} + w_{rd}n_{rd} \tag{B.18}$$

The expected value of noise is

$$\begin{aligned} \mathrm{E}\{(\mathrm{w_{sd}n_{sd}} + \mathrm{w_{rd}n_{rd}})^2\} &= \mathrm{E}\{\mathrm{w_{sd}^2 n_{sd}^2} + \mathrm{w_{rd}^2 n_{rd}^2} + 2\mathrm{w_{sd}n_{sd}w_{rd}n_{rd}}\} \\ &= w_{sd}^2 \underbrace{\mathrm{E}\{\mathrm{n_{sd}^2}\}}_{\sigma^2} + w_{rd}^2 \underbrace{\mathrm{E}\{\mathrm{n_{rd}^2}\}}_{\sigma^2} + 2w_{sd}w_{rd} \underbrace{\mathrm{E}\{\mathrm{n_{sd}n_{rd}}\}}_{=0, \text{ from (B.8)}} \end{aligned} \tag{B.19}$$

hence, (B.19) can be written as,

$$\begin{aligned} &= w_{sd}^2\sigma^2 + w_{rd}^2\sigma^2 \\ &= \sigma^2(w_{sd}^2 + w_{rd}^2) \end{aligned} \tag{B.20}$$

Equation (B.20) can be written in the form of squared vector norm as,

$$= \sigma^2 \|\mathbf{w}_{\mu d}\|^2 \tag{B.21}$$

where, $\|\mathbf{w}_{\mu d}\|^2 = (w_{sd}^2 + w_{rd}^2)$ and equation (B.21) represents the noise power. We will substitute this value of noise power in equation (B.17) of SNR, once we will be done with the calculation of signal power as well.

Signal Power

From (B.16), we know

$$\mathbf{w}_{\mu d}^{T}\mathbf{h}_{\mu d} = \begin{bmatrix} w_{sd} & w_{rd} \end{bmatrix} \begin{bmatrix} h_{sd} \\ h_{rd} \end{bmatrix} = w_{sd}h_{sd} + w_{rd}h_{rd} \tag{B.22}$$

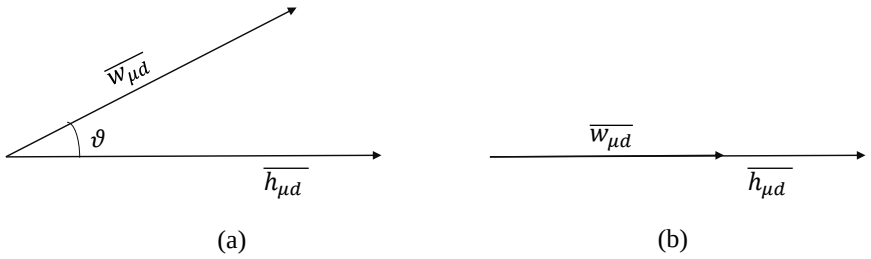

Figure B.1: Two vectors with angle θ and 0

By the definition of dot product of two vectors it can be shown,

$$|\mathbf{w}_{\mu d}^{T}.\mathbf{h}_{\mu d}| = \|\mathbf{w}_{\mu d}\|.\|\mathbf{h}_{\mu d}\| cos\theta \tag{B.23}$$

where $cos\theta$ is the angle between the two vectors.

$$|\mathbf{w}_{\mu d}^{T}.\mathbf{h}_{\mu d}|^2 = \|\mathbf{w}_{\mu d}\|^2.\|\mathbf{h}_{\mu d}\|^2 cos^2\theta \tag{B.24}$$

Now if values for signal and noise power components are incorporated in SNR equation (B.17), as under

$$\gamma = \frac{P|\|\mathbf{w}_{\mu d}\|^2\|\mathbf{h}_{\mu d}\|^2 cos^2\theta}{\sigma^2\|\mathbf{w}_{\mu d}\|^2} \tag{B.25}$$

$$\gamma = \frac{P\|\mathbf{h}_{\mu d}\|^2 cos^2\theta}{\sigma^2} \tag{B.26}$$

It is clear from (B.26) that SNR γ is maximum when $cos^2\theta = 1$. It is only possible if the value of $\theta = 0$, as shown in Figure B.1(b), i.e., two vectors are pointing along the same direction. Moreover, it can be said that $\mathbf{w}_{\mu d} \propto \mathbf{h}_{\mu d}$. Furthermore, (B.26) can be simplified as

$$\begin{aligned} \gamma &= \frac{P\|\mathbf{h}_{\mu d}\|^2}{\sigma^2} \\ &= \frac{P(|h_{sd}|^2 + |h_{rd}|^2)}{\sigma^2} \end{aligned} \tag{B.27}$$

As, $\mathbf{w}_{\mu d} \propto \mathbf{h}_{\mu d}$, so that $\mathbf{w}_{\mu d}$ should be set in such a way that norm of vector $\mathbf{w}_{\mu d}$ is unity. It can be done as follows

$$\mathbf{w}_{\mu d} = \frac{1}{\|\mathbf{h}_{\mu d}\|}\begin{bmatrix} h_{sd} \\ h_{rd} \end{bmatrix} = \frac{1}{\sqrt{(|h_{sd}|^2 + |h_{rd}|^2)}}\begin{bmatrix} h_{sd} \\ h_{rd} \end{bmatrix} \tag{B.28}$$

where, $\mathbf{w}_{\mu d}$ is the optimal *combining weight vector*.

B.3 Estimation of $\hat{x_s}$ in CMRC

In, B.2, we have derived the weights considering the real channel coefficients. For complex channel coefficients instead of using $\mathbf{w}_{\mu d}^{T}$, $\mathbf{w}_{\mu d}^{H}$ is used, where H represents the *Hermitian*.

$$\mathbf{w}_{\mu d}^{H}\mathbf{y}_{\mu d} = \begin{bmatrix} w_{sd}^{*} & w_{rd}^{*} \end{bmatrix}\begin{bmatrix} y_{sd} \\ y_{rd} \end{bmatrix} = w_{sd}^{*}y_{sd} + w_{rd}^{*}y_{rd} \tag{B.29}$$

Nonetheless, optimal *combining weight vector* can be still given as

$$\mathbf{w}_{\mu d} = \frac{\mathbf{h}_{\mu d}}{\|\mathbf{h}_{\mu d}\|} \tag{B.30}$$

Hence, we can write it further in terms of cooperative maximum ratio combining as

$$\begin{aligned} y_{cmrc} &= \sum_{\mu \in \{s,r\}} w^*_{\mu d} y_{\mu d} \\ y_{cmrc} &= \sum_{\mu \in \{s,r\}} w^*_{\mu d} \big[h_{\mu d} x_\mu + n_{\mu d} \big] \end{aligned} \tag{B.31}$$

The estimated symbol $\hat{x_s}$ can be obtained like

$$\hat{x}_s = arg\min_{x_s} |(w^*_{sd} y_{sd} + w^*_{rd} y_{rd}) - (w^*_{sd} h_{sd} + w^*_{rd} h_{rd}) x_s|^2 \tag{B.32}$$

By putting the values of y_{sd} and y_{rd} from (5.3), in (B.32)

$$\hat{x}_s = arg\min_{x_s} |(w^*_{sd}(h_{sd} x_s + n_{sd}) + w^*_{rd}(h_{rd} x_r + n_{rd})) - (w^*_{sd} h_{sd} + w^*_{rd} h_{rd}) x_s|^2 \tag{B.33}$$

Moreover, in our work we have assumed, that $x_r = x_s$, because the relay is placed closer to the source and forward error correction codes are employed to have an error free transmission at the relay in a two hop system, hence,

$$\hat{x}_s = arg\min_{x_s} |(w^*_{sd}(h_{sd} x_s + n_{sd}) + w^*_{rd}(h_{rd} x_r + n_{rd})) - (w^*_{sd}(h_{sd} x_s) + w^*_{rd}(h_{rd} x_s)|^2 \tag{B.34}$$

In this way $\hat{x}_s$, can be estimated using complex weighted coefficients as it is done in classical maximum ratio combining.

Bibliography

[1] Mischa Dohler, Yonghui Li, "Cooperative Communications Hardware, Channel & PHY," *WILEY*, Mar. 2010.

[2] V. Chandrasekhar, J. Andrews, A. Gatherer, "Femtocell networks: a survey," *IEEE Commun Mag. Communications Magazine, IEEE*, vol. 46, pp 59 - 67, Sept. 2008.

[3] S. Basagni, M. Conti, S. Giordano, I. Stojmenovic, "Mobile Ad Hoc Networking," *John Wiley & Sons*, Oct. 2004.

[4] X. Shen, "Device-to-device communication in 5G cellular networks," *IEEE Network*, vol. 29, pp. 2-3, Mar-Apr. 2015.

[5] I. F. Akyildiz, W. Su, Y. Sankarasubramaniam, E. Cayirci, "A survey on sensor networks," *IEEE Commun. Mag.*, vol. 40, pp. 102 – 114, Aug. 2002.

[6] A. Goldsmith, "Wireless Communications," *Cambridge University Press*, 2005.

[7] S. ten Brink, "Webdemos," https://webdemo.inue.uni-stuttgart.de, 2013.

[8] B. SKalar, "Rayleigh fading channels in mobile digital communication systems, Part I, characterization," *IEEE communication magazine*, pp. 90-100, Jul. 1997.

[9] M. K. Simon, M. S. Alouini, "Digital Communication over Fading Channels: A Unified Approach to Performance Analysis, " *John Wiley*, Jan, 2002.

[10] R. G. Gallager, "Low-density parity-check codes," *IEEE Transactions on Information Theory*, vol. IT-8, pp. 21-28, Jan. 1962.

[11] D. J. C. MacKay, R. M. Neal, "Good codes based on very sparse matrices," *Cryptography and Coding 5th IMA Conf., C. Boyd, Ed., Lecture Notes in Computer Science*, pp. 100–111, 1995.

[12] T. J. Richardson, M. A. Shokrollahi, R. L. Urbanke, "Design of Capacity-Approaching Irregular Low-Density Parity-Check Codes, "*IEEE Transaction on Information Theory*, vol.47, Feb. 2001.

[13] W. E. Ryan, "An Introduction to LDPC codes," in *CRC Handbook for Coding and Signal Processing for Recording Systems*, B. Vasic and E.M. Kurtas, Eds. Boca Raton, FL: CRC, 2005.

[14] M. G. Luby, M. Mitzenmacher, M. A. Shokrollahi, D. A. Spielman, "Analysis of low density codes and improved designs using irregular graphs," *Proceedings of the 30th annual ACM symposium on theory of computing*, May, 1998.

[15] R. M. Tanner, "A Recursive Approach to Low Complexity Codes," *IEEE Transaction on Information Theory*, vol. IT-27, Sept. 1981.

[16] D. Divsalar, H. Jin, R. J. McEliece, "Coding Theorems for Turbo-Like Codes," *Proc. 36th Allerton Conf. on Communication, Control and Computing*, vol. 36, pp. 201-210, Sept. 1998.

[17] H. Jin, A. Khandekar, R. McEliece, "Irregular Repeat–Accumulate Codes," *Proc. 2nd Int. Symp. Turbo Codes and Related Topics*, pp. 1-8, Sept. 2000.

[18] M. Yang, W. E. Ryan, Y. Li, "Design of Efficiently Encodable Moderate-Length High-Rate Irregular LDPC Codes," *IEEE Transaction on Communications*, vol. 52, Apr. 2004.

[19] Y. Kou, S. Lin, M. Fossorier, "Low density parity check codes based on finite geometries: A rediscovery and new results," *IEEE Transactions on Information Theory*, vol. 47, Nov. 2001.

[20] S.Lin, and D.J. Costello, " Error control coding: Fundamentals and applications," *Englewood Cliffs, Prentice-Hall*, 1983.

[21] C. M. Jorge and G. F. Patrie, "Essentials of error-control coding," *John Wiley and Sons, Ltd.*, Aug. 2006.

[22] S. Johnson, "Low-Density Parity-Check Codes from Combinatorial Designs," *PhD Thesis*, University of Newcastle, Australia, Apr. 2004.

[23] A. A. Sani, L. Zhong, A. Sabharwal, "Directional antenna diversity for mobile devices: characterizations and solutions," *Proceedings of the sixteenth annual international conference on Mobile computing and networking*, pp. 221-232, Sept. 2010.

[24] T. Wang, A. Cano, J. N Laneman, "High-Performance Cooperative Demodulation with Decode-and-Forward Relays," *IEEE Transactions on Communications*, vol. 55, pp. 1427–1438, Jul. 2007.

[25] S. S. Eldin, M. Nasr, S. Khamees, E. Sourour, "LDPC coded MIMO OFDM based IEEE 802.11n wireless LAN," *WOCN Conf.*, Apr. 2009.

[26] H. Hourani, "An overview of diversity techniques in wireless communication systems," *IEEE JSAC*, Oct. 2004.

[27] T. Wang, A. Cano, G. B. Giannakis, J. N. Laneman, "High performance cooperative demodulation with decode-and-forward relays," *Communications, IEEE Transactions*, vol. 55, pp. 1427 – 1438, Jul. 2007.

[28] M. Janani, A. Hedayat, T. E Hunter, A. Nosratinia, "Coded cooperation in wireless communications: space-time transmission and iterative decoding," *IEEE Transactions on Signal Processing*, vol. 52, Feb. 2004.

[29] H. Shin, J. B Song, "MRC Analysis of Cooperative Diversity with Fixed-Gain Relays in Nakagami-m Fading Channels," *IEEE Transactions on Wireless Communications*, Jul. 2008.

[30] N. G. M. N. Alliance, "5G white paper," *Next generation mobile networks*, pp. 1-125, Feb. 2015.

[31] J. W. Wallace, M. A. Jensen, "Modeling the indoor MIMO wireless channel," *IEEE Journal of Transactions on Antennas and Propagation*, vol. 50, pp. 591-599, May, 2002.

[32] G . German, Q. Spencer, L. Swindlehurst and R. Valenzuela, "Wireless indoor channel modeling: statistical agreement of ray tracing simulations and channel sounding measurements," *IEEE International Conference on Acoustics, Speech, and Signal Processing. Proceedings*, vol. 4, pp. 2501-2504, 2001.

[33] Z. Irahhauten, H. Nikookar and G. J. M. Janssen, "An overview of ultra wide band indoor channel measurements and modeling," *IEEE Microwave and Wireless Components Letters*, vol. 14, pp. 386-388, Aug. 2004.

[34] D. Moltchanov, Y. Koucheryavy, J. Harju, "Simple, Accurate and Computationally Efficient Wireless Channel Modeling Algorithm," *Wired/Wireless Internet Communications*, vol. 3510, 2005.

[35] S. Jaruwatanadilok, "Underwater Wireless Optical Communication Channel Modeling and Performance Evaluation using Vector Radiative Transfer Theory," *IEEE Journal on Selected Areas in Communications*, vol. 26, pp. 1620-1627, Dec. 2008.

[36] A. Iyer, C. Rosenberg, A. Karnik, "What is the right model for wireless channel interference?," *IEEE Transactions on Wireless Communications*, vol. 8, pp. 2662-2671, May, 2009.

[37] C. Wang, X. Cheng, D. I. Laurenson, "Vehicle-to-vehicle channel modeling and measurements: recent advances and future challenges," *IEEE Communications Magazine*, vol. 47, pp. 96-103, Nov. 2009.

[38] Z. Sun, I. F. Akyildiz, "Channel modeling and analysis for wireless networks in underground mines and road tunnels," *IEEE Transactions on Communications*, vol. 58, pp. 1758-1768, Jun. 2010.

[39] J. M. Jornet, I. F. Akyildiz, "Channel Modeling and Capacity Analysis for Electromagnetic Wireless Nanonetworks in the Terahertz Band," *IEEE Transactions on Wireless Communications*, vol. 10, pp. 3211-3221, Oct. 2011.

[40] L. Liu et al., "Position-Based Modeling for Wireless Channel on High-Speed Railway under a Viaduct at 2.35 GHz," *IEEE Journal on Selected Areas in Communications*, vol. 30, pp. 834-845, May, 2012.

[41] M. R. Akdeniz et al., "Millimeter Wave Channel Modeling and Cellular Capacity Evaluation," *IEEE Journal on Selected Areas in Communications*, vol. 32, pp. 1164-1179, June 2014.

[42] J. N. Laneman, D. N. C. Tse and G. W. Wornell, "Cooperative diversity in wireless networks: Efficient protocols and outage behavior," *IEEE Transactions on Information Theory*, vol. 50, pp. 3062-3080, Dec. 2004.

[43] A. Chakrabarti, A. D. Baynast, A. Sabharwal and B. Aazhang, "Low density parity check codes for the relay channel," *IEEE Journal on Selected Areas in Communications*, vol. 25, pp. 280-291, Feb. 2007.

[44] A. Müller, H. C. Yang, "Dual-hop adaptive packet transmission with regenerative relaying for wireless TDD systems," *IEEE Global Telecommunications Conference*, pp. 1-6, 2009.

[45] A. J. Goldsmith, S.-G. Chua, "Adaptive coded modulation for fading channels," *IEEE Trans. Commun.*, vol. 46, pp. 595-602, May, 1998

[46] H. Su and Y. He and L. Zhou , "Adaptive transmission based on multi-relay selection and rate-compatible LDPC codes, *AIP Conference Proceedings*, vol. 1864, pp. 20-154, 2017

[47] D. J. C. Mackay, R. M. Neal, "Near Shannon limit performance of low density parity check codes," *IEEE Electron. Letters*, vol. 32, pp. 1645-1646, Aug. 1996.

[48] S. Y. Chung, G. D. Forney, T. J. Richardson, R. L. Urbanke, "On the design of low-density parity check codes within 0.0045 dB of the Shannon limit", *IEEE Communications Letters*, vol. 5, pp. 58-60, Feb. 2001.

[49] A. Müller, "Analysis and Optimization of Wireless Communication Systems with Regenerative Relaying," *PhD dissertation*, Telecommunication department, University of Stuttgart, Stuttgart, 2011.

[50] M. Wu, P. Weitkemper, D. Wübben, K. D. Kammeyer, "Comparison of distributed LDPC coding schemes for decode-and-forward relay channels," *IEEE International ITG Workshop on Smart Antennas*, pp. 127-134 , 2010.

[51] A. Müller and J. Speidel, "Adaptive modulation for wireless multihop systems with regenerative relays," *IEEE 68th Vehicular Technology Conference*, pp. 1-5, 2008.

[52] Z. Lin, E. Erkip and M. Ghosh, "CTH15-5: Rate adaptation for cooperative systems," *IEEE Globecom, San Francisco, CA*, pp. 1-5, 2006.

[53] S.A. Hassan, M.A. Ingram, "A quasi-stationary Markov chain model of a cooperative multi-hop linear network," *IEEE Transactions on Wireless Communications*, vol. 10, pp. 2306-2315, Jul. 2011.

[54] I. Ez-Zazi, M. Arioua, A. El Oualkadi, P. Lorenz, "A hybrid adaptive coding and decoding scheme for multi-hop wireless sensor networks," *Wireless Personal Communications, Springer*, pp. 1-17, 2016.

[55] S.A. Hassan, Y. G. Li, P. S. S. Wang, and M. Green, "A full rate dual relay cooperative system for wireless communications," *IEEE Journal on Communications and Networks (JCN)*, vol. 12, pp. 442-448, Oct. 2010.

[56] J. Liu and Rodrigo C. de Lamare, "Rate-Compatible LDPC codes based on puncturing and extension techniques for short block lengths," *International Journal of Electronics and Communications*, vol. 69, pp. 1582 - 1589, Jul. 2015.

[57] R. Hormis, X. Wang, "Notes on a posteriori probability (APP) metrics for LDPC," *IEEE 802.3an Task Force, Columbia University, New York*, Nov. 2004.

[58] N. A. Rahim, M. Nguyen, K. D. and Lechner, "SC-LDPC code design for half-duplex relay channels," *G. Wireless Pers Commun.*, vol. 92, pp.771-783, Jan. 2017.

[59] E. C. Van der Meulen, "Three-terminal communication channels," *Adv. Appl. Prob.*, vol. 3, pp. 120-154, 1971.

[60] T. Cover and A. A. El Gamal, "Capacity theorems for the relay channel," *IEEE Trans. Inf. Theory*, vol. IT-25, pp. 572–584, Sept. 1979.

[61] A. A. El Gamal and M. Aref, "The capacity of the semi-deterministic relay channel," *IEEE Trans. Inf. Theory* , vol. IT-28, pp. 536, May, 1982.

[62] D. Qiao, M. C. Gursoy and S. Velipasalar, "Analysis of Energy Efficiency in Fading Channels under QoS Constraints," *IEEE Global Telecommunications Conference, New Orleans, LO*, pp. 1-5, 2008.

[63] J. N. Laneman and G. W. Wornell, "Distributed space-time-coded protocols for exploiting cooperative diversity in wireless networks," *IEEE Trans. Inf. Theory*, vol. 49, pp. 2415-2425, Oct. 2003.

[64] L. Wu, J. Lin, K. Niu, Z. He, "Error analysis of generalized selection combining over relay channel," *The Journal of China Universities of Posts and Telecommunications*, vol. 17, pp. 50-66 , 2010.

[65] A. Yılmaz, O. Kucur, "End-to-end performance of transmit antenna selection and generalized selection combining in dual-hop amplify-and-forward relay network in the presence of feedback errors," *Journal of Wireless Communications and Mobile Computing, Wiley Online Library*, vol. 14, pp. 689-703, May, 2014.

[66] S. ten Brink, "Convergence of iterative decoding," *Electronic Letters*, vol. 35, pp. 806-808, 1999.

[67] A. Ashikmin, G.Kramer, S.ten Brink, "Extrinsic Information Transfer Functions: Model and Erasure Channel Property," *IEEE Trans. Inform. Theory*, vol. 50, pp. 2657-2673, 2004.

[68] S. Asoodeh, H Ramezani, S. Hossein, " Gaussian Approximation for LDPC Codes," *IEEE Wireless Communications, Networking and Mobile Computing*, pp. 1437 - 1440, 2007.

[69] M. Martalò, G. Ferrari, A. Abrardo, M. Franceschini, R. Raheli, "Density evolution-based analysis and design of LDPC codes with a priori information," *Information Theory and Applications Workshop (ITA), San Diego, CA*, pp. 1-9 2010.

[70] T. Wang, A. Cano, G. B Giannakis, and J. N. Laneman, "High-performance cooperative demodulation with decode-and-forward relays," *IEEE Transactions on Communications*, vol. 55, pp. 1427-1438, Jul. 2007.

[71] S.S Ikki, A. Abdaoui, and M. H. Ahmed, "Performance analysis of adaptive decode-and-forward cooperative diversity networks with the best relay selection scheme," *IEEE Transactions on Communications*, vol. 58, pp. 68-72, Oct. 2010.

[72] T. Q. Duong, V. N. Q. Bao, and H. J. Zepernick, "On the performance of selection decode-and-forward relay networks over Nakagami-m fading channels," *IEEE Communications Letters*, vol. 13, pp. 172-174, 2009.

[73] S. X. Ng et al., "Distributed irregular codes relying on decode-and-forward relays as code components," *IEEE Transactions on Vehicular Technology*, vol. 64, pp. 4579-4588, 2015.

[74] Y. Gu, S. Aissa, "RF-based energy harvesting in decode-and-forward relaying systems: Ergodic and outage capacities," *IEEE Transactions on Wireless Communications*, vol. 14, pp. 6425-6434, 2015.

[75] B. Zafar, S. Gherekhloo and M. Haardt, "Analysis of multihop relaying networks: Communication between range-limited and cooperative nodes," *IEEE Vehicular Technology Magazine*, vol. 7, pp. 40-47, Sept. 2012.

[76] L. Chen et al., "Mobile relay in LTE-advanced systems," *IEEE Communications Magazine*, vol. 51, pp. 144-151, Nov. 2013.

[77] M. M. Fareed and M. Uysal, "BER-Optimized Power Allocation for Fading Relay Channels," *IEEE Trans. Wireless Commun.*, vol. 7, pp. 2350-2359, Jun. 2008.

[78] Z. Li, H. Hu, Y. Zhao and L. Jia, "Power allocation methods in relay-assisted network with mobile-to-mobile channels," *IEEE International Conference on Communications Technology and Applications*, pp. 940-945, 2009.

[79] L. K. Jayasinghe, and R. M. A. P. Rajatheva, "Optimal Power Allocation for Relay Assisted Cognitive Radio Networks," *IEEE 72nd Vehicular Technology Conference*, pp. 1-5, 2010.

[80] P. Ubaidulla, S. Aissa, "Optimal relay selection and power allocation for cognitive two-way relaying networks," *IEEE Wireless Communications Letters*, pp. 225-228, 2012.

[81] M. Chen, S. Serbetli, A. Yener, "Distributed power allocation strategies for parallel relay networks," *IEEE Transactions on Wireless Communications*, vol. 7, 2008.

[82] S. Kadloor, R. Adve, "Relay selection and power allocation in cooperative cellular networks," *IEEE Transactions on Wireless Communications*, vol. 9, 2010.

[83] D. Michalopoulos and G. Karagiannidis, "Performance analysis of single relay selection in Rayleigh fading, " *IEEE Transactions on Wireless Communications*, vol. 7, no. 10, pp. 3718–3724, Oct. 2008.

[84] Y. Liu, "Wireless information and power transfer for multirelay-assisted cooperative communication," *IEEE Communications Letters*, vol. 20, pp. 784-787, 2014.

[85] Z. Moe, Win, and J. H. Winters, "Analysis of hybrid Selection/Maximal-Ratio Combining in Rayleigh Fading," *IEEE Transactions on Communications*, vol. 47, No. 12, pp. 1773-1776, Dec. 1999.

[86] H. Xu, "Symbol Error Rate of Generalized Selection Combining with Signal Space Diversity in Rayleigh Fading Channels," *SAIEE Africa Research Journal*, vol. 106, pp 201-211, 2015.